



UvA-DARE (Digital Academic Repository)

Bulk locality breakdown

Kabir, L.R.

[Link to publication](#)

Citation for published version (APA):

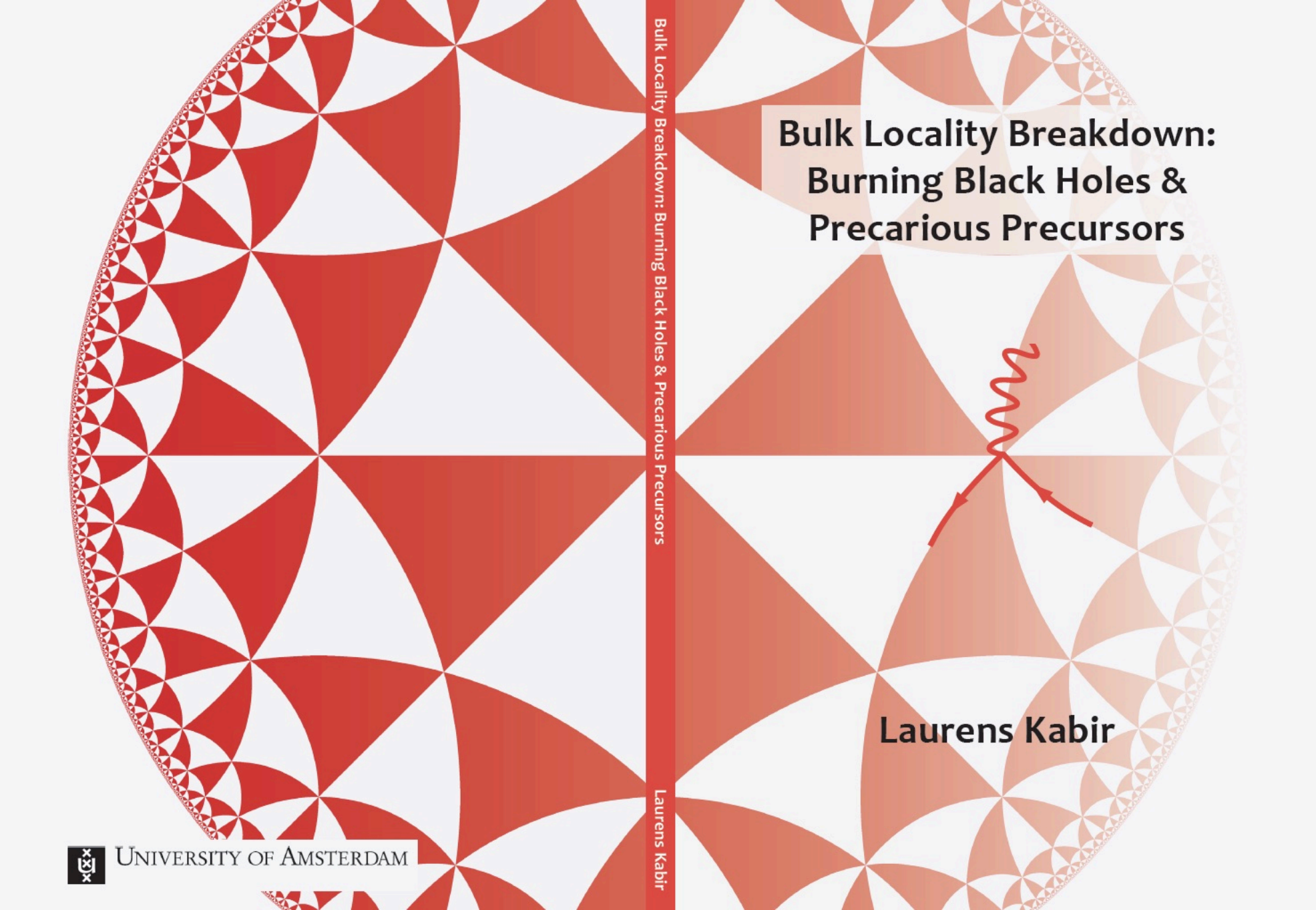
Kabir, L. R. (2017). Bulk locality breakdown: Burning black holes & precarious precursors

General rights

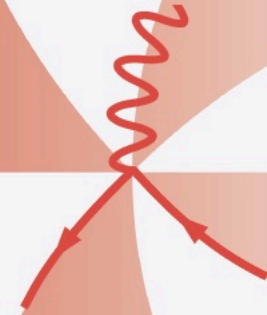
It is not permitted to download or to forward/distribute the text or part of it without the consent of the author(s) and/or copyright holder(s), other than for strictly personal, individual use, unless the work is under an open content license (like Creative Commons).

Disclaimer/Complaints regulations

If you believe that digital publication of certain material infringes any of your rights or (privacy) interests, please let the Library know, stating your reasons. In case of a legitimate complaint, the Library will make the material inaccessible and/or remove it from the website. Please Ask the Library: <http://uba.uva.nl/en/contact>, or a letter to: Library of the University of Amsterdam, Secretariat, Singel 425, 1012 WP Amsterdam, The Netherlands. You will be contacted as soon as possible.



**Bulk Locality Breakdown:
Burning Black Holes &
Precarious Precursors**



Laurens Kabir

Bulk Locality Breakdown: Burning Black Holes & Precarious Precursors

Laurens Kabir



UNIVERSITY OF AMSTERDAM

BULK LOCALITY BREAKDOWN:
BURNING BLACK HOLES &
PRECARIOUS PRECURSORS

This work has been accomplished at the Institute for Theoretical Physics (ITFA) of the University of Amsterdam (UvA) and is part of the Delta ITP consortium, a program of the Netherlands Organisation for Scientific Research (NWO) that is funded by the Dutch Ministry of Education, Culture and Science (OCW).



UNIVERSITY OF AMSTERDAM

ISBN: 978-94-6233-630-8

© Laurens Kabir, 2017.

Cover: local interaction on an AdS_3 time slice (Poincaré hyperbolic disk) tessellation.

All rights reserved. Without limiting the rights under copyright reserved above, no part of this book may be reproduced, stored in or introduced into a retrieval system, or transmitted, in any form or by any means (electronic, mechanical, photocopying, recording or otherwise) without the written permission of both the copyright owner and the author of the book.

BULK LOCALITY BREAKDOWN:
BURNING BLACK HOLES &
PRECARIOUS PRECURSORS

ACADEMISCH PROEFSCHRIFT

ter verkrijging van de graad van doctor

aan de Universiteit van Amsterdam

op gezag van de Rector Magnificus

prof. dr. ir. K.I.J. Maex

ten overstaan van een door het College voor Promoties ingestelde

commissie, in het openbaar te verdedigen in de Agnietenkapel

op Vrijdag 23 Juni 2017, te 14.00 uur

door

LAURENS RAHIED KABIR

geboren te Leuven, België

PROMOTIECOMMISSIE

PROMOTOR

prof. dr. J. de Boer, Universiteit van Amsterdam

CO-PROMOTORES

dr. B.W. Freivogel, Universiteit van Amsterdam

dr. J.P. van der Schaar, Universiteit van Amsterdam

OVERIGE LEDEN

prof. dr. D.D. Baumann, Universiteit van Amsterdam

dr. A. Castro Anich, Universiteit van Amsterdam

dr. K. Papadodimas, Rijksuniversiteit Groningen

prof. dr. S.J.G. Vandoren, Universiteit Utrecht

prof. dr. E.P. Verlinde, Universiteit van Amsterdam

FACULTEIT DER NATUURWETENSCHAPPEN, WISKUNDE EN INFORMATICA

Publications

THIS THESIS IS BASED ON THE FOLLOWING PUBLICATIONS:

- [1] B. Freivogel, R. Jefferson, L. Kabir and I-S. Yang
Geometry of the Infalling Causal Patch
Phys. Rev. D **91** no. 4, 044036 (2015), arXiv:1406.6043 [hep-th].

- [2] B. Freivogel, R. Jefferson and L. Kabir
Precursors, Gauge Invariance, and Quantum Error Correction in AdS/CFT
JHEP **1604**, 119 (2016), arXiv:1602.04811 [hep-th].

- [3] A. Belin, B. Freivogel, R. Jefferson and L. Kabir
Sub-AdS Scale Locality in AdS₃/CFT₂
JHEP **1704**, 147 (2017), arXiv:1611.08601 [hep-th].

- [4] J. de Boer, B. Freivogel, L. Kabir and S.F. Lokhande
Precursors and BRST Symmetry
arXiv:1612.05265 [hep-th].

OTHER PUBLICATIONS BY THE AUTHOR:

- [5] B. Freivogel, R. Jefferson, L. Kabir, B. Mosk and I-S. Yang
Casting Shadows on Holographic Reconstruction
Phys. Rev. D **91** no. 8, 086013 (2015), arXiv:1412.5175 [hep-th].

- [6] F. Dimitrakopoulos, L. Kabir, B. Mosk, M. Parikh and J.P. van der Schaar
Vacua and Correlators in Hyperbolic de Sitter Space
JHEP **1506**, 095 (2015), arXiv:1502.00113 [hep-th].

Preface & Overview

BULK LOCALITY BREAKDOWN: BURNING BLACK HOLES & PRECARIOUS PRECURSORS

This thesis is an exposition of some of the research that I carried out during my doctoral studies. Broadly speaking, my research focused on how fundamental subjects such as general relativity, thermodynamics and quantum information appear to be connected. Various connections exist, manifested notably in black holes, holography, and the AdS/CFT correspondence in particular. All three of these related subjects will be touched upon in this work, with locality playing an inter-connecting role. In what follows, I will briefly summarize and motivate the central elements in this thesis.

Introduction

To begin with, I will set the stage by providing some background information in chapter 1 on a level that should be accessible to readers holding a master in theoretical physics. The introduction contains two main parts, the first of which is focused on black holes. These fascinating objects have been studied for over 50 years, and form an excellent playground for theorists to study properties of (quantum) gravity. I will explain that black holes radiate and can be attributed various thermodynamical properties, such as a temperature and an entropy. Thereafter, I will discuss the thermodynamical stabilities of black holes, since it will be relevant for chapter 2.

The second part of the introduction is about holography and in particular the AdS/CFT correspondence. I will explain how black hole entropy leads to the holographic principle, and motivate how theoretical physicists could come up with this remarkable duality between string theory and conformal field theory living in one dimension less. Then I will proceed to discuss various aspects of AdS/CFT, especially concepts such as HKLL reconstruction and bulk locality, as they will be frequently used in chapters 3, 4 and 5.

I think it is fair to say that while AdS/CFT has been one of the most powerful tools in theoretical physics in the last 20 years, many parts of this duality are still poorly understood. In particular an understanding of core aspects of the duality related to reconstructing bulk physics from boundary data, and the miraculous property of (sub-AdS scale) locality, is still lacking. It is in these two areas that I have tried to make progress with my research, therefore, I will spend a significant part of this thesis explaining the problems and outlining my contributions.

Burning Black Holes

Almost 40 years after Hawking showed that black holes have a temperature and radiate, it is clear that they still keep many secrets until this very day. A famous consequence of Hawking's result is the information paradox: collapsing a pure state into a black hole and letting it evaporate seems to lead to a mixed state of thermal radiation, which cannot happen in a unitary theory. Various resolutions have been proposed: from the pragmatic black hole complementarity to more exotic (Planck-sized) remnants, large modifications of (semi-)classical gravity, or even soft hair. Although none of these suggestions seem completely satisfactory, I do think that holography (and more specifically, AdS/CFT) suggests that black hole evaporation is unitary, although it is far from clear how that would work from a bulk point of view.

In 2012 a new thought experiment surfaced, involving an observer falling into an evaporating black hole. Some older information paradox-like ingredients were repackaged in a sharper paradox: it was pointed that there is a trilemma between unitary black hole formation and evaporation, locality, and the equivalence principle. Some theoretical physicists gave up the latter, suggesting that an infalling observer experiences a 'firewall' instead of a smooth event horizon. Others proposed drastic violations of locality, such as ER=EPR that involves tiny wormholes connecting the interior of the black hole with the exterior. The firewall paradox is puzzling, because common sense says that doing low energy effective field theory in a weakly curved region of spacetime (such as the event horizon of a large black hole) should give perfectly accurate results. It is unclear why quantum gravity effects would suddenly be important in this particular problem.

In chapter 2, I will elaborate on this important problem in modern theoretical physics. First, I will discuss the paradox in detail, and continue by disproving the paradox at the level of s -wave Hawking quanta. I will geometrically show that the paradox generically can not be posed in the causal patch of an infalling observer, suggesting that no physical observer ever witnesses a violation of the laws of physics. While this may not be enough to settle the debate, it requires a more

careful formulation of the paradox. In particular, it seems that the holographic versions that appeared later seem quite robust to the causal patch arguments I will make. They necessitate a detailed study of bulk reconstruction (in particular near or even behind the black hole horizon) and sub-AdS scale locality, a topic which I will address extensively later in this thesis.

A complete understanding of this paradox remains elusive until this very day, with various conflicting proposals dividing the community. Further research is needed, and I am a strong proponent that a better understanding will lead to fundamental insights in the properties of bulk locality and quantum gravity.

Precarious Precursors

The rest of this thesis will focus on bulk reconstruction and locality in AdS/CFT, and consists of chapters 3, 4 and 5. One of my favorite diagnostics are precursors: non-local operators in the CFT that are dual to a local bulk field in the appropriate limit. As the title suggests, precursors often have surprising and even paradoxical properties since bulk locality is a highly non-trivial property of AdS/CFT. That is why I find it interesting to study them, since it leads to a better understanding of AdS/CFT and, eventually, quantum gravity.

In chapter 3, I will discuss some of the puzzles associated to precursors. I will explain that different precursors can be dual to the same bulk field, but bulk locality implies that these different precursors can not be equal as true operators. I will introduce a simple holographic toy model to study the redundant way in which local bulk operators are encoded in the CFT. This redundancy can be tracked to an ambiguity in the smearing function on one hand, but equivalently can be understood using the language of quantum error correction on the other hand. Interestingly, I will show using the two aforementioned approaches that this ambiguity can be used to localize the information of the bulk field in a particular region of the CFT, e.g. a Rindler wedge, provided that bulk field is contained in the corresponding bulk wedge.

Next, in chapter 4, I will dive deeper in the ambiguity that many non-local operators in the CFT seem to be dual to the same local bulk operator. I will recast this problem in the language of BRST symmetry, and make a conjecture relating two precursors corresponding to the same bulk operator. As a check, I will re-derive an earlier expression of a precursor ambiguity that appeared in the literature, which exactly translates into the smearing function ambiguity used in the toy model of chapter 3. The results suggest that precursors are related to the underlying gauge symmetry of the field theory. Once this ambiguity between precursors is understood, I will show that this ambiguity contains enough freedom to localize the bulk

information in the CFT, order by order in $1/N$. This suggests that the procedure I explicitly undertook in chapter 3 to leading order in $1/N$, could be carried out order by order in $1/N$.

Thereafter, in chapter 5, I discuss the broader issue of bulk locality in $\text{AdS}_3/\text{CFT}_2$ in detail, and focus on the question which CFTs have local bulk duals. In order to make some progress on this rather grand question, I will explore the breakdown of sub-AdS scale locality in the same toy model that I introduced in chapter 3. While the model is not modular invariant, it has the right low- and high energy density of states to be dual to Einstein gravity coupled to matter in AdS_3 . Surprisingly, non-local effects seem to emerge at order $1/N$ due to the presence of an infinite tower of higher spins in the bulk. This leads me to formulate a conjecture about the spectrum of modular invariant CFT_2 's in order to have local bulk duals, however, an explicit proof is still lacking.

Finally, I will wrap up in chapter 6 by summarizing and concluding the material presented in this thesis. Doing so, I will try at the same time to provide an outlook of which problems remain, and what would constitute some interesting next steps of research.

The thesis will end with a few mandatory parts: the bibliography, a short outline of my contributions to the publications on which this thesis is based, and a popular-scientific summary in Dutch. I will finish by acknowledging everyone that made it possible to complete this thesis.

Before continuing, a final word on writing style is in order. Throughout the thesis, I will refrain from using the pronoun 'I', but rather use the pronoun 'we' when talking about ideas and the research performed during my studies. This is not only more conventional in the field when writing papers, but also indicates better the way in which my research was performed, which was always in close collaboration with my colleagues.

Contents

Preface & Overview	vii
1 Introduction	1
1.1 20 th Century Physics	1
1.2 Black Holes	3
1.2.1 From Einstein to Hawking and Bekenstein	3
1.2.2 Thermodynamic Stability of Black Holes	4
1.3 Holography & AdS/CFT	9
1.3.1 Towards AdS/CFT	10
1.3.2 Symmetries	15
1.3.3 Weak vs. Strong Coupling	16
1.3.4 Dictionary	17
1.3.5 HKLL Reconstruction	19
1.3.6 Bulk Locality	21
2 Firewalls	25
2.1 Introduction	25
2.2 Static Black Holes in Higher Dimensions	30
2.2.1 Black Holes in Asymptotically Minkowski Spacetime	30
2.2.2 Black Holes in de Sitter	31
2.2.3 Black holes in Anti-de Sitter	33
2.3 Black Holes in 3+1 Dimensions	35
2.4 Entropy and Information	42
3 Localizing Precursors in AdS/CFT	45
3.1 Introduction	45
3.2 Toy Model of the AdS/CFT Correspondence	49
3.3 Localizing the Precursor via Gauge Freedom	50
3.4 Localizing the Precursor via Entanglement	56
3.4.1 Mapping the Precursor into the Eastern Rindler Wedge	57
3.4.2 Mapping the Precursor in the ‘Wrong’ Rindler Wedge	59
3.A Relating Fourier Transforms of the Smearing Function	61

3.B	Evaluating the Smearing Function	64
3.C	Computing the Two-Point Function	64
4	QEC from BRST	69
4.1	Introduction	69
4.2	Proposal: Precursor Ambiguities from BRST	71
4.3	BRST Symmetry of N Real Scalars	72
4.3.1	The BRST Charge	72
4.3.2	Reduction to a Global $SO(N)$ Symmetry	74
4.4	Localizing Precursors in a Toy Model	75
4.4.1	The Model	75
4.4.2	Precursor Localization Perturbatively in $1/N$	76
4.4.3	N -Scaling	79
5	Sub-AdS Scale Locality in AdS_3/CFT_2	81
5.1	Introduction	81
5.2	Some Criteria for Bulk Locality	83
5.3	The Holographic Toy Model Revisited	87
5.3.1	The Model	87
5.3.2	Spectrum of Primaries	88
5.3.3	Density of States	89
5.4	Bulk Locality in the Toy Model	93
5.4.1	Locality and Reconstruction	93
5.4.2	3- and 4-point Correlation Functions	95
5.A	Holomorphic Primaries	97
6	Conclusions & Outlook	99
6.1	Burning Black Holes	99
6.2	Precairous Precursors	101
	Bibliography	107
	Contributions to Publications	117
	Samenvatting	119
	Acknowledgments	125

Introduction

1.1 20th Century Physics

The beginning of the last century gave birth to two cornerstones of modern physics. First of all, the foundations of quantum mechanics were established, describing physics on (sub)atomic scales. At the same time, Einstein developed his theory of special and general relativity, reformulating the laws of gravity which govern physics on much larger scales. The combination of quantum mechanics with the principles of special relativity ultimately gave rise to the development of quantum field theory. This new theoretical framework, together with the experimental advancement of particle accelerators, led to one of the greatest triumphs in modern physics: the Standard Model of particle physics. It provides us with a unified description of the fundamental particles and three out of four forces in nature: the strong, weak and electromagnetic interaction.

General relativity however, describing gravity – the fourth and weakest force in nature – remains a separate subject that has not yet been incorporated in our theory of fundamental interactions. Surprisingly maybe, that did yet not result in a mismatch between experiments and theoretical predictions. This is due to gravity's weakness compared to the other three fundamental interactions; neglecting gravity at the typical energies one produces nowadays with particle accelerators is an excellent approximation. As everyone who ever lifted a paperclip by holding a magnet over it knows: even though gravity is omnipresent, it can be overcome rather easily. Nonetheless in very high energy situations, such as black holes or early universe physics, the gravitational force can have a strength comparable to elementary particle interactions, and both frameworks need to be combined in a more general theory: a quantum theory incorporating gravity, that reduces to the Standard Model and general relativity in the appropriate limit.

The absence of gravity is not the only reason why the Standard Model is not the end of our work. First of all, the Standard Model contains at least 19 free param-

eters, which is not only aesthetically unpleasant, but also leaves a lot of questions unanswered. There are also more technical indications that one gets into trouble when applying gravity at high energies: Einstein's gravity is non-renormalizable, which means that at small scales it contains divergences that require an infinite number of counterterms. We typically interpret this as a breakdown of our current theory, and a signal that a more general theory will have to take over.

These shortcomings motivated people to look for a 'better' theory: a proper quantum theory that contains the Standard Model as well as gravity. Out of the many candidates that have been formulated, it seems that string theory emerged as one of the most promising and successful candidates. The fundamental constituents of string theory are not particles, but one dimensional objects localized in space-time: 'strings'. These strings can vibrate, and the various vibrational modes are interpreted as different particles. Originally, string theory was developed in the 60's as an attempt to explain asymptotic freedom present in the the strong interaction. However, the appearance of a massless spin-2 particle in the closed string spectrum made theorists realize that theory's true potential did not lie in a theory of hadrons, but in a quantum theory of gravity where the massless spin-2 particle could play the prominent role of the graviton.

From then on, string theory has gone through several developments. Particularly important milestones were the incorporation of supersymmetry in the theory, and the discovery of D -branes with their associated fluxes. This means that string theory is not only a theory of strings, but rather a more general theory of higher-dimensional extended objects. Together with supersymmetry, a way of relating bosonic and fermionic degrees of freedom with each other, it can be used to produce Standard Model-like features. That made theorists hopeful that one day, string theory should be capable of describing gravity together with all the elementary particles and their interactions.

Studying string theory turned out to be a vast but fruitful task, leading to a plethora of phenomena much richer than one could have imagined 50 years ago: it includes the counting of black hole microstates and connections with mathematics such as moonshine, as well as more phenomenologically oriented fields such as building cosmological models and looking for Standard Model-like solutions in one of string theory's 10^{500} vacua.

Last but not least, string theory is helping us understand the features a respectable theory of quantum gravity should have, in particular by providing us with one of the most remarkable and powerful dualities in theoretical physics: the AdS/CFT correspondence. This non-perturbative definition of quantum gravity in AdS in terms of a CFT, gives us a unique opportunity to study quantum gravity. Since it will play a central role in this thesis, it will be introduced in section 1.3.

1.2 Black Holes

1.2.1 From Einstein to Hawking and Bekenstein

Soon after Einstein published his theory of general relativity [7], Schwarzschild found the first nontrivial exact solution of Einstein's field equations [8]. It was only many years later until physicists started to understand its various mysterious properties. The spherically symmetric solution is singular at one point (the origin), but has an event horizon, where effectively time and space switch roles. Behind this event horizon, the gravitational force is so strong that not even light can escape, hence it was given the name *black hole*. It was later understood that these solutions are the natural end-products when very massive stars collapse under their own weight. Since black holes are in some sense nature's most dense objects, they are a perfect playground for theorists to study how the gravitational force works on various energy scales.

In the early 70s, many similarities between black hole physics and thermodynamics were discovered. In 1971 Hawking showed that the area of the event horizon can not decrease [9]. This remarkable result got known as the second law of black hole mechanics, due to its similarity with the second law of thermodynamics. Continuing in this spirit, in 1973 Bekenstein suggested in [10] that a black hole can be attributed an entropy, which is proportional to its event horizon. A year later, Hawking showed in [11] that black holes emit thermal radiation and he computed the temperature of a black hole that a far away observer would measure. Using thermodynamic relations, he confirmed Bekenstein's conjecture and fixed the constant of proportionality:

$$S_{\text{BH}} = \frac{A_{\text{BH}}}{4} \frac{k_B c^3}{\hbar G}. \quad (1.1)$$

Let us make a few comments on this important formula.

1. It contains Boltzmann's constant k_B (thermodynamics), the speed of light c (relativity), Planck's constant \hbar (quantum mechanics) and Newton's constant G (gravity)! All the fundamental domains in physics seem to be hiding behind what may well be the most beautiful formula in theoretical physics.
2. The entropy associated to the black hole horizon is based purely on thermodynamical arguments. Boltzmann taught us that entropy has an underlying statistical explanation; it counts the number of microstates. An obvious question arises: is it possible to count 'black hole microstates' and give a statistical interpretation to this formula? The answer seems affirmative. Strominger and Vafa famously derived in [12] the Bekenstein-Hawking entropy

relation (1.1) for a class of five-dimensional extremal black holes in string theory. In this case, the counting of microstates is a counting of geometric degrees of freedom, that tells us in how many ways one can wrap D-branes around the extra dimensions. An explanation on the level of microstates for black hole entropy, can be considered as one of the great successes of string theory, and is still the subject of ongoing research.

3. Another striking feature of this formula is its universality. It seems to apply to a whole zoo of black holes, irrespective if they are rotating or charged. Gibbons and Hawking showed in [13] that it even applies to cosmological horizons, such as the one in the static patch of de Sitter space. It is unclear whether there exists a statistical explanation for that entropy, since the cosmological horizon is observer dependent.
4. Finally, it is remarkable that the entropy of nature's most dense objects is not proportional to the volume, but rather scales like the area enclosing the volume. This will lead us to the holographic principle in section 1.3.

1.2.2 Thermodynamic Stability of Black Holes

The fact that black holes have thermodynamical properties is surprising, and strongly suggests an underlying microscopic description. In this section we will discuss the thermodynamics of various black hole solutions, and in particular show that some solutions are unstable with respect to evaporation. This will be important for chapter 2, where we will investigate a paradox that comes with black hole evaporation.

To keep things from being cluttered, the black hole metrics in D spacetime dimensions we will consider are all of the form

$$ds^2 = -f(r)dt^2 + \frac{dr^2}{f(r)} + r^2 d\Omega_{D-2}^2. \quad (1.2)$$

Black Holes in Flat Space

Consider a Schwarzschild black hole in flat space. The metric is of the form (1.2) with

$$f(r) = 1 - \left(\frac{r_h}{r}\right)^{D-3}. \quad (1.3)$$

While this metric looks singular at the horizon $r = r_h$, one can show that it is perfectly regular by changing to Kruskal coordinates, as the equivalence principle requires: a freely falling observer should not experience anything when he crosses the horizon of a large (such that tidal effects can be ignored) black hole.

A simple way of showing that an observer at fixed radius is accelerating and observes a black hole as thermally radiating, is by invoking the equivalence principle which implies that the near-horizon region of a black hole is well approximated by the Minkowski vacuum. Writing the Minkowski vacuum as a Rindler decomposition gives

$$|0\rangle = \bigotimes_{\omega,k} \sqrt{1 - e^{-2\pi\omega}} \sum_n e^{-\pi\omega n} |n\rangle_L \otimes |n\rangle_R. \quad (1.4)$$

Tracing over the $|n\rangle_L$ modes representing the interior of the black hole (which the hovering observer cannot access) leads to a thermal density matrix.

The temperature of the Schwarzschild solution (1.2) can be computed using a neat trick: send $t \rightarrow i\tau$ and do an expansion near the horizon $r = r_h$. A conical defect in the resulting Euclidean metric can be avoided by imposing the right periodicity in the new imaginary time variable $\tau \sim \tau + \beta$, which in turn gets interpreted as the inverse temperature via $\beta = T^{-1}$:

$$\begin{aligned} ds^2 = \rho^2 \left(d \left(\frac{f'(r_h)\tau}{2} \right) \right)^2 + d\rho^2 &\Rightarrow \frac{f'(r_h)}{2}\tau \sim \frac{f'(r_h)}{2}\tau + 2\pi \\ &\Leftrightarrow \tau \sim \tau + \frac{4\pi}{f'(r_h)} \end{aligned} \quad (1.5)$$

from which we can conclude that

$$T = \frac{1}{\beta} = \frac{f'(r_h)}{4\pi}. \quad (1.6)$$

For a Schwarzschild black hole in four dimensions we have that $r_h = 2GM$, which gives the following temperature an observer at rest at infinity would measure:

$$T = \frac{1}{8\pi GM}. \quad (1.7)$$

We define the heat capacity as

$$C = \frac{\partial E}{\partial T} = \frac{\partial M}{\partial T} \quad (1.8)$$

where we have used that $dM = dE$. In particular, notice that the temperature vs. mass curve of a Schwarzschild black hole (sketched in figure 1.1(a)) is monotonically decreasing. This means that the heat capacity is negative, therefore black holes in flat space are thermodynamically unstable: they become hotter and smaller until they are completely evaporated. For the curious reader: collapsing the earth will give a black hole that is roughly 2 centimeters in size, has a temperature of 0.02 Kelvin and a lifetime of $5 \cdot 10^{50}$ years!

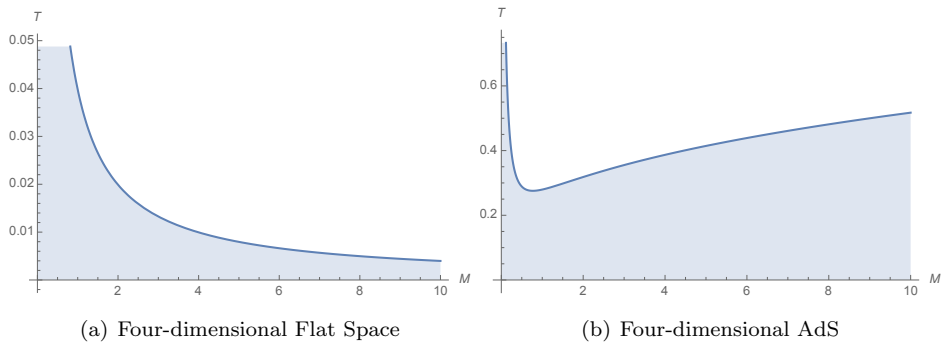


Figure 1.1: Plotting the black hole temperature vs. mass. G and L_{AdS} have been set to one.

Black Holes in AdS

Putting a black hole in Anti-de Sitter space (a vacuum solution of the Einstein equations with negative cosmological constant) leads to a much richer thermodynamic structure. This is because the negative cosmological constant effectively acts as a box. In particular, we will see that there is an important distinction between the microcanonical and canonical ensemble, as well as between AdS_3 and higher dimensional versions of AdS, since gravity in three dimensions is topological (meaning that there are no propagating degrees of freedom in the metric).

Three-Dimensional AdS

Even though gravity in AdS_3 is topological, there exists a black hole solution called the BTZ black hole [14]. When it does not have any electric charge or angular momentum, it is of the form (1.2) with

$$f(r) = \frac{r^2 - r_h^2}{L_{\text{AdS}}^2}. \quad (1.9)$$

We can immediately see that the BTZ black hole always has positive heat capacity, hence it is (locally) thermodynamically stable. For completeness, we note that there is a mass gap in AdS_3 , meaning that if we take $r_h \rightarrow 0$ we don't recover empty AdS, but a conical defect.

In what follows, we will focus on $D > 3$. The metric of a black hole in AdS_D with $D > 3$ is of the form (1.2) with

$$f(r) = 1 - \frac{GM}{r^{D-3}} + \frac{r^2}{L_{\text{AdS}}^2}. \quad (1.10)$$

The temperature vs mass curve can be found in figure 1.1(b).

Canonical Ensemble

For a given T (sufficiently large such that black solutions exist), we can see there are two black hole solutions $M_1 < M_2$. Only the heavier one has positive heat capacity and is stable. The smaller one will just keep absorbing energy until it becomes the heavier one. We can also see that there exists a critical temperature T_0 . Below that temperature black holes can not exist and the space is filled with thermal radiation. When we start increasing the temperature $T > T_0$, black hole solutions exist, however, they do not dominate the ensemble (i.e. have lower free energy than the state with thermal radiation) until the temperature reaches a critical value T_{HP} , called the Hawking-Page temperature [15]. When we increase the temperature even further, stable radiation solutions will cease to exist and always form a large black hole.

Microcanonical Ensemble

In the microcanonical ensemble we have to keep the total energy (mass) fixed. To see whether the black hole or radiation phase dominates, one has to maximize the entropy. A particular important result is that small black holes, even though they have negative heat capacity, can coexist peacefully with some thermal radiation in AdS, and hence are stable with respect to evaporation. On a more personal note: the question of how black holes with negative heat capacity can be stable, often led to confusion between me and my colleagues, and I vividly recall spending a few lunches debating this topic. So, let us set this straight once and for all.

We will demonstrate this surprising fact using a small black hole in AdS_{4+1} ¹ (up to $O(1)$ numerical factors), that is $r_h \ll L_{\text{AdS}}$. If this condition is obeyed, we have that

$$r_h^2 \approx GM. \tag{1.11}$$

Consider a system of a small black hole with energy $E_1 = M_1$, and some thermal gas with energy $E - E_1$, where we keep the total energy $E = M$ fixed. This gives

$$S_{\text{BH}} = \frac{A}{4G} \propto \frac{r_h^3}{G} = \frac{(GM_1)^{\frac{3}{2}}}{G} = \sqrt{GM_1^{\frac{3}{2}}}. \tag{1.12}$$

We know that the energy and entropy of a thermal photon gas in 5D goes like

$$E_{\text{gas}} \propto VT^5 \Rightarrow S_{\text{gas}} \propto VT^4 = V \left(\frac{E_{\text{gas}}}{V} \right)^{\frac{4}{5}} = (L_{\text{AdS}} E_{\text{gas}})^{\frac{4}{5}} \tag{1.13}$$

hence

$$S_{\text{total}} \approx \sqrt{GM_1^{\frac{3}{2}}} + L_{\text{AdS}}^{\frac{4}{5}} (M - M_1)^{\frac{4}{5}}. \tag{1.14}$$

¹With AdS/CFT in the back of mind, we could consider a small black hole in $\text{AdS}_5 \times S^5$ which initially is uniform over the S^5 . That is, however, unstable to localising on the the S^5 due to Gregory-Laflamme instability. In this case, one should consider a 10-dimensional small black hole. Nonetheless, the qualitative results that we obtain in this section remain true.

This entropy reaches a maximum for $M_1 \in [0, M]$, implying that there exist a stable equilibrium between the black hole and some thermal radiation. Extremizing the entropy yields

$$\frac{\partial S_{\text{total}}}{\partial M_1} = 0 \Rightarrow \frac{3}{2}\sqrt{GM_1} - \frac{4}{5}L^{\frac{4}{5}}(M - M_1)^{-\frac{1}{5}} = 0 \quad (1.15)$$

which we can rewrite as (neglecting $O(1)$ coefficients)

$$\frac{1}{T_{\text{BH}}} - \frac{1}{T_{\text{gas}}} = 0 \Rightarrow T_{\text{BH}} = T_{\text{gas}} \quad (1.16)$$

since the temperature of a 5D Schwarzschild black hole $\propto (GM)^{-\frac{1}{2}}$ and the temperature of our 5D photon gas is $\propto (E_{\text{gas}}/V)^{\frac{1}{5}}$. Notice that the black hole has negative heat capacity, as we expect from the flat space result. Since the entropy needs to obtain a maximum:

$$\frac{\partial^2 S}{\partial M_1^2} < 0 \Rightarrow -\frac{1}{T_{\text{BH}}^2}C_{\text{BH}}^{-1} + \frac{1}{T_{\text{gas}}^2}\frac{\partial T_{\text{gas}}}{\partial M_1} = -\frac{1}{T_{\text{BH}}^2}C_{\text{BH}}^{-1} - \frac{1}{T_{\text{gas}}^2}C_{\text{gas}}^{-1} < 0 \quad (1.17)$$

where we've defined the heat capacity

$$C \equiv \frac{\partial E}{\partial T}. \quad (1.18)$$

Note the sign change in front of the heat capacity of the gas, because it is defined by differentiating wrt to $M - M_1$ instead of M_1 . At equilibrium we have $T_{\text{BH}} = T_{\text{gas}}$, so the equation reduces to

$$-C_{\text{BH}}^{-1} - C_{\text{gas}}^{-1} < 0. \quad (1.19)$$

Since the black hole heat capacity is negative, we have at equilibrium

$$|C_{\text{gas}}| < |C_{\text{BH}}|. \quad (1.20)$$

Imagine the small 5D black hole in AdS in equilibrium with some thermal gas at temperature T_{eq} , with $C_{\text{BH}} < 0$ and $C_{\text{gas}} > 0$ while $|C_{\text{BH}}| > |C_{\text{gas}}|$. Consider a fluctuation where the black hole loses some mass and radiates a small amount of energy $\delta E > 0$ in the photon gas. Due to the condition on the heat capacities, we see that $T_{\text{eq}} < T_{\text{BH}} < T_{\text{gas}}$, that is, both the black hole and the gas increases its temperature (energy is of course always conserved, since the increase in the energy of the gas gets compensated by the decrease in energy of the black hole), but the temperature increase of the gas is larger then the one in the black hole. Because of this difference in temperature, some energy δE will flow back from the gas into the black hole, lowering both temperatures back to the equilibrium temperature T_{eq} . The case for a fluctuation where both the black hole and gas cool down, is completely similar.

Notice that in the case the gas is coupled to an infinite heat bath at temperature T , as is the case in the canonical ensemble, black holes with a negative heat capacity can never be stable. One can see this by considering a black hole at temperature T . When the black hole radiates some energy δE in the gas, it will increase its temperature with respect to the gas: $T_{\text{BH}} > T_{\text{gas}}$. Because the black hole temperature is higher, it wants to deposit more energy in the gas, making it hotter and hotter, rendering the solution unstable.

This concludes the brief introduction on black holes and their thermodynamic stabilities. In chapter 2 we will revisit evaporating black holes and the information paradox, and show that the equivalence principle, unitarity and locality seem to be inconsistent for an infalling observer. Before doing that, we will try to provide a pedagogical introduction to some aspects of holography and the AdS/CFT correspondence, building on a way it was presented by the author in [16]. In particular, we will elaborate on things like bulk reconstruction and locality in AdS/CFT, as it will play a prominent role in chapters 3, 4 and 5.

1.3 Holography & AdS/CFT

Our starting point this time will again be the remarkable and, at the same time, the very first formula in this thesis (1.1):

$$S_{\text{BH}} = \frac{A_{\text{BH}}}{4G} \tag{1.21}$$

which tells us that the Bekenstein-Hawking entropy of a black hole is proportional to the area of its event horizon. Note that we've set $c = k_B = \hbar = 1$ and will continue to do so.

It was Bekenstein himself who concluded from this that the maximal amount of entropy contained in a certain volume of space is proportional to the *area* that encloses the volume. To see this, consider a region V that has more entropy than a black hole of the same size, but has less energy. By adding some matter, we could collapse it to a black hole and decrease its entropy, thereby violating the second law. It was 't Hooft that took this idea a step further in [17], and conjectured that any physical theory in a volume V can be described by a set of degrees of freedom (1 per Planck area) residing on the surface enclosing V . This idea got known as the 'holographic principle', and was further developed by Susskind in [18], who argued that string theory should obey the holographic principle as well.

1.3.1 Towards AdS/CFT

Over the years various developments culminated in 1997, where Maldacena made an extraordinary conjecture [19]: he claimed that a particular string theory is dual (i.e. equivalent) to a gauge theory living in one dimension less. More precisely,

$$\begin{aligned} \text{Type IIB string theory on AdS}_5 \otimes S^5 \\ \Leftrightarrow \\ d = 4, \mathcal{N} = 4, \text{SU}(N) \text{ super-Yang-Mills theory.} \end{aligned} \tag{1.22}$$

This is a particular realization of the holographic principle, since the gravitational theory is completely captured by a field theory living on its boundary. It became famous under the name AdS/CFT correspondence. AdS stands for Anti-de Sitter space, a vacuum solution of Einstein's field equations with negative cosmological constant. CFT stands for conformal field theory: a (quantum) field theory where the usual Poincaré symmetry group has been extended to include scale transformations and inversion (the conformal group). It is a very nontrivial statement: it relates a string theory – which contains gravity – and a gauge theory – which does not contain gravity – living in different dimensions and spaces.

String Theory and the $N \rightarrow \infty$ Limit of Gauge Theory

We will start by arguing why string theory could be dual to a gauge theory. This kind of argument was first given by 't Hooft in [20], but in a rather different context. The problem at interest was the strong interaction. This is described by a SU(3) Yang-Mills theory, and while it has a nice perturbative description at high energies, it gets strongly coupled at low energies (i.e. it is asymptotically free). However, it appeared that approximating the strong interaction by taking the large N limit (doing 'planar QCD'), we can make reasonably accurate predictions. 't Hooft's hope was that, while the gauge theory description is useful at high energies, he could construct and use the string theory dual (which is weakly coupled in the $N \rightarrow \infty$ limit) to make predictions at low energies.

To start, consider a non-Abelian SU(N) gauge theory with coupling constant g_{YM} . In the limit where N becomes very large, 't Hooft showed that it is useful to introduce an effective coupling constant $\lambda \equiv g_{\text{YM}}^2 N$, from now on called the '*t Hooft coupling*'. In a gauge theory, typical problems at hand are computing the partition function and correlation functions. In the limit where g_{YM} is sufficiently small, we can write down a perturbative expansion for these correlators in terms of Feynman graphs. It is possible to supply the Feynman graphs with an additional structure: the double line or fat graph notation [21]. Expanding the correlators using Wick's theorem yields various contractions, which tell us how to connect the

fat graphs. This way, we get connected diagrams and can associate a genus to each graph, as is depicted in figure 1.2. For a given genus g , the graphs can be organized as an expansion in the 't Hooft coupling λ . Schematically:

$$\log \mathcal{Z} = \sum_{\text{genus } g} N^{2-2g} \sum_{i=1}^{\infty} \lambda^i f_i(\dots) \quad (1.23)$$

It becomes clear why the large N limit is sometimes called the planar limit: graphs organize themselves in groups depending on the topology. The higher the genus of the graph, the more it becomes suppressed. Large N limits can thereby greatly simplify our life, since we only have to take the planar diagrams into account. Furthermore, if λ is sufficiently small, we can describe the gauge theory perturbatively in λ .

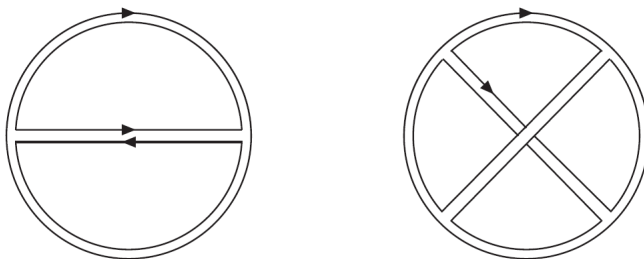


Figure 1.2: A planar diagram (genus 0, i.e. it can be drawn on a sphere without crossing any lines) on the left and a non-planar diagram (genus 1, i.e. it can be drawn on a torus without crossing any lines) on the right. The right diagram will be suppressed relative to the planar one by a factor $1/N^2$.

To see what this has to do with string theory, consider the scattering of four closed strings. String theory allows us to calculate the S-matrix of this process perturbatively. This has to be done by summing over all possible world sheet topologies, as is represented in figure 1.3. Schematically:

$$\text{S-matrix} = \sum_{\text{genus } g} g_s^{2g-2} F_g(\alpha')[\dots] \quad (1.24)$$

where g_s is the string coupling and $\alpha' = l_s^2$.

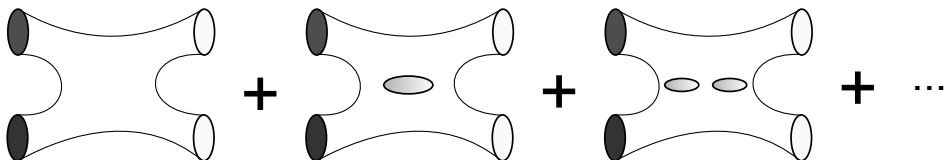


Figure 1.3: Sum over topologies in the scattering of four closed strings.

The similarities between the two perturbative expansions are striking. In particular, we would suspect $g_s \propto \frac{1}{N}$: taking the large N (planar) limit corresponds with a weakly coupled string theory, i.e. we only take the worldsheets without holes into account.

Maldacena’s Decoupling Argument

We will now present a simple argument that should lead us to the AdS/CFT correspondence (1.3.1).

Consider a stack of N $D3$ -branes. We can regard them as hyperplanes in flat space, where the endpoints of open strings can propagate on. We call this the ‘open string’ description. On the other hand, we can also regard them as (black) branes emitting closed strings, the ‘closed string’ description. In particular, they will emit gravitons since they can be found in the closed string spectrum, which will deform the background. Both viewpoints should be equivalent: they are a different description of the same system. This equivalence is also known as open-closed duality in string theory, and is illustrated in figure 1.4.

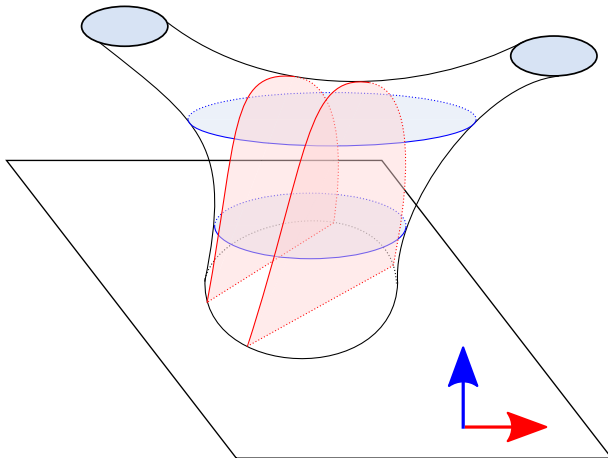


Figure 1.4: Cartoon picture of open-closed duality. We can view the brane as an hypersurface where the endpoints of open strings can end and propagate on (red). On the other hand, we can cut the string worldsheet differently, and regard the branes as if they were emitting closed strings (blue). Time directions are denoted by the arrows.

First, consider the open string description. The endpoints of open strings realize a (supersymmetric) $U(1)$ gauge theory on the brane’s worldvolume. Since we are considering a stack of N $D3$ -branes, the endpoints of the string can start and end on N different branes and in total there are N^2 possibilities. The lowest excitation modes are massless when the branes are coincident, and via the Chan-

Paton mechanism one can see that they carry the appropriate charges to enhance the $U(1)^N$ symmetry to a (supersymmetric) $SU(N)$ symmetry.

In this open string description, the action describing the brane's dynamics looks schematically as follows

$$S = S_{\text{brane}} + S_{\text{interaction}} + S_{\text{bulk}}. \quad (1.25)$$

- S_{brane} contains the $d = 4$, $\mathcal{N} = 4$ super-Yang-Mills (dimensional reduction of $d = 10$, $\mathcal{N} = 1$ SYM) in lowest order, plus stringy corrections which are $O(\alpha')$ and higher.
- $S_{\text{interaction}}$ couples the brane and the bulk, and does only contains terms which are $O(\alpha')$ and higher.
- S_{bulk} contains type IIB supergravity in lowest order, plus stringy corrections which are $O(\alpha')$ and higher.

We can now take a low energy limit $\alpha' \rightarrow 0$ to obtain

- $S_{\text{brane}} \rightarrow d = 4$, $\mathcal{N} = 4$ $SU(N)$ super-Yang-Mills
- $S_{\text{interaction}} \rightarrow 0$
- $S_{\text{bulk}} \rightarrow$ type IIB supergravity

and we see that the dynamics on the brane and in the bulk decouple.

Let us take another, but equivalent, viewpoint: the closed string (gravitational) description. We regard the stack of branes as massive objects, deforming the geometry. The following metric is a solution of the type IIB supergravity equations of motion, and describes a stack of N coincident $D3$ -branes:

$$ds^2 = \frac{1}{\sqrt{H(r)}} \eta_{\mu\nu} dx^\mu dx^\nu + \sqrt{H(r)} (dr^2 + r^2 d\Omega_5^2) \quad (1.26)$$

$$H(r) = 1 + \frac{L_{\text{AdS}}^4}{r^4} \quad L_{\text{AdS}}^4 = 4\pi\alpha'^2 g_s N \quad r = \sqrt{y^a y^a}. \quad (1.27)$$

Here $\mu, \nu = 0, \dots, 3$, $a = 4, \dots, 9$ and r measures the distance transverse to the branes. Note that $H(r)$ is an harmonic function of the coordinates transverse to the brane. We can take two interesting limits:

- $r \rightarrow \infty$: $ds^2 \rightarrow 10D$ flat Minkowski space
- $r \rightarrow 0$: $ds^2 \rightarrow \frac{r^2}{L_{\text{AdS}}^2} \eta_{\mu\nu} dx^\mu dx^\nu + \frac{L_{\text{AdS}}^2 dr^2}{r^2} + L_{\text{AdS}}^2 d\Omega_5^2 = \text{AdS}_5 \otimes S^5$

Now take the low energy limit for an observer at $r = \infty$. There are two types of low energy excitations, as illustrated in figure 1.5. First of all, there are the massless modes surrounding the observer: this is regular type IIB supergravity. Nearby the stack of branes however, *any* excitation will be low energy with respect to our far away observer since this excitation has to climb out of the gravitational well and gets redshifted. This redshift will be huge for excitations very close to the brane, since we can read off from the metric: $\delta E_{\text{proper}} = \frac{L_{\text{AdS}}}{r} \delta E_{\infty}$. Thereby, the *full* string theory (and not only the massless modes) will be low energy with respect to this observer and it decouples from the free type IIB supergravity which surrounds the observer in $D = 10$ flat space.

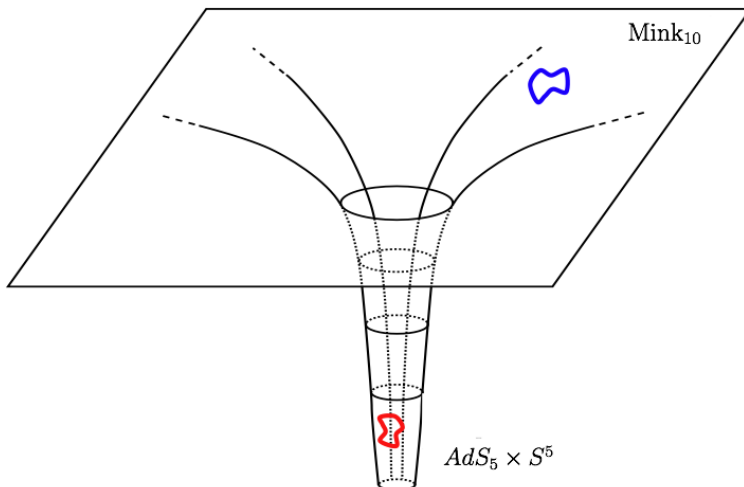


Figure 1.5: Geometry of a stack of D3-branes which interpolates between $AdS_5 \otimes S^5$ near the branes, and flat space far away from the branes.

Let us summarize what we have found. Taking the low energy limit in the open string (‘gauge theory’) description resulted in a $d = 4$, $\mathcal{N} = 4$ $SU(N)$ SYM near the branes, decoupled from $D = 10$ type IIB SUGRA at infinity. On the other hand, taking the low energy limit in the closed string (‘gravitation’) description, resulted in full type IIB string theory on $AdS_5 \otimes S^5$ near the branes, decoupled from $D = 10$ type II SUGRA at infinity. Both theories at $r = 0$ and $r = \infty$ decouple, but the open and closed string descriptions should be equivalent.

This finally motivates the AdS/CFT correspondence (1.3.1): Type IIB string theory on an $AdS_5 \otimes S^5$ background, should correspond with $d = 4$, $\mathcal{N} = 4$ $SU(N)$ super-Yang-Mills theory.

1.3.2 Symmetries

Claiming that two theories are equivalent with each other, requires at least a complete match of the symmetries. On the gravitational side, we can embed AdS₅ in 6-dimensional pseudo-Euclidean space with metric $\text{diag}(- + + + + -)$ as the hyperboloid

$$-x_0^2 + x_1^2 + x_2^2 + x_3^2 + x_4^2 - x_5^2 = -L_{\text{AdS}}^2. \quad (1.28)$$

The isometry group of AdS₅ is therefore SO(4, 2). The isometry group of S⁵ is given by SO(6).

Let us try to see how these symmetries manifest themselves on the gauge theory side. Since $d = 4$, $\mathcal{N} = 4$ SYM can be obtained by dimensional reduction of $d = 10$, $\mathcal{N} = 1$ SYM, we get the following Lagrangian [22]:

$$\begin{aligned} \mathcal{L} = \text{Tr} \{ & \frac{1}{2} F_{\mu\nu} F^{\mu\nu} + 2\bar{\lambda}^\alpha \gamma^\mu D_\mu P_L \lambda_\alpha + D_\mu X^i D^\mu X^i \\ & + g_{\text{YM}} ((C^\alpha_\beta)^i \bar{\lambda}_\alpha P_L [X^i, \lambda^\beta] + \text{h.c.}) + \frac{g_{\text{YM}}^2}{2} \sum_{i,j} [X^i, X^j]^2 \} \end{aligned} \quad (1.29)$$

containing the gauge potential A_μ , four chiral fermion fields $P_L \chi^\alpha$, and six scalars X^i (originating from dimensional reduction of the $d = 10$ vector). The C matrices are gamma matrices for SO(6). The first symmetry of the theory is manifest: rotating the six scalars among each other. It is a SO(6) symmetry and corresponds with the R-symmetry of the theory.

The other symmetry of the theory is a conformal symmetry. This happens because the gauge theory is not only invariant under Poincaré transformations, but also under inversion $x_\mu \rightarrow x'_\mu = x_\mu/x^2$ and scale transformations $x_\mu \rightarrow x'_\mu = \lambda x_\mu$. All transformations combine in what is known as the conformal group, which is given by SO(4, 2) in four dimensions. Therefore, we have checked that the (bosonic) symmetries of the theories match.

However, $d = 4$, $\mathcal{N} = 4$ SYM has another remarkable property: it remains conformal at quantum level. This is rather special, since quantizing a field theory typically leads to divergences, which one has to solve by introducing a cutoff in the theory and renormalizing it. But introducing such a (energy) scale μ in the theory, manifestly breaks conformal invariance. Renormalization typically leads to a ‘running’ coupling constant g_{YM} when varying the energy scale μ . This running is captured in the beta function of the theory, which satisfies the renormalization group equation:

$$\mu \frac{\partial g_{\text{YM}}}{\partial \mu} = \beta(g_{\text{YM}}). \quad (1.30)$$

It has been shown that the beta function of $d = 4$, $\mathcal{N} = 4$ SYM vanishes at all loops, and the theory has a superconformal $SU(2, 2|4)$ symmetry at quantum level. A more detailed analysis of the superstring theory in $AdS_5 \otimes S^5$ shows that the fermionic symmetries also match. We conclude that there is a complete match of symmetries. Furthermore, one can also show there is a match between the spectrum of IIB fields on $AdS_5 \otimes S^5$, and operators in the dual field theory [23].

1.3.3 Weak vs. Strong Coupling

The brane description of the gauge theory relates the string coupling constant g_s and gauge theory coupling g_{YM} with each other. Summarizing the various parameters of interest:

Gauge Theory	String Theory
g_{YM}^2	$g_s = g_{YM}^2/4\pi$
$\lambda = g_{YM}^2 N$	$\lambda = L_{AdS}^4/\alpha'^2 = L_{AdS}^4/l_s^4$

(1.31)

Most of the time we work in the useful 't Hooft limit where $N \rightarrow \infty$ and $g_{YM}^2 \rightarrow 0$ while λ is kept fixed. This corresponds with planar $\mathcal{N} = 4$ SYM. Or equivalently on the string theory side: $g_s \rightarrow 0$ while λ is kept fixed which corresponds with 'free' string theory.

We can now distinguish two interesting regimes. The first one is taking $\lambda \rightarrow 0$. This means that the gauge theory simplifies and becomes perturbative planar SYM, but on the string theory side we see that $L_{AdS} \ll l_s$: the AdS length scale becomes small compared with the string length scale, and the supergravity approximation of string theory breaks down. This is the tensionless limit of string theory, where all the stringy modes become important and there is no classical geometric picture of the bulk anymore. On the other hand, we can take $\lambda \rightarrow \infty$. This means that $L_{AdS} \gg l_s$: we are taking the point limit of strings. In this limit, the geometry is classical and we can safely use the supergravity approximation to string theory. Since g_s was assumed to be very small, quantum effects are suppressed and we can do classical (tree-like) supergravity. The gauge theory side however, gets strongly coupled.

This shows that the AdS/CFT correspondence can be very powerful: when it becomes 'difficult' to do a calculation at one side of the duality, we can go to the other side where the problem becomes 'easy'. For example, it allows us to make predictions about strongly coupled SYM by doing supergravity, and vice versa. The downside is that it becomes very hard to prove these statements, since one should do the calculation on both sides of the duality and see whether they agree.

1.3.4 Dictionary

We showed that, depending on the problem, it is beneficial to work on a particular ‘side’ of the duality. To do so, we want to be able to translate string theory problems into gauge theory ones, and vice versa. This can be done, if we have a precise correspondence between the observables at our disposition: a dictionary. Two dictionaries exist: the ‘differentiate’ dictionary, initiated by Witten, Gubser, Klebanov and Polyakov in [24, 25], and the ‘extrapolate’ dictionary, first used in [26], and stated explicitly by Banks, Horowitz, Douglas and Martinec in [27].

There is a 1:1 correspondence between fields in the bulk and operators in the CFT. As an example, one can derive a relation between the mass m of a scalar field Φ in the bulk, and the scaling dimension Δ of the corresponding dual operator in the CFT. In AdS_{d+1} we have that

$$\Delta_{\pm} = \frac{1}{2} \left(d \pm \sqrt{d^2 + 4m^2 L_{\text{AdS}}^2} \right). \quad (1.32)$$

Usually only the solution $\Delta = \Delta_+$ is admissible, but for masses in the Breitenlohner-Freedman window

$$\frac{-d^2}{4} < m^2 < \frac{-d^2}{4} + 1 \quad (1.33)$$

both Δ_- and Δ_+ are allowed [28].

Unitarity of the CFT requires Δ to be real and positive, so it is interesting to note that this implies that negative masses are allowed as long as

$$m^2 \geq \frac{-d^2}{4L_{\text{AdS}}^2}. \quad (1.34)$$

Intriguingly, this result was already known ten years before the AdS/CFT correspondence, by analyzing particle states in AdS [29]. Particles are always classified in irreducible representations of the symmetry group of the theory. As was mentioned before, for the case of AdS_5 this symmetry group is given by $\text{SO}(4, 2)$, which has maximal compact subgroup $\text{SO}(4) \otimes \text{SO}(2)$. Δ can be viewed as the lowest eigenvalue of the $\text{SO}(2)$ generator, and demanding unitary representations of the AdS group leads exactly to the same stability bound.

Differentiate Dictionary

Consider Poincaré AdS_5 :

$$ds^2 = \frac{L_{\text{AdS}}^2}{z^2} (dz^2 + \eta_{\mu\nu} dx^\mu dx^\nu). \quad (1.35)$$

The boundary of this space is at $z \rightarrow 0$ and is given by four dimensional Minkowski space, up to a conformal factor. We can now write

$$\Phi_0(\vec{x}) = \Phi(\vec{x}, z) \Big|_{z=0}. \quad (1.36)$$

We interpret the boundary value Φ_0 as a source for the CFT operator \mathcal{O} , that has the same symmetry representations as the bulk field Φ . Consider the generating function $\mathcal{Z}_{\mathcal{O}}[\Phi_0]$ for correlation functions of \mathcal{O} , which can be obtained by adding the term

$$\int d^4x \Phi_0(\vec{x}) \mathcal{O}(\vec{x}) \quad (1.37)$$

to the $\mathcal{N} = 4$ Lagrangian. We have that

$$\langle \mathcal{O}(x_1) \cdots \mathcal{O}(x_n) \rangle = \frac{\delta^n}{\delta \Phi_0(x_1) \cdots \delta \Phi_0(x_n)} \mathcal{Z}_{\mathcal{O}}[\Phi_0] \Big|_{\Phi_0=0}. \quad (1.38)$$

Witten argued that

$$\mathcal{Z}_{\mathcal{O}}[\Phi_0]_{\text{CFT}} = \langle e^{\int d^4x \Phi_0(\vec{x}) \mathcal{O}(\vec{x})} \rangle_{\text{CFT}} = \mathcal{Z}_{\text{string}}[\Phi(\vec{x}, z)] \Big|_{\Phi(0, \vec{x}) = \Phi_0}. \quad (1.39)$$

The right hand side is the string (or, in the appropriate limit, supergravity) partition function with the boundary condition that the bulk scalar takes the value Φ_0 on the AdS boundary. The left hand side is the generating functional for correlators of the operator \mathcal{O} in the CFT.

Extrapolate Dictionary

The second dictionary, as the name suggests, consists of taking bulk fields and extrapolating them to the boundary.

$$\lim_{z \rightarrow 0} z^{-\Delta} \Phi(x, z) = \mathcal{O}(x). \quad (1.40)$$

In this limit they vanish, but extracting the leading behavior gives the dual operator. In this sense, the extrapolate dictionary relates a field close to the boundary to a local CFT operator. We can use this to compute bulk correlators and pull them to the boundary. Extracting the leading behavior gives the correlators of the dual operators:

$$\langle \mathcal{O}(x_1) \cdots \mathcal{O}(x_n) \rangle_{\text{CFT}} = \lim_{z \rightarrow 0} z^{-n\Delta} \langle \Phi(x_1, z) \cdots \Phi(x_n, z) \rangle_{\text{bulk}}. \quad (1.41)$$

In this dictionary, the crucial step is to extrapolate bulk fields to the boundary and write them as (smeared) CFT operators. We will explore this in detail in the next section 1.3.5.

Both dictionaries were proved to be equivalent by Harlow and Stanford in [30]. They showed that

$$\frac{\delta}{\delta\beta(x_1)} \cdots \frac{\delta}{\delta\beta(x_n)} \mathcal{Z}_{\text{bulk}}[\beta] \Big|_{\beta=0} \sim \lim_{z \rightarrow 0} z^{-n\Delta} \langle \Phi(x_1, z) \cdots \Phi(x_n, z) \rangle_{\text{bulk}} \quad (1.42)$$

where β is the coefficient of the non-normalizable mode (i.e. putting the boundary condition $\Phi \sim z^{d-\Delta} \beta$ when $z \rightarrow 0$).

1.3.5 HKLL Reconstruction

One of the central problems in AdS/CFT is to reconstruct bulk physics from boundary data. In the large N limit, we expect the bulk to be classical and composed of local bulk fields on a fixed, curved background. An important series of works came from the authors Hamilton, Kabat, Lifschytz and Lowe, and is known as the HKLL prescription [31–41].

We saw in (1.40) that a bulk field Φ , in the limit that it goes to the boundary, is dual to a local CFT operator \mathcal{O} . A natural question to ask is how we can relate a local bulk field which is a finite distance in the bulk to a CFT operator. At leading order in $1/N$, HKLL proposed that

$$\Phi(X) = \int d^d x K(X|x) \mathcal{O}(x) \quad (1.43)$$

for an appropriate smearing function $K(X|x)$. Note that with capital X we denote a point in the AdS_{d+1} , while with a small x we denote a point on the boundary CFT_d . One can see that if the smearing function K satisfies a free Klein-Gordon equation, so will the bulk field Φ :

$$(\square - m^2)\Phi = 0 \Leftrightarrow (\square - m^2)K(X|x) = 0 \quad (1.44)$$

where \square acts on the bulk coordinates X . In the case where K exists and can be computed, its support on the boundary gives a measure for what region in the CFT contains the information of the local bulk field $\Phi(X)$. One way of computing the smearing function is by expanding the bulk field Φ in orthogonal solutions of the Klein-Gordon equation Φ_k [42]:

$$\Phi(X) = \int dk a_k \Phi_k(X) + \text{h.c.} \quad (1.45)$$

Now take the bulk point X to the boundary and define $\phi_k \equiv z^{-\Delta} \Phi_k$ which gives

$$\mathcal{O}(x) = \int dk a_k \phi_k(x) + \text{h.c.} \quad (1.46)$$

If the ϕ_k are orthogonal, we can invert this equation and write

$$a_k = \int dx \mathcal{O}(x) \phi_k^*(x). \quad (1.47)$$

Plugging back in yields

$$\Phi(X) = \int dk \left(\int dx \mathcal{O}(x) \phi_k^*(x) \right) \Phi_k(X) + \text{h.c.} \quad (1.48)$$

Provided we can interchange the integrals, this finally gives

$$\Phi(X) = \int dx K(X|x) \mathcal{O}(x) \quad (1.49)$$

where

$$K(X|x) = \int dk \Phi_k(X) \phi_k^*(x) + \text{h.c.} \quad (1.50)$$

The smearing function K can be computed this way for the case of Poincaré or global AdS. Interestingly, the smearing function K is not unique, a property which we will explore in chapter 3. In the case when there is an horizon present (such as Rindler AdS or black hole solution), the integral of momenta does not converge and there is no (position space representation of the) smearing function.

At order $1/N$, the bulk field Φ will satisfy an interacting wave equation that can be perturbatively solved. Expand the bulk field as $\Phi = \Phi^{(0)} + \frac{1}{N} \Phi^{(1)}$. The leading part will satisfy the free wave equation and can be reconstructed using the techniques described above. At order $\frac{1}{N}$, the bulk field satisfies an interacting wave equation $(\square - m^2)\Phi^{(1)} = (\Phi^{(0)})^2$ which can be solved by putting

$$\Phi^{(1)}(X) = \int d^{d+1} X' G(X|X') \Phi^{(0)}(X') \Phi^{(0)}(X') \quad (1.51)$$

where G is a bulk-to-bulk propagator (Green's function) that satisfies

$$(\square - m^2)G(X|X') = \frac{1}{\sqrt{|g|}} \delta^{d+1}(X - X'). \quad (1.52)$$

We can in principle reconstruct the interacting bulk field order by order in $1/N$ in the CFT. The first order correction to the HKLL formula (1.43) is now given by:

$$\Phi^{(1)}(X) = \int d^d x \int d^d x' \tilde{K}(X|x, x') \mathcal{O}(x) \mathcal{O}(x') \quad (1.53)$$

where

$$\tilde{K}(X|x, x') \equiv \int d^{d+1} X' \sqrt{|g|} G(X|X') K(X'|x) K(X'|x'). \quad (1.54)$$

1.3.6 Bulk Locality

One of the core aspects of holography is the emergence of spacetime and the reconstruction of (local) bulk physics from CFT data. As we will see in chapter 2, locality plays an important role in the firewall paradox, and its status in quantum gravity remains unclear. Since the AdS/CFT correspondence provides us with a definition of quantum gravity, we can hope that this duality will shed some light on the possible breakdown of locality. However, bulk locality and reconstruction, while crucial in AdS/CFT, still remains poorly understood after more than 15 years.

When doing QFT on a fixed background (no dynamical gravity), by locality we usually mean that operators which are spacelike separated commute:

$$[\mathcal{O}(x), \mathcal{O}(y)] = 0 \quad \forall (x - y)^2 > 0. \quad (1.55)$$

When we add gravity to the mix, i.e. we add diffeomorphisms to our ‘ordinary’ gauge symmetries, an object such as $\Phi(X)$ is not gauge invariant anymore, and for example would need to be dressed by a gravitational Wilson line in order to make it gauge invariant. This is usually summed up in the common lore that there are no gauge invariant local observables in a theory of quantum gravity. This is the case for string theory, that will be manifestly non-local on length scales comparable to the string length l_s . However, based on the expectations from our everyday real world which include gravity and is perceived to be local, we would want a good candidate of quantum gravity to be local in the right regime. Since the AdS/CFT correspondence provides us with an unique window on quantum gravity, we are interested in studying questions related to how local bulk physics emerges from the CFT, or which CFTs will have local bulk duals.

A particularly mysterious property of AdS/CFT is that of sub-AdS scale locality. Consider two bulk wavepackets that are separated a distance l in the radial (i.e. the emergent) direction denoted by the coordinate r . From a local bulk point of view, these excitation should not interact. While both of them have the same position in the CFT, they will have different energies since

$$E \sim \frac{r}{L_{\text{AdS}}^2}. \quad (1.56)$$

It should be clear that if they are separated sufficiently far from each other in the bulk, their energies will differ a lot, and they will not interact with each other by locality in the RG -flow. However, this heuristic argument will start to break down when

$$\frac{\delta E}{E} = \frac{\delta r}{r} = O(1). \quad (1.57)$$

If we use that the AdS metric in the radial direction looks like $ds^2 = L_{\text{AdS}}^2 dr^2/r^2$, we see that bulk locality is not guaranteed anymore by having different energies when the two wave packets are separated a distance $l \sim L_{\text{AdS}}$. This means that bulk locality on scales much larger than L_{AdS} is a rather trivial property, but on scales smaller than L_{AdS} , it becomes very nontrivial. However, we can make the AdS radius as large as we want, in particular much larger than the string length l_s . But we would want a realistic theory of quantum gravity to be local at scales much smaller than L_{AdS} , up to l_s for example.

In [43], the authors argued for a criterion that a CFT needs to satisfy in order to be local below sub-AdS length scales. Consider a string excitation in AdS_{4+1} , which will have a mass on the order of $1/l_s$. The conformal dimension of the dual operator satisfies

$$\Delta(\Delta - 4) = m^2 L_{\text{AdS}}^2 \sim \left(\frac{L_{\text{AdS}}}{l_s} \right)^2 = \sqrt{\lambda} \quad (1.58)$$

where λ is the 't Hooft coupling. To have local physics below the AdS scale we want $\lambda \gg 1$, and this means that all operators dual to stringy excitations will have parametrically large dimensions. Based on these observations, the authors in [43] motivated the conjecture that any CFT which has a large N expansion², and in which all single trace operators of spin > 2 have large Δ , will have a bulk dual with sub-AdS scale locality. This criterion is often summarized as the requirement of having a sparse spectrum. We will elaborate further on criteria for bulk locality in chapter 5.

In the same paper, an intuitive diagnostic for bulk locality was proposed. Consider a four-point function in the (Lorentzian) CFT, where the four insertions are placed in such a way that they are not on each other's boundary lightcones, but the four bulk lightcones intersect in a point (see figure 1.6). In this setup, we can think of it as a $2 \rightarrow 2$ scattering process in the bulk. In a local bulk theory, the four-point function in the CFT will have particular singularities. From the CFT point of view this is a rather mysterious property: changing one of the insertions slightly will cause a dramatic fall-off of the four-point function. On the other hand, from the bulk point of view this makes complete sense: the singularity is caused by the interaction of the two scattering particles. Two short comments are in order. First of all, the two- and three-point functions in a CFT are fixed by conformal invariance, while the four-point function contains dynamical information (it will depend on the OPE coefficients). It makes good sense that a diagnostic for bulk locality should depend on this information.

²In order for a CFT to have a holographic dual, it needs enough degrees of freedom to make up the holographic dimension, so large N (central charge) is always an assumption.

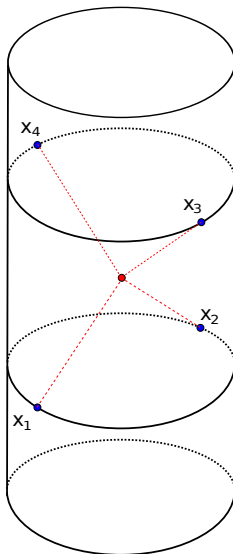


Figure 1.6: Four CFT insertions that are not lightlike separated in the CFT, but whose bulk lightcones intersect in a point.

Secondly, if we would take weakly coupled $\mathcal{N} = 4$ SYM, there would be no such singularity (a weaker singularity will be present), rather, the real singularity will emerge in the strong coupling limit $\lambda \rightarrow \infty$. That makes sense, since it is only in this regime that we would expect the bulk theory to be local.

This concludes the introduction to holography and AdS/CFT. We will pick it back up in chapters 3, 4 and 5, where we will study issues related to bulk reconstruction and locality using precursor puzzles and holographic toy models. The AdS/CFT conjecture has, as the name implies, not yet been formally proven. However, the evidence is overwhelming and it is fair to say that it made holography one of the most valuable and interesting tools in theoretical high energy physics for the last 20 years.

Firewalls

This chapter is based on the paper [1].

In the introduction we saw that black holes radiate and have interesting thermodynamical properties. While our current understanding of black holes advanced a lot over the past decades, some issues, in particular the ones involving black hole evaporation, remain poorly understood. In this chapter, we will address the recent firewall paradox that involves an observer falling into an old black hole. It states that the observer must see a violation of either unitarity, locality, or the equivalence principle. Motivated by this remarkable conflict, we analyze the causal structure of black hole spacetimes in order to determine whether all the necessary ingredients for the paradox fit within a single observer's causal patch. We particularly focus on the question of whether the interior partner modes of the outgoing Hawking quanta can, in principle, be measured by an infalling observer. Since the relevant modes are spread over the entire sphere, we answer a simple geometrical question: can any observer see an entire sphere behind the horizon?

We find that for all static black holes in 3+1 and higher dimensions, with any value of the cosmological constant, no single observer can see both the early Hawking radiation and the interior modes. We present a detailed description of the causal patch geometry of the Schwarzschild black hole in 3+1 dimensions, where an infalling observer comes closest to being able to measure the relevant modes.

2.1 Introduction

In 2012, Almheiri, Marolf, Polchinski and Sully (AMPS) [44] identified a remarkable conflict between some fundamental physical principles. Consider an 'old' black hole – one that has already emitted more than half of the Hawking quanta – and focus on the emission of the next Hawking quanta H . We expect the following three statements to be true.

1. For a large black hole, the spatial curvature at the event horizon is small, so we expect low energy effective field theory should suffice to describe physics in the region near the horizon (we definitely do not expect quantum gravity to be necessary). The equivalence principle says that the region near the horizon should look locally like the Minkowski vacuum. In particular, an infalling observer should not experience anything special when he crosses the event horizon, which requires H to be strongly entangled with its ‘partner mode’ P behind the horizon (see figure 2.1).
2. The black hole can be formed by collapsing a pure state, and unitarity requires the final state (some radiation) to end up in a pure state as well. When the black hole starts evaporating, the Hawking radiation becomes more and more mixed. When the black hole emitted approximately half of its Hawking quanta however, unitarity requires the Hawking quanta that are subsequently emitted to purify the earlier radiation, in order for the total entanglement entropy to go back to zero when the black hole has completely evaporated. This requires that H is strongly entangled with the radiation R that has already been emitted. It is often visually represented as a kink in the Page-curve (which plots the entanglement entropy of the black hole with the radiation over time), named in honor of its inventor [45, 46].
3. Locality of the (gravitational) theory dictates that P and H can not physically influence each other, because commutators of spacelike separated observables should vanish.

The AMPS paper noted that the above three statements are inconsistent. To see this, consider the strong subadditivity property of entanglement (Von Neumann) entropy. This says

$$S_{PHR} + S_H \leq S_{PH} + S_{HR} \tag{2.1}$$

where S_X is the entanglement entropy of subsystem X with everything else. Since we just argued that the mode H is (close to) maximally entangled with two different subsystems P and R , the RHS of this inequality is (close to) zero. Since S_H will be order one due to its entanglement, one of the aforementioned assumptions must be wrong.

One could argue that the essential conflict stated here was in some sense already present in Hawking’s original work [47] and the information paradox that comes with it. This says that collapsing a pure state in a black hole and letting it evaporate will lead to final state consisting of mixed thermal radiation, which can not happen under unitary time evolution. Some time later, the problem was stated in terms of entanglement by [48, 49]. Before the work of AMPS, the information paradox could be addressed by invoking black hole complementarity (BHC) [50–

54]. In a nutshell, BHC simply states that no observer ever witnesses a violation of any physical law. Observers who remain outside the black hole have access to H and R and can thus confirm the unitarity of black hole evaporation, while an infalling observer has access to H and P and can verify the equivalence principle.

The key innovation of AMPS was to consider the causal patch of an observer who falls into an old black hole. Such an observer would seem to have access to all 3 ingredients necessary for the paradox. If that's the case, then BHC is no longer sufficient to resolve the information paradox. That explains why it is useful to study the geometrical limitations of a causal patch, such as those proposed in [55,56].

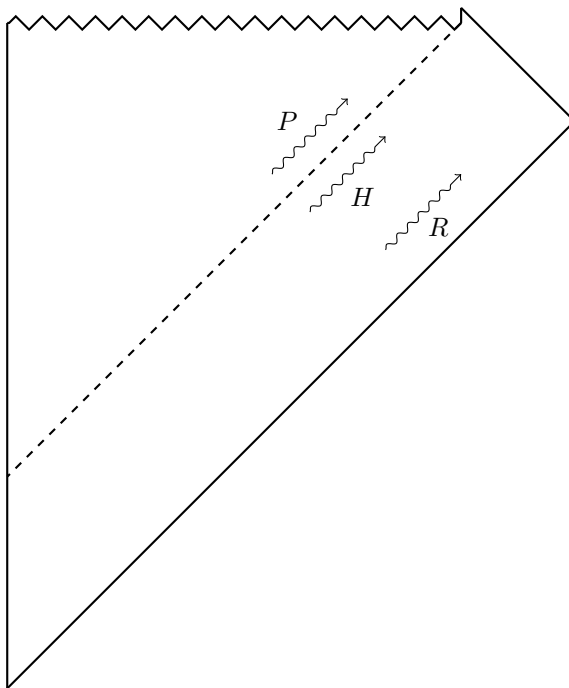


Figure 2.1: Penrose diagram of a Schwarzschild black hole depicting the near-horizon Hawking mode H , its behind-the-horizon partner P , and the early radiation R .

In the rest of this chapter we therefore ask a simple geometric question: can any single observer see the entire sphere behind the horizon? This seems a very relevant question because the simplest and most robust version of the paradox requires that the s -wave Hawking quantum H actually escapes from the black hole.

Consider a massless free Klein-Gordon field on top of a four dimensional static and spherically symmetric black hole background, such as the one considered in (1.2).

The wave equation for the field can be rewritten in terms of a Schrödinger-like problem with effective potential

$$V_l(r) = f(r) \left[\frac{l(l+1)}{r^2} + \frac{f'(r)}{r} \right] \quad (2.2)$$

which is plotted in figure 2.2. We see that there is an angular momentum barrier (present even for modes with $l = 0$), that effectively confines the Hawking radiation in a thermal atmosphere between $r = 2GM$ and $r = 3GM$, sometimes called ‘the zone’. Due to this barrier, Hawking radiation that escapes to infinity occurs almost exclusively in modes with low angular momentum l . That is why we focus on the s -wave firewall, i.e. H should be spread over the entire sphere near the horizon. This means that its entangled partner mode P is also spread over the entire sphere. Therefore, an observer who cannot see the entire behind-the-horizon sphere will have difficulties recognizing the entanglement between these two modes.

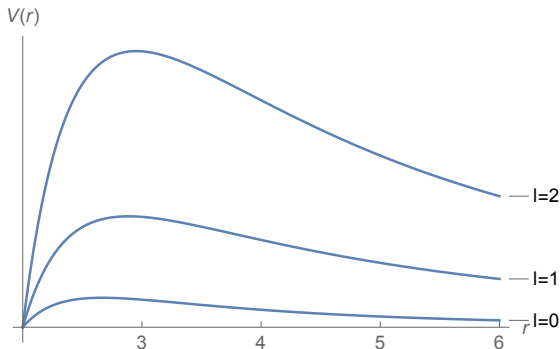


Figure 2.2: Effective potential $V_l(r)$ for a massless scalar field vs. a radial Schwarzschild coordinate in units of GM .

We analyze this question for static black holes in all dimensions, in spacetimes with positive, negative, and zero cosmological constant. For static black holes in asymptotically Minkowski spacetime, an infalling observer cannot receive signals from the entire sphere behind the horizon before hitting the singularity. The most interesting case is 3+1 dimensions, where an observer can see nearly the entire sphere, but it comes with an important caveat: there is a tradeoff between the radial and angular extent of the causal patch, as we will describe in section 2.3. In higher dimensions, less than half the sphere fits within one causal patch.

Adding a negative cosmological constant decreases the region that is causally accessible; for large black holes in asymptotically Anti-de Sitter spacetime, in 3+1 and higher dimensions, an infalling observer can only see a small fraction of the horizon sphere, with physical size of order the AdS radius. This result is potentially important for the AdS version of the firewall paradox [57, 58], which some

consider to be the most robust against the concerns of computation time [59] and back-reaction [60]. Since an infalling observer can only see sub-AdS scales near the horizon, the subtle issue of reconstructing these modes from CFT data can play an important role in the firewall paradox [42, 61, 62]. Interestingly, as we learned in section 1.3.6, it is on these sub-AdS scales that reconstruction and locality is not well understood.

Adding a positive cosmological constant increases the angular size of the causal patch. However, we show that once the cosmological constant is large enough to allow an observer to collect information from the entire sphere, the information contained in the Hawking radiation cannot fit within the cosmological horizon. In other words, as the cosmological constant is increased, an infalling observer begins to be able to measure P but loses the ability to measure R .

These geometrical results motivate a possible resolution of the firewall paradox: even for an old black hole, some degrees of freedom that are smeared over the entire sphere in the near-horizon zone are entangled with the early radiation, while localized modes in the near-horizon zone are entangled with their partners behind the horizon. This would then avoid an observable conflict between the equivalence principle and unitarity.

Some firewall-related cases and issues will not be addressed in this thesis. BTZ black holes is one of them: it seems that an infalling observer can collect a sufficient amount of information. However, we saw that these black holes are quite different from their higher-dimensional relatives. For example, they do not emit Hawking radiation. Rotating black holes are another issue. In this case, there is no spherical symmetry, so it is less obvious which sphere must be contained within the causal patch in order to formulate the paradox. The last issue concerns black hole mining [63]: inserting a device such as a string that collects radiation from deep in the zone and transports it to the exterior. This could, in principle, give access to modes with high l , which according to AMPS should also be entangled with the early radiation. Since it is not clear how this process would work, and it will most probably disrupt the entanglement structure, we will not consider this case any further.

The rest of this chapter is organized as follows: in section 2.2 we discuss results for various static black holes, except for Schwarzschild black holes in $3+1$ dimensions, which we treat separately in section 2.3. The reason for this separation is that with the exception of the latter, it is clear that the geometry of the causal patch alone offers an escape from the firewall paradox. In the case of $(3+1)$ -dimensional Schwarzschild black holes however, a more detailed analysis is required. Then, in section 2.4, we discuss the consequences for entropy and information in the context of the causal patch considerations in the $D = 3 + 1$ Schwarzschild background.

2.2 Static Black Holes in Higher Dimensions

In this section, we consider arbitrary dimensional static black holes in spacetimes with positive, negative, and zero cosmological constant. We postpone a detailed discussion of the critical $(3 + 1)$ -dimensional static black hole in flat space to the next section, as the geometry of the causal patch, and its implications for the firewall discussion, are more subtle in this case. In what follows, we've set the gravitational constant $G = 1$.

2.2.1 Black Holes in Asymptotically Minkowski Spacetime

To address the question of how much of the sphere an infalling observer can see, we need to calculate the maximum angle a light ray can travel between the horizon and the singularity. For static black holes in $D > 3$ spacetime dimensions, the metric is of the form (1.2):

$$ds^2 = -f(r)dt^2 + \frac{dr^2}{f(r)} + r^2 d\Omega_{D-2}^2 \quad (2.3)$$

where

$$f(r) = \left[1 - \left(\frac{r_-}{r} \right)^{D-3} \right] \left[1 - \left(\frac{r_+}{r} \right)^{D-3} \right] \quad (2.4)$$

with

$$r_{\pm} = \frac{1}{2} \left(r_h \pm \sqrt{r_h^2 - 4r_Q^2} \right). \quad (2.5)$$

Here r_+ and r_- are the radii of the outer and inner horizons, respectively; the parameter r_Q is determined by the charge of the black hole. For uncharged black holes, $r_Q = 0$ and the above reduces to the Schwarzschild solution ($r_- \rightarrow 0$, $r_+ \rightarrow r_h$). For the Reissner-Nordstrom solution ($Q^2 > 0$), the inner horizon is believed to be unstable to perturbations, so the natural question is how far light rays can travel between the outer horizon and inner horizon in the angular direction.

Inside the outer horizon, the r and t coordinates switch roles, such that r is temporal and t is spatial. Hence to move the maximum distance along the sphere, the ray should not move in the t direction. Therefore the null ray that travels the maximal angle satisfies

$$r^2 d\theta^2 = -\frac{dr^2}{f(r)} \quad (2.6)$$

and the angle is given by

$$\Delta\theta = \int_{r_-}^{r_+} \frac{dr}{r\sqrt{-f(r)}} = \frac{\pi}{D-3}. \quad (2.7)$$

Thus for higher-dimensional black holes, it is impossible for a single observer to see the entire horizon, and hence no paradox can result. For the limiting case $D = 4$, there is at most just enough time for the information to be collected at a point (but no time for it to be processed), which we investigate in more detail in section 2.3. If the same property holds for all black holes, it suggests a principle: a freely falling observer cannot access the entire horizon sphere, and therefore cannot measure modes of definite angular momentum.

2.2.2 Black Holes in de Sitter

In this section we will show that introducing a positive cosmological constant increases the visible angle $\Delta\theta$, allowing the infalling observer to fit the entire infalling sphere inside the causal diamond. However, at the same time the cosmological horizon moves closer to the black hole. Interestingly, we find that by the time the cosmological constant is large enough to allow the infalling observer to see the entire sphere, the cosmological horizon is too small to allow for the early radiation to be collected.

3+1 dimensions

Introducing a positive cosmological constant will change the metric so that now

$$f(r) = 1 - \frac{M}{r} - \frac{r^2}{L_{\text{dS}}^2} \quad (2.8)$$

where M is the black hole mass and $L_{\text{dS}}^2 \equiv 3/\Lambda$. We want to know how this affects the angle computed above: will putting black holes in de Sitter space allow the infalling observer to see the entire horizon sphere?

Using again (2.7) for the angle, we get

$$\Delta\theta = \int_0^{r_h} \frac{dr}{r\sqrt{-1 + \frac{M}{r} + \frac{r^2}{b^2}}} = L_{\text{dS}} \int_0^{r_h} \frac{dr}{\sqrt{r}\sqrt{(r-r_1)(r-r_2)(r-r_3)}} \quad (2.9)$$

where the r_i are the 3 roots of the equation $f(r) = 0$. If we assume that $M < M_c \equiv \frac{2L_{\text{dS}}}{3\sqrt{3}}$, these three roots are the black hole horizon r_h , the cosmological horizon r_c , and a third negative root $r_3 = -r_h - r_c$. Defining a dimensionless

variable $u = r/r_h$ and rearranging gives

$$\Delta\theta = L_{\text{dS}} \int_0^1 \frac{du}{\sqrt{u-u^2} \sqrt{r_c(r_c+r_h) - r_h^2(u+u^2)}}. \quad (2.10)$$

Note that in the limit that the dS radius is much bigger than the black hole, $r_c \approx L_{\text{dS}}$ and the second factor approaches 1, giving the flat space result.

We would like to approximate the formula for $r_h \ll r_c$. First we use that the product of the 3 roots is $\prod_i r_i = -ML_{\text{dS}}^2$, so

$$r_c(r_c+r_h) = \frac{ML_{\text{dS}}^2}{r_h} \quad (2.11)$$

so that

$$\Delta\theta = \int_0^1 \frac{du}{\sqrt{u-u^2} \sqrt{\frac{M}{r_h} - \frac{r_h^2}{L_{\text{dS}}^2}(u+u^2)}}. \quad (2.12)$$

Now, perturbatively solving (2.8) for r_h and taking the limit where $r_h \approx M$ yields

$$\frac{M}{r_h} = 1 - \frac{M^2}{L_{\text{dS}}^2} + \dots \quad (2.13)$$

so that finally the integral of interest is

$$\Delta\theta \approx \int_0^1 \frac{du}{\sqrt{u-u^2} \sqrt{1 - \frac{r_h^2}{L_{\text{dS}}^2}(1+u+u^2)}} \approx \pi + \frac{15\pi}{16} \frac{r_h^2}{L_{\text{dS}}^2}. \quad (2.14)$$

A nice way to summarize this result is to write it in terms of the entropy of the two horizons:

$$\Delta\theta = \pi + \frac{15\pi}{16} \frac{S_{\text{BH}}}{S_{\text{dS}}}. \quad (2.15)$$

This shows that in principle an observer inside has access to the entire horizon sphere in some location. Now suppose that we want to collect the information at least a Planck distance from the singularity – then instead of integrating all the way to $r = 0$ we should integrate to the location $r = r_P$ where

$$\int_0^{r_P} \frac{dr}{\sqrt{-f(r)}} \approx \int_0^{r_P} dr \sqrt{\frac{r}{M}} = \frac{2}{3} \frac{r_P^{3/2}}{\sqrt{M}} \equiv l_P \quad (2.16)$$

so that $r_P = \left(\frac{3}{2}\right)^{2/3} l_P^{2/3} M^{1/3}$, giving a lower cutoff on the u integral of $u_P = r_P/r_h \approx \left(\frac{3}{2}\right)^{2/3} \left(\frac{l_P}{M}\right)^{2/3}$, where we used that $r_h \approx M$. This corrects the angle by about

$$\int_0^{u_P} \frac{du}{\sqrt{u}} = 2\sqrt{u_P} \approx 12^{1/3} \pi^{1/6} S_{\text{BH}}^{-1/6}. \quad (2.17)$$

So overall, the angular distance that light can travel behind the horizon of a Schwarzschild black hole in de Sitter space before reaching regions of Planckian curvature is

$$\Delta\theta = \pi + \frac{15\pi}{16} \frac{S_{\text{BH}}}{S_{\text{dS}}} - 12^{1/3} \pi^{1/6} S_{\text{BH}}^{-1/6} \quad (2.18)$$

and, at this level of analysis, we can see the entire horizon as long as

$$S_{\text{dS}} < S_{\text{BH}}^{7/6} \quad (2.19)$$

where we have neglected order one factors. However, the amount of information that can be stored inside the horizon in any ordinary system is [64]

$$S_R < S_{\text{dS}}^{3/4}. \quad (2.20)$$

Since we need to be able to collect a number of bits comparable to the black hole entropy, $S_R \sim S_{\text{BH}}$. Therefore, the combined constraints on the size of the cosmological horizon give

$$S_{\text{BH}}^{4/3} < S_{\text{dS}} < S_{\text{BH}}^{7/6}. \quad (2.21)$$

But since S_{dS} is larger than one, $S_{\text{BH}}^{4/3} > S_{\text{BH}}^{7/6}$, so the combined inequality cannot be satisfied.

Therefore, whenever the cosmological constant is large enough to allow the infalling observer to see the partner modes behind the horizon, the AMPS paradox cannot be constructed for another reason: the Hawking radiation will not fit inside the cosmological horizon.

Higher dimensions

For dS black holes in higher dimensions, (2.20) becomes $S_R < S_{\text{dS}}^{(D-1)/D}$. This means that for black holes whose radiation can be collected within the causal patch, the cosmological horizon r_c is much larger than the black hole horizon r_h . In this limit, the higher-order corrections to the flat space result $\Delta\theta = \frac{\pi}{D-3}$ are small, so they do not change the conclusion that the observer is missing an order one fraction of the sphere. Therefore, as long as S_R fits inside the cosmological horizon, the infalling observer cannot see the entire horizon sphere.

2.2.3 Black holes in Anti-de Sitter

We will work in general D -dimensional spacetime, where $D > 3$. The metric function for an AdS black hole is given by

$$f(r) = 1 + \frac{r^2}{L_{\text{AdS}}^2} - \frac{R_S^{D-3}}{r^{D-3}} \quad (2.22)$$

where for AdS we have $L_{\text{AdS}}^2 \equiv -3/\Lambda > 0$. The relevant integral is

$$\Delta\theta = \int_0^{r_h} \frac{dr}{r\sqrt{-f(r)}}. \quad (2.23)$$

For a large black hole with horizon radius much larger than the AdS radius, it is important to ask how large the part of the horizon is that fits inside one causal patch: is it many AdS radii, or not? Taking the large black hole limit, we get

$$\Delta\theta \approx \int_0^{r_h} \frac{dr}{r\sqrt{\frac{R_S^{D-3}}{r^{D-3}} - \frac{r^2}{L_{\text{AdS}}^2}}}. \quad (2.24)$$

$$= \int_0^{r_h} \frac{dr}{R_S^{\frac{D-3}{2}} r^{\frac{5-D}{2}} \sqrt{1 - \frac{r^{D-1}}{R_S^{D-3} L_{\text{AdS}}^2}}}. \quad (2.25)$$

In the $L_{\text{AdS}}^2 \ll r_h^2$ limit we can use that $r_h^{D-1} \approx R_S^{D-3} L_{\text{AdS}}^2$ and change variables to get the dependence on parameters outside the integral, giving

$$\Delta\theta = \frac{L_{\text{AdS}}}{r_h} \int_0^1 du \frac{u^{\frac{D-5}{2}}}{\sqrt{1-u^{D-1}}} \sim \frac{L_{\text{AdS}}}{r_h} \quad (2.26)$$

where the integral can be evaluated exactly to give an $O(1)$ number for $D = 4$ which is monotonically decreasing with increasing D . This shows that for a big black hole in AdS, only a small fraction of the horizon fits inside the causal patch of an infalling observer. The corresponding physical length along the horizon that fits in one causal patch is

$$\Delta x \sim L_{\text{AdS}}. \quad (2.27)$$

We can conclude that an observer falling into a large AdS-Schwarzschild black hole¹ in a D -dimensional spacetime has access to only a small part of the horizon, with physical size of order one AdS radius.

This fact may have important consequences for the AdS/CFT version of the firewall argument [58]. Existing techniques for mapping bulk to boundary fail when applied to fields localized to less than one AdS radius in the near-horizon region [61]. Ultraviolet divergences in the CFT prevent the HKLL construction from working on these scales [35]. It is very intriguing that the arguments for a firewall in AdS black holes must focus on phenomena within a single AdS radius. It is precisely in this regime that the AdS/CFT duality is not well-understood, and there are obstacles to reconstructing bulk physics from the CFT.

¹We saw that these black holes are thermodynamically stable, so they never get ‘old’. In this case, different arguments for a firewall than the ones presented in section 2.1 can be made [57].

2.3 Black Holes in 3+1 Dimensions

As indicated by (2.7), for 3+1 dimensional black holes in asymptotically Minkowski spacetime, an infalling observer can see the entire sphere just as he hits the singularity. This case calls for a more detailed analysis of the causal patch.

A full analysis requires the inclusion of both interior and exterior s -wave partners, and thus we must identify a spacelike slice that crosses the horizon of the black hole. We want to know about the physics of observers who fall in to the black hole from infinity. The Gullstrand-Painlevé (GP, a.k.a. ‘rain-frame’) coordinates are ideally suited for such purposes: the GP time variable T is the proper time along the worldline of observers falling into the black hole, starting from rest at infinity. The slices of constant T are orthogonal to such observers. Therefore, analyzing the entanglement in this frame is directly relevant to the question of whether such infalling observers detect any violation of the equivalence principle.

The GP coordinates are defined as follows [65]: beginning with the Schwarzschild metric, define a new coordinate

$$T = t + r_h \left(2\sqrt{\frac{r}{r_h}} + \log \left| \frac{\sqrt{\frac{r}{r_h}} - 1}{\sqrt{\frac{r}{r_h}} + 1} \right| \right) \quad (2.28)$$

called the Gullstrand-Painlevé time, with which the metric may be rewritten

$$ds^2 = -f dT^2 + 2\sqrt{\frac{r_h}{r}} dT dr + dr^2 + r^2 d\Omega^2 \quad (2.29)$$

which has the appeal of being regular at $r = r_h$. Another nice feature that is apparent from the metric is that constant T -slices are spatially flat. See figure 2.3 for a depiction of the constant T slices.

We want to determine the causal structure, so we need the equation for null geodesics in these coordinates. The conserved quantities for the GP metric are

$$E = f\dot{T} - \sqrt{\frac{r_h}{r}} \dot{r} \quad (2.30)$$

$$l = r^2 \dot{\theta} \quad (2.31)$$

where the dot denotes differentiation with respect to some affine parameter. By using the second of these to replace $\dot{\theta}$ in the null geodesic equation $ds^2 = 0$, and using the resulting expression for \dot{T} in (2.30), one obtains a third conservation expression:

$$E^2 = \dot{r}^2 + \frac{f}{r^2} l^2 \quad (2.32)$$

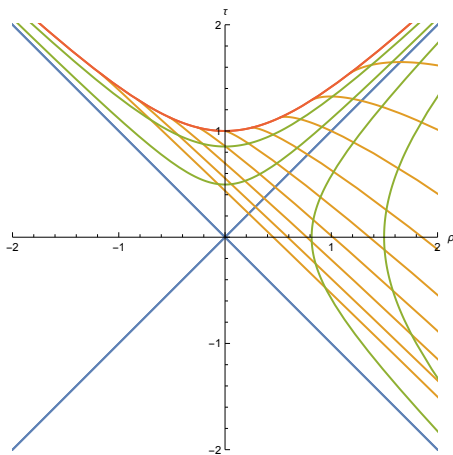


Figure 2.3: Schwarzschild black hole in Gullstrand-Painlevé coordinates, with singularity at $r = 0$ (red), showing constant r slices (green), and constant T slices (orange). The vertical and horizontal axes are Kruskal-Szekeres time and radius, respectively, while the Schwarzschild radius has been set to $r = 1$.

which we may use to eliminate the affine parameter and obtain an expression for the angular distance traversed by an arbitrary null geodesic:

$$\frac{\dot{\theta}}{\dot{r}} = \frac{d\theta}{dr} \implies \Delta\theta = \int_0^{r'} \frac{\pm dr}{\sqrt{\epsilon^2 r^4 + r^2 f}} \quad (2.33)$$

where $\epsilon \equiv \frac{E}{l}$, and the \pm sign selects the polar direction in which the null ray travels. Note the fundamental difference between this expression and (2.7): our null rays are no longer constrained to move along constant Schwarzschild t -slices in the black hole interior.

Similarly, we obtain an expression for the Gullstrand-Painlevé time difference corresponding to (2.33):

$$\frac{\dot{T}}{\dot{r}} = \frac{dT}{dr} \implies \Delta T = \int_0^{r'} \frac{1}{f} \left(\sqrt{\frac{r_h}{r}} \pm \frac{\epsilon r}{\sqrt{\epsilon^2 r^2 - f}} \right) dr. \quad (2.34)$$

Henceforth we will absorb the \pm sign in our expressions for ΔT into ϵ by allowing the latter to take negative values.

Now we would like to determine which part of the constant time surface fits within a single causal patch. We fix a single observer, who determines the causal patch, just above the singularity at Schwarzschild time $t = 0$, at the north pole of the sphere, $\theta = 0$. This observer will collect measurements transmitted to her from

an infalling distributed measuring device; say, a ring of probes spread around the horizon. At some specified GP time T , the probes will perform a measurement of the interior s -wave and transmit this information to the observer to be collected for analysis. The intersection of the observer's past light cone with this T -slice determines the causal patch under consideration (see figure 2.4.)

The Schwarzschild time of the observer ($t = 0$) intersects this T -slice at $r = r_0$. We wish to know the geometry of this causal patch as a function of the choice of T (equivalent to considering observers who fall in at different Schwarzschild times), which requires numerically evaluating (2.33) along the T -slice.

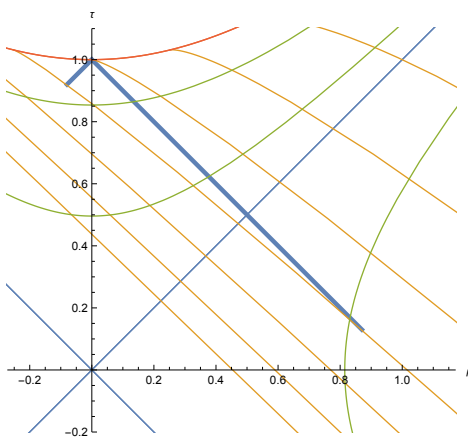


Figure 2.4: Past light-cone (bold blue) of an observer hovering just above the singularity at $(t, r) \approx (0, 0)$. The interior and exterior radial null rays (left and right cone sides, respectively) intersect the T -slice at $r_{\epsilon \rightarrow \infty}$, $r_{\epsilon \rightarrow -\infty}$, respectively. The geometry of the patch is determined by evaluating $\Delta\theta$ along the T -slice for the null rays between these two radial extremes.

Performing this evaluation requires a specification of ϵ . For each point in the causal patch, there intersects in principle an infinite number of possible null rays, parameterized by ϵ , only one of which will have the correct trajectory to be collected by the observer. Furthermore, this value of ϵ is dependent on the upper limit of integration, i.e. on the r -position along the T -slice: $\epsilon = 0$ corresponds to $l \rightarrow \infty$, for which (2.33) reduces to (2.7), while $\epsilon \rightarrow \pm\infty$ corresponds to radial null rays with $l = 0$, whose intersections with the T -slice give the minimal (at $r = r_{\epsilon \rightarrow \infty}$) and maximal ($r = r_{\epsilon \rightarrow -\infty}$) radii of the casual patch.

The distance between the observer and our chosen T -slice, denoted T_* , is given by $\Delta T = T_* - T(r = 0, t = 0) = T_*$. Thus we may numerically obtain the values of ϵ for radii along $T = T_*$ by finding the root of $T_* - \Delta T(\epsilon)$, where $\Delta T(\epsilon)$ is given

by (2.34), with ϵ as the free parameter. With these values of ϵ in hand, we may proceed to the numerical evaluation of (2.33). Results are shown in figure 2.5.

As $|\Delta T|$ is increased, the observer sees less of the interior and more of the exterior of the black hole. This is consistent with an inspection of the geometry in figure 2.4: as T_* becomes more and more negative, $r_{\epsilon \rightarrow \infty}$ approaches the horizon radius, while $r_{\epsilon \rightarrow -\infty}$ increases without bound; conversely, as T_* approaches $t = 0$, both $r_{\epsilon \rightarrow \infty}$ and $r_{\epsilon \rightarrow -\infty}$ shrink, allowing the observer to see more of the black hole interior at the cost of her external view.

In order to try to fit all the ingredients necessary for the firewall paradox inside a single causal patch, we wish to examine a causal patch that contains both an outgoing Hawking quantum and its interior partner mode. Hence for our purposes, the regime of interest is when $|\Delta T|$ becomes large, which allows the observer to maximize both her internal and external angular visibility, and hence affords the best chance of measuring both an outgoing s -wave and its entangled interior partner. However, as pointed out in [55], the wavelength of the interior mode may pose some difficulty to fitting it inside such a patch. In particular, because of the aforementioned trade-off between angular and radial depth visibility, it may not be possible to keep the wavelength of the interior mode above the Planck scale while effecting sufficient angular resolution.

For $|\Delta T|$ sufficiently large to close the exterior visibility region, the exclusion region resembles a raindrop (see figure 2.6). In the limit of large $|\Delta T|$, $r_{\epsilon \rightarrow \infty}$ approaches r_h , and the radial depth available to interior s -wave modes vanishes. Since the energy is $\sim \lambda^{-1}$, this places a lower limit on the energy of the measurable modes, namely $E \gtrsim (r_h - r_{\epsilon \rightarrow \infty})^{-1}$.

Although an analytical expression for the droplet geometry is not available, it is possible to obtain an approximation in the large $|\Delta T|$ limit, where the droplet begins to look like that in figure 2.6 for $|\Delta T| = 3$. By approximating (2.33) and (2.34) in the small- ϵ limit, we find:

$$\Delta\theta \approx \pi - 2\sqrt{1 - r + \epsilon^2} \tag{2.35}$$

$$\Delta T \approx 2\sqrt{r} + 2 \log \left(\frac{1 - \sqrt{r}}{\epsilon + \sqrt{1 - r + \epsilon^2}} \right) + 2 \log \left(\epsilon + \sqrt{1 - \epsilon^2} \right). \tag{2.36}$$

Note that $\Delta T < 0$ (consistent with an infalling observer, since we integrated outwards from the singularity $r = 0$).

These results can be plotted against the numerical exclusion region (i.e. the droplet) by solving (2.36) for ϵ , and substituting the result into (2.35) to obtain an expres-

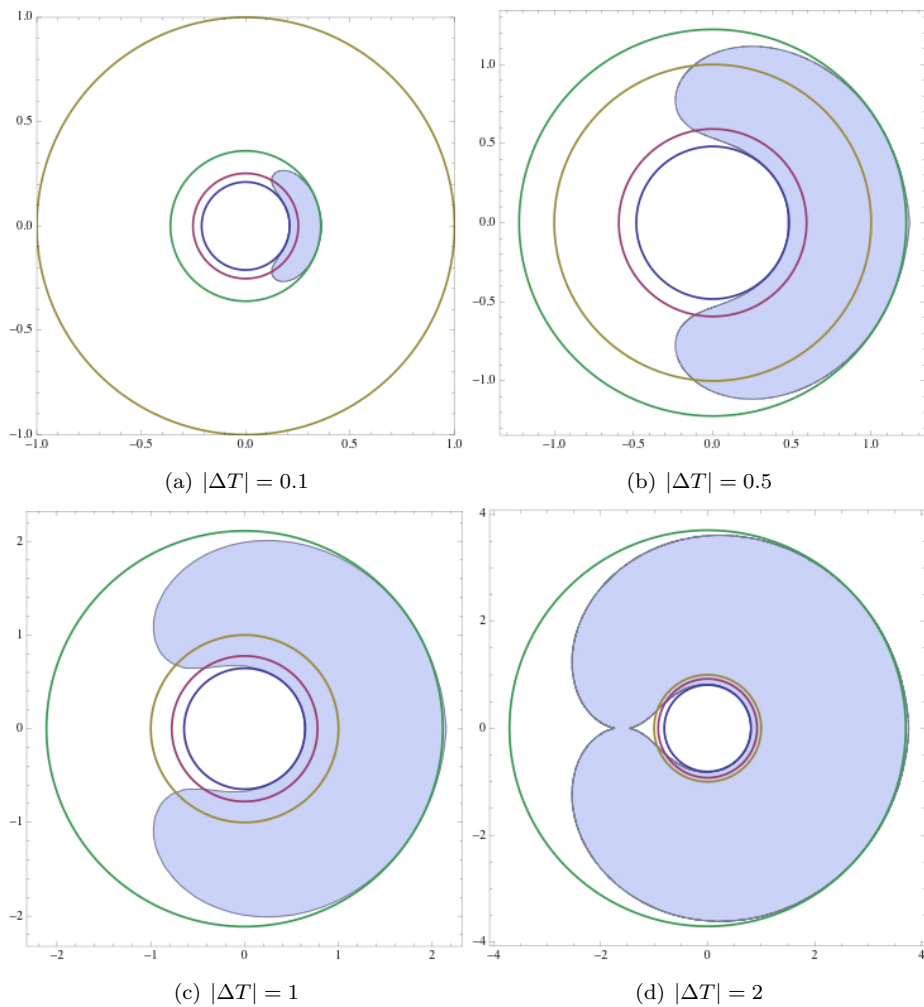


Figure 2.5: Causal patch geometry for several values of ΔT . The shaded region depicts the portion of the spacelike T -slice (as $r(\theta)$) visible to the observer. The concentric rings show the horizon $r_h = 1$ (yellow), $r_{\epsilon \rightarrow -\infty}$ (green), r_0 (red), and $r_{\epsilon \rightarrow \infty}$ (blue). (Note that the axes are rescaled between images). Increasing $|\Delta T|$ corresponds to selecting a T -slice closer to the past horizon in figure 2.4.

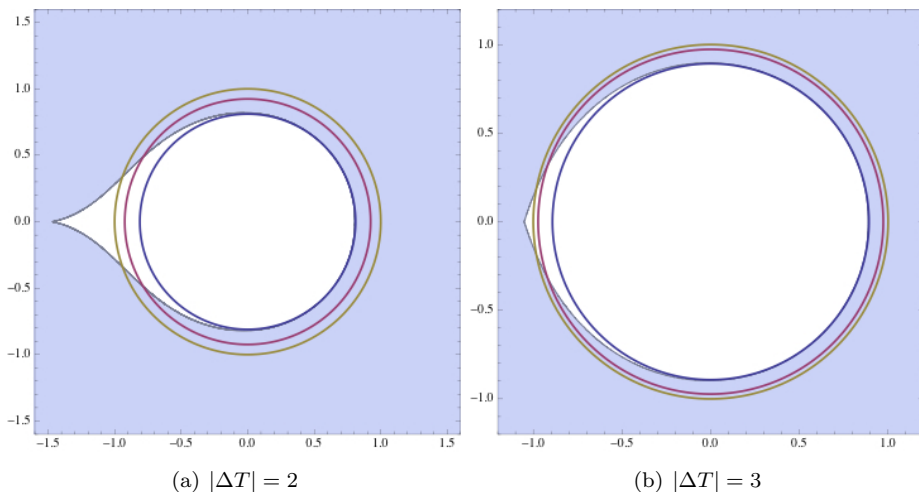


Figure 2.6: Rain in the rain-frame: close-up of exclusion regions. The pointed end of the rain-drop diminishes, and the droplet approaches a circular region with radius $r \rightarrow r_h$, in the limit of large ΔT .

sion for $\Delta\theta(r)$. We find:

$$\Delta\theta \approx \pi - 2\sqrt{\frac{(-1 + r + \sqrt{r} \sinh(\Delta T/2 - \sqrt{r}) + \cosh(\Delta T/2 - \sqrt{r}))^2}{2 - r - 2\sqrt{r} \sinh(\Delta T/2 - \sqrt{r}) - 2 \cosh(\Delta T/2 - \sqrt{r})}}. \quad (2.37)$$

Two example cases which serve to demonstrate the validity of this result are shown in figure 2.7.

We may obtain a more aesthetically pleasing approximation to (2.36) by expanding in the near-horizon region. We find:

$$\pi - \Delta\theta \approx \sqrt{h} + \frac{1 - r}{\sqrt{h}} \quad (2.38)$$

where

$$\sqrt{h} \equiv 2e^{\Delta T/2 - 1} \quad (2.39)$$

our choice of the notation ‘ \sqrt{h} ’ will become clear shortly. The accuracy of (2.38) is comparable to (2.37) near the horizon (and hence also on the tip for sufficiently large $|\Delta T|$), but cannot be used along the rest of the droplet body.

At the horizon itself ($r = 1$), the second term in (2.38) vanishes and we obtain an approximation for the angular width of the droplet tip at the Schwarzschild radius as a function of GP time:

$$\pi - \Delta\theta \approx \sqrt{h} = 2e^{\Delta T/2 - 1}. \quad (2.40)$$

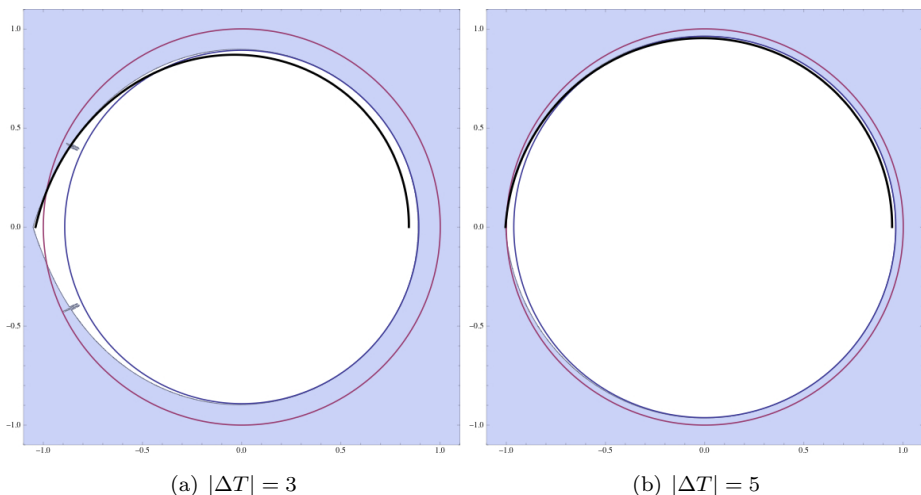


Figure 2.7: $r(\theta)$ (thick black curve), determined by (2.37), plotted against the droplet for $|\Delta T| = 3$ (left) and 5 (right), showing improvement as $|\Delta T|$ is increased. The concentric circles are r_h (red) and $r_{\epsilon \rightarrow \infty}$ (blue). The tick marks in the left image are due to a rendering glitch.

Two other droplet parameters are of interest: the height of the tip above the horizon, and the depth of the antipodal point within. The former is defined by $\Delta\theta = \pi$, hence $\epsilon = \sqrt{r-1}$ and (2.36) becomes

$$\Delta T \approx 2\sqrt{r} + 2 \log \left(\frac{1 - \sqrt{r}}{\sqrt{r-1}} \right) \quad (2.41)$$

where we have discarded the negligible third term. Defining the height of the tip $h \equiv r - 1 > 0$, and expanding around $h = 0$, we find

$$\Delta T \approx 2 + \frac{h}{2} - \log(4) + \log(h). \quad (2.42)$$

We may then drop the term linear in h relative to the log, and solve:

$$h \approx 4e^{\Delta T - 2} \quad (2.43)$$

cf. (2.39). To obtain a similar expression for the depth of the antipodal point requires a formula valid in the limit $\epsilon \rightarrow \infty$. One can show that

$$\lim_{\epsilon \rightarrow \infty} \Delta T = 2\sqrt{r} + r + 2 \log(1 - \sqrt{r}). \quad (2.44)$$

Defining the depth $d \equiv 1 - r > 0$ and expanding, we find:

$$\Delta T \approx 3 - \frac{3}{2}d - \log(4) + 2 \log(d). \quad (2.45)$$

As before, we drop the linear d term and solve:

$$d \approx 2e^{(\Delta T - 3)/2} = e^{-1/2} \sqrt{h}. \quad (2.46)$$

We summarize our results for the droplet parameters in figure 2.8.

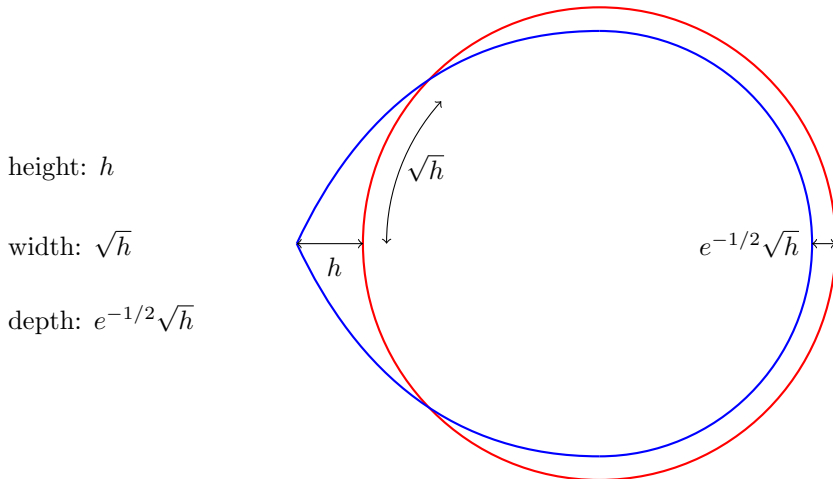


Figure 2.8: Sketch of a heavily distorted droplet (blue) against the horizon $r_h = 1$ (red) with parameters of interest labelled. Note that distances are not to scale, although the height is indeed less than the width for $h \ll 1$ ($|\Delta T|$ large).

2.4 Entropy and Information

Having obtained a geometric picture of the infalling observer’s causal patch in the case of Schwarzschild black holes in 3 + 1 dimensions, we now wish to ask what this implies for the AMPS paradox. We appear to have a trade-off between the energy scale of the measurable modes and the angular resolution of the horizon. What can we then conclude about the entanglement of the partner modes?

For an infalling observer, the entanglement entropy across the horizon may be thought of as being organized into localized Bell pairs, each of which contains a single bit of entanglement entropy [66]. Consider the total number of bits within the droplet $m = \theta_{\text{missing}}^2 / \lambda^2$, out of a total $N = 1/\lambda^2$ bits distributed over the entire circle. The wavelength of measurable quanta is limited by the distance between the droplet and the horizon, which for partner modes must be equal inside and outside the black hole. If we take $\lambda \leq h$ with $\Delta\theta_{\text{missing}} \sim \sqrt{h}$, that implies

$$m = \frac{(\Delta\theta_{\text{missing}})^2}{\lambda} \left(\frac{1}{\lambda} \right) \sim \frac{h}{\lambda} \sqrt{N} \implies m \gtrsim \sqrt{N} \quad (2.47)$$

since $\lambda \leq h$. Thus we find that an observer focussing on modes with $\lambda \leq h$ is always missing at least about \sqrt{N} out of N bits. Insofar as N is proportional to λ^{-2} , only high energy modes stand a chance of reducing the missing fraction to the point where collection of sufficient information is possible. Another obvious though important consequence is that, since one cannot speak of trans-Planckian modes in the absence of a full theory of quantum gravity, m will *never* be zero: even the most determined observer is missing at least one bit.

We may also compute the entropy associated with this missing area. Computing the solid angle in the small h approximation, we find

$$A_{\text{missing}} \approx \pi(\sqrt{h})^2 r_h^2 \implies \quad (2.48)$$

$$S_{\text{missing}} = \frac{A_{\text{missing}}}{4l_P^2} \approx \frac{\pi h r_h^2}{4l_P^2} \quad (2.49)$$

Via (2.43), this can be written as

$$S_{\text{missing}} \approx \frac{\pi r_h^2}{l_P^2} e^{\Delta T - 2}. \quad (2.50)$$

Thus, an observer who wishes to measure a mode with wavelength of order $\lambda \sim h \approx 4e^{\Delta T - 2}$ does so at an entropy cost given by (2.50), which we may think of as the entropy associated with the missing \sqrt{N} bits.

A natural question is precisely how much of the horizon area – equivalently, how many bits m – the infalling observer can afford to lose before measurement of the ingoing Hawking mode becomes impossible. Questions of reconstructing information from some subset of bits are considered in quantum information theory in the context of (k, n) threshold schemes [67], in which a quantum ‘secret’ is divided into n shares such that any $k \leq n$ of those shares can be used to reconstruct the original secret, but any $k - 1$ or fewer cannot. The authors of [67, 68] demonstrated that the only general constraint on such threshold schemes is due to monogamy: one must have $n < 2k$ else the quantum no-cloning theorem is violated.

Consider, as above, an s -wave immediately behind the horizon with an outgoing partner mode directly outside, with the entanglement information distributed in N localized Bell pairs. Further suppose that the information necessary to reconstruct the entangled state is encoded in a (k, n) threshold scheme ($n = N$). The question at hand is then: what is the value of k needed to reconstruct the state?

If reconstruction requires the full N bits ($k = n = N$), then our results imply that doing so is impossible, since one reaches the Planck scale in wavelength before the missing number of bits $m \rightarrow 0$. Conversely, if the information can be retrieved from some sufficiently large fraction $\frac{N-m}{N}$, then the infalling observer may still

be able to reconstruct high energy modes. In the absence of a precise statement about how black holes encode their secrets, the general bounds $k \leq n < 2k$ are not sufficiently strict to rule-out the possibility that an infalling observer could reconstruct the state despite missing a large number of bits.

However, this still involves a trade-off between the energy scale of the measurable modes and the angular occlusion. It may be that one can only have sufficient angular resolution for modes whose energy exceeds some critical value, $\lambda_{\text{crit}}^{-1}$, in which case the $O(1)$ corrections to modes as was claimed by AMPS, would only be detectable for very high-energy modes indeed. More work is needed to determine precisely how small the fraction m/N need be.

Localizing Precursors in AdS/CFT

This chapter is based on the paper [2].

In this chapter we will investigate a puzzling aspect of the AdS/CFT correspondence: a single bulk operator can be mapped to multiple different boundary operators, or precursors. By improving upon a recent model [69], we will demonstrate explicitly how this ambiguity arises in a simple model of the field theory. In particular, we will utilize the freedom in the smearing function used in the bulk-boundary mapping, and explicitly show how this freedom can be used to localize the precursor in different spatial regions. Later, in chapter 4, we will explain how this freedom connects with boundary gauge invariance. We will also show how the ambiguity can be understood in terms of quantum error correction, by appealing to the entanglement present in the CFT. The concordance of these two approaches suggests that gauge invariance and entanglement in the boundary field theory are intimately connected to the reconstruction of local operators in the dual spacetime.

3.1 Introduction

In AdS/CFT, much interest has focused on the emergence of the bulk spacetime from boundary CFT data, but a complete understanding of bulk locality remains elusive. We saw in section 1.3.5 that the HKLL construction allows us to write the boundary dual of a local bulk field Φ located a finite distance z away from the boundary as an integral of the corresponding local CFT operator \mathcal{O} over space and time:

$$\Phi(t, x, z) = \int dx' dt' K(t, x, z|x', t') \mathcal{O}(x', t') + O(1/N) \quad (3.1)$$

where the kernel K is called the smearing function. In the cases where K exists and can be computed, its support on the boundary is a measure for what subregion

of the boundary stores the information of a given bulk point.

A perplexing feature of this procedure is that there is a freedom in choosing the smearing function K , allowing for a family of different CFT operators corresponding to a given bulk operator. As we will explain later, this can be understood because the dual operator does not have support on a complete set of Fourier modes. These different CFT operators, when evolved back to one time, can even have support in different spatial regions of the CFT (see figure 3.1). We refer to these CFT operators as ‘precursors’, because in general they contain information about bulk events before signals from these events have had time to reach the boundary [70–72].

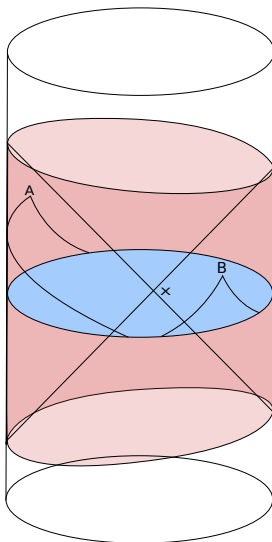
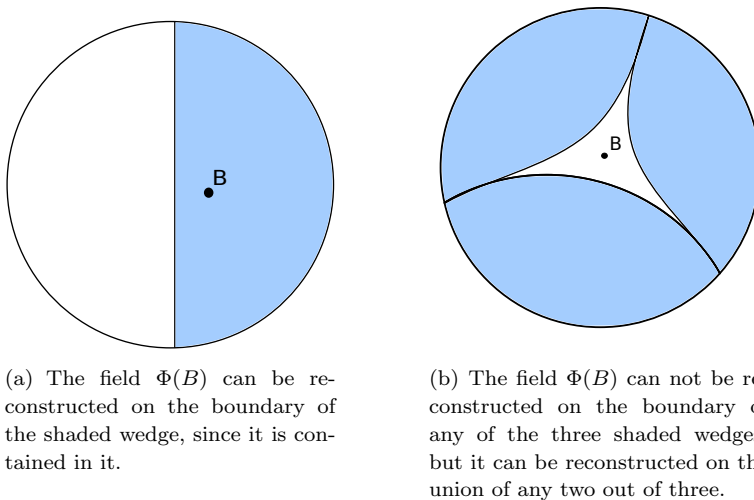


Figure 3.1: Global AdS_3 , showing the light-cone for a bulk point x , which defines a spacelike separated region on the boundary (shaded red). The corresponding non-local boundary operator is defined à la (3.1) as an integral over this region. The local CFT operators can be time-evolved to a single Cauchy slice. This is illustrated schematically for points A and B , where we’ve indicated the null lines on the boundary. In our model, the boundary operators factorize along the light-cone directions, and are trivially evolved to bilocals at the $t = 0$ Cauchy slice (blue).

Almheiri, Dong, and Harlow [73] pointed out that these different CFT operators cannot be really equal as operators. To see this, consider a precursor corresponding to a bulk point in the middle of AdS. Bulk locality requires this operator to commute with all local operators in the CFT on a fixed time slice containing the bulk point. But an operator which commutes with all local operators (at a fixed time) must be proportional to the identity. This follows from Schur’s lemma for QFT on a lattice, and in the continuum it is known as the time-slice axiom [74].



(a) The field $\Phi(B)$ can be reconstructed on the boundary of the shaded wedge, since it is contained in it.

(b) The field $\Phi(B)$ can not be reconstructed on the boundary of any of the three shaded wedges, but it can be reconstructed on the union of any two out of three.

Figure 3.2: Time slice of global AdS with a bulk point B , and boundary regions with their corresponding causal wedges (blue, shaded).

It is believed to be a fundamental property of physically relevant quantum field theories [75]. From this they concluded that bulk locality can not be respected at the level of the algebra of operators.

Another precursor puzzle is what we will call in this thesis the precursor ‘ambiguity’: a local bulk field can correspond with many different precursors. To see this, it is sufficient to note that we can use the HKLL construction (in empty AdS) of a local bulk field in a particular region of the boundary as long as it is contained in the corresponding Rindler wedge. Have a look at figure 3.2(a). Since there are many different Rindler wedges containing the same bulk field, we run in a problem. A more interesting example is depicted in figure 3.2(b), where the boundary is divided in three regions. We see that none of the three regions can reconstruct the bulk field, but any two out of three regions can. This property is very reminiscent of (quantum) error correction.

To resolve the aforementioned conundrums, the authors proposed that the different CFT operators (corresponding with a local bulk field) are only equivalent when acting on a certain subclass of states (the ‘code subspace’), casting the bulk reconstruction problem in the language of quantum error correction (QEC) and quantum secret sharing [67, 68], in which increasing radial depth into the bulk is interpreted as improved resilience of the boundary theory against local quantum erasures. This idea has been beautifully implemented in several tensor network models [76–78].

Subsequently, Mintun, Polchinski, and Rosenhaus (MPR) [69] argued that the structure of QEC emerges naturally when one considers the gauge invariance of the boundary field theory. MPR reconciles the representation of a local bulk operator by a number of different CFT operators by pointing out that an operator can be modified by a ‘pure-gauge’ contribution that changes its support on the boundary without changing its action on physical states. This suggests that the emergence of local operators in the dual spacetime may be deeply connected with gauge symmetries in the CFT. We will further explore this interesting connection in chapter 4, where we will derive and generalize the results of MPR using the BRST formalism.

In this chapter, we will clarify the relationship between quantum error correction, gauge freedom, and the localization of precursors, in the context of an explicit holographic toy model in AdS₃/CFT₂. We will first point out a shortcoming of the MPR model: the particular boundary conditions specified by MPR lead to a theory with no bulk dynamics. This difficulty is easily fixed by choosing different boundary conditions, and we revise their model of the CFT accordingly in section 3.2. We show that with these revisions, the model provides a nice, tractable model for understanding the CFT encoding of bulk information, including such issues as the role of quantum error correction.

We show in section 3.3 that the known ambiguity in the choice of smearing function arises from the gauge freedom in the $N \rightarrow \infty$ limit, and explicitly show how to use this freedom to localize the precursor in different spatial regions. We begin with a standard representation of a local bulk operator spread over the entire CFT, as illustrated in figure 3.1, and show that the gauge freedom allows us to localize the precursor within a single boundary Rindler wedge. This result agrees with the claims of MPR, but now in a model with genuine bulk dynamics. We find that this localization procedure works when the bulk field is located inside the corresponding entanglement wedge¹, consistent with general expectations for bulk reconstruction. This result is independent of the weakly coupled CFT model, and relies only on the freedom in the choice of smearing function.

In section 3.4, we take a quantum error correction approach to localizing the precursor in a boundary region A : we use the entanglement of the ground state to map operators acting on the complement \bar{A} into operators acting on A . We point out how this procedure can fail, and show that it is successful when the above condition is satisfied: the bulk point must lie in the entanglement wedge corresponding to the boundary region under consideration.

¹For most of this work, the entanglement and causal wedges agree, and we use the terms interchangeably. We will discuss the crucial difference between them in chapter 6.

3.2 Toy Model of the AdS/CFT Correspondence

In this section, we describe the MPR model [69] along with our improvements. In the former, the CFT consists of N free massless scalars ϕ^i in $d = 1 + 1$ dimensions, where i is a global $O(N)$ index. The global $O(N)$ symmetry is not gauged, but we take it as a simple model for the gauge invariance of the full theory, so ‘gauge invariant’ operators are defined to be operators that are invariant under global $O(N)$ transformations. MPR considers a massless bulk field Φ in AdS_3 , and from the two possible consistent quantization schemes we discussed in section 1.3.4,

$$\Delta_{\pm} = \frac{d}{2} \pm \sqrt{\frac{d}{2} + m^2} \quad (3.2)$$

they choose boundary conditions such that the bulk field is dual to a $\Delta_- = 0$ operator, which they take to be $\phi_i \phi^i$.

The choice $\Delta = 0$ is unfortunate for a number of related reasons. From the CFT point of view, $\Delta = 0$ saturates the unitarity bound. In any dimension, an operator \mathcal{O} saturating the unitarity bound must obey the *boundary* equation of motion $\square \mathcal{O} = 0$, meaning that it acts like a free field on the boundary. From the bulk point of view, when we impose the boundary condition $\Phi \propto z^{\Delta_-}$ as $z \rightarrow 0$, with $\Delta_- = 0$, there are no solutions to the bulk equation of motion except for the special modes satisfying the boundary wave equation. Therefore, this field does not have true bulk dynamics and is not a good setting to discuss bulk reconstruction; see [79] for a more detailed discussion of the $\Delta = 0$ limit.

This problem is easily fixed: we simply choose the other boundary condition $\Phi \rightarrow z^2$ ($\Delta_+ = 2$), and take the boundary operator dual to the bulk field to be

$$\mathcal{O} = \partial_{\mu} \phi^i \partial^{\mu} \phi_i \quad (3.3)$$

where the ϕ^i are free massless scalar fields as in the MPR model. Strictly speaking, this is also a poor model for perturbative bulk physics, since the CFT is weakly coupled. However, at the level of two-point functions it suffices to capture the salient features. This improved model is almost identical to [72], which in turn was closely related to [70].

In the following we suppress the $O(N)$ index i and use light-cone coordinates $x_{\pm} = t \pm x$ in the boundary, so we can write simply

$$\mathcal{O} = \partial_+ \phi \partial_- \phi . \quad (3.4)$$

We expand the CFT field ϕ in terms of creation and annihilation operators as

$$\phi(x_+, x_-) = \int \frac{d\nu_+}{\nu_+} \alpha_{\nu_+} e^{-i\nu_+ x_+} + \int \frac{d\nu_-}{\nu_-} \tilde{\alpha}_{\nu_-} e^{-i\nu_- x_-} \quad (3.5)$$

where α and $\tilde{\alpha}$ correspond to the right and left movers, respectively. This then yields a simple formula for the primary operator \mathcal{O} ,

$$\mathcal{O}(x_+, x_-) = - \int d\nu_+ d\nu_- e^{-i(\nu_+ x_+ + \nu_- x_-)} \alpha_{\nu_+} \tilde{\alpha}_{\nu_-} . \quad (3.6)$$

In the large N limit, as is explained in [69] and we will derive in chapter 4, the global $O(N)$ gauge invariance includes the freedom to add $L^{ij} A_{ij}$ to any operator within correlation functions, where L^{ij} is the generator of global $O(N)$ transformations and A_{ij} is any operator in the adjoint. This translates to the freedom of adding $\alpha_{\nu_+} \tilde{\alpha}_{\nu_-}$ as long as $\nu_+ \nu_- < 0$. One can check it annihilates the vacuum in both directions, so it can be freely added within two-point functions.

3.3 Localizing the Precursor via Gauge Freedom

The aforementioned freedom appears distinct from the freedom in the choice of smearing function, but we will show that they are in fact identical. We will then show explicitly how this freedom can be used to localize the precursor within a given boundary region, in an effort to make more precise the role that gauge invariance plays in the localization and non-uniqueness of boundary data.

The precursor for a local bulk field Φ is defined with support on the entire boundary by (3.1), in the $N \rightarrow \infty$ limit,

$$\Phi(t, x, z) = \int dx' dt' K(t, x, z|x', t') \mathcal{O}(x', t') . \quad (3.7)$$

The smearing function K in Poincaré-AdS₃ for a field with conformal dimension $\Delta = 2$ is given by [31]

$$K(t, x, z|t', x') = \log \left(\frac{|z^2 + (x - x')^2 - (t - t')^2|}{2z} \right) \equiv K. \quad (3.8)$$

The ambiguity in the smearing function consists of the freedom to add a function δK which in Fourier space satisfies $\nu_+ \nu_- < 0$. This can be understood from the fact that satisfying the bulk wave equation, $\square \Phi = 0$, in global AdS implies that modes with frequency ω and boundary momentum κ satisfying $\omega^2 < \kappa^2$ (or in light-cone coordinates, $\nu_+ \nu_- < 0$) are disallowed. Since the dual operator has no support on the space of these modes: $\int d^2x \mathcal{O} \delta K = 0$.

Focusing on a particular Fourier mode, the change in the smearing function is

$$\delta K(x_+, x_-) = e^{i(\nu_+ x_+ + \nu_- x_-)} . \quad (3.9)$$

The corresponding change in the precursor is therefore

$$\delta\Phi = \int dx_+ dx_- e^{i(\nu_+ x_+ + \nu_- x_-)} \mathcal{O} . \quad (3.10)$$

Plugging in the expansion for the field in terms of creation and annihilation operators (3.6) then gives

$$\delta\Phi = - \int dx_+ dx_- e^{i(\nu_+ x_+ + \nu_- x_-)} \int d\nu'_+ d\nu'_- e^{-i(\nu'_+ x_+ + \nu'_- x_-)} \alpha_{\nu'_+} \tilde{\alpha}_{\nu'_-} . \quad (3.11)$$

The spatial integrals can be performed, yielding

$$\delta\Phi = -\alpha_{\nu_+} \tilde{\alpha}_{\nu_-} . \quad (3.12)$$

This demonstrates that the freedom identified in MPR corresponds precisely to the freedom in the choice of smearing function. In this narrow sense, we will refer to the function δK satisfying $\nu_+ \nu_- < 0$ as ‘pure gauge’ henceforth.

We are now prepared to demonstrate that this freedom in the smearing function can be used to localize the precursor to within a single boundary Rindler wedge. In Poincaré light cone coordinates, the metric for Rindler-AdS₃ is

$$ds^2 = \frac{-dx_+ dx_- + dz^2}{z^2} \quad (3.13)$$

which naturally leads to a bulk Rindler horizon at $x_+ = x_- = 0$. This horizon defines the bulk Rindler or causal wedge, and our aim is to localize the precursor for a given field in this wedge within the corresponding boundary region. This requires finding the most general pure-gauge function δK that we can add such that the new smearing function, $\hat{K} = K + \delta K$, only has support within that region.

To proceed, we need to know how the pure-gauge mode functions (that is, the Poincaré modes with $\nu_+ \nu_- < 0$) look in the various Rindler wedges. This can be done by studying the analyticity of the mode functions in the complex plane.

It is convenient to work in terms of the Rindler modes²

$$x_+^{i\omega_+} x_-^{i\omega_-} \quad (3.14)$$

where x_{\pm} are the Poincaré light-cone coordinates, as above. The Rindler plane is sketched in figure 3.3. The above Rindler modes (3.14) are then defined as-is in the northern quadrant, where $x_+ > 0$, $x_- > 0$. We would then like to know what this looks like in the remaining three quadrants. However, getting there requires navigating the branch cuts at $x_+ = 0$ and/or $x_- = 0$.

²In fact, working in terms of the Rindler modes is more than a convenience, it is a necessity, because the resulting smearing function can only be written in Fourier space; it cannot be transformed to position space.

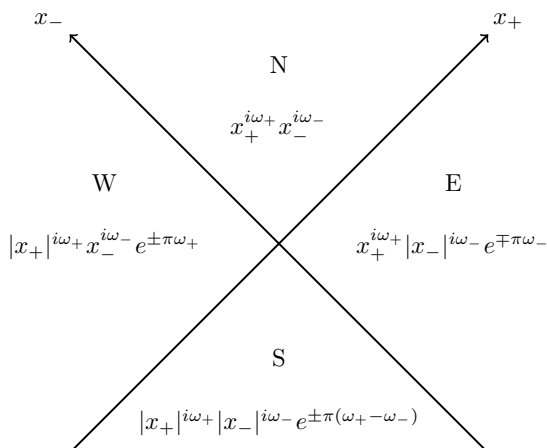


Figure 3.3: Rindler plane in light cone coordinates, indicating the phase changes in the mode functions (3.14) when crossing the branch cuts at $x_{\pm} = 0$. The sign choice is arbitrary, but must be consistent across all four quadrants in order to obtain a pure-gauge Poincaré mode. We refer to these quadrants throughout as the northern (N), southern (S), eastern (E), and western (W) wedges.

Consider moving into the western wedge. We have a choice of contour upon crossing the branch cut at $x_+ = 0$. Suppose we take the function to be analytic in the lower-half complex x_+ plane. Then the transformation from the northern wedge ($x_+ > 0$) across $x_+ = 0$ into the western wedge ($x_+ < 0$), is $x_+ \rightarrow |x_+|e^{-i\pi}$, where the minus sign in the exponential corresponds to our choice of contour. The Rindler mode changes as

$$x_+^{i\omega_+} x_-^{i\omega_-} \rightarrow |x_+|^{i\omega_+} x_-^{i\omega_-} e^{\pi\omega_+} . \quad (3.15)$$

Since we chose x_+ to be analytic in the lower half-plane, our mode is a superposition of positive frequency Poincaré modes $\nu_+ > 0$.³ Had we made the opposite choice for the analyticity of the function, we would take the opposite sign of ν_+ . Hence the general transformation across the $x_+ = 0$ branch cut into the western wedge is

$$x_+^{i\omega_+} x_-^{i\omega_-} \rightarrow |x_+|^{i\omega_+} x_-^{i\omega_-} e^{\pm\pi\omega_+} \quad (\text{N} \rightarrow \text{W}) \quad (3.16)$$

where the upper sign is for $\nu_+ > 0$, lower for $\nu_+ < 0$. From this relation one immediately writes down the transformation from the northern quadrant across $x_- = 0$ into the east ($x_- < 0$):

$$x_+^{i\omega_+} x_-^{i\omega_-} \rightarrow x_+^{i\omega_+} |x_-|^{i\omega_-} e^{\mp\pi\omega_-} \quad (\text{N} \rightarrow \text{E}) \quad (3.17)$$

³Any function $f(x)$ built out of positive frequency Fourier modes (that is $e^{-i\nu x}$ with $\nu > 0$) must be analytic in the lower half of the complex x -plane, and vice versa.

where the upper sign is for $\nu_- < 0$, lower for $\nu_- > 0$. Similarly, the transformation of the precursor into the southern quadrant, with two branch crossings, is

$$x_+^{i\omega_+} x_-^{i\omega_-} \rightarrow |x_+|^{i\omega_+} |x_-|^{i\omega_-} e^{\pm\pi\omega_+ \mp \pi\omega_-} \quad (\text{N} \rightarrow \text{S}) . \quad (3.18)$$

The crucial fact is that the above, with a consistent sign choice (upper or lower), corresponds to a pure-gauge function in Poincaré, since we have $\nu_+ \nu_- < 0$ by construction. The nice feature of this method is that we're guaranteed this without having to explicitly work with Poincaré modes, where the meaning of $\nu_+ \nu_- < 0$ in the various quadrants is not readily visualized.

From this analyticity analysis, we can immediately write down the general form of the pure-gauge function δK :

$$\delta K = \int d\omega_+ d\omega_- \left(c_{\omega_+ \omega_-} f_{\omega_+ \omega_-}^{\text{upper}} + d_{\omega_+ \omega_-} f_{\omega_+ \omega_-}^{\text{lower}} \right) \quad (3.19)$$

with, from (3.16), (3.17), and (3.18),

$$\begin{aligned} f_{\omega_+ \omega_-} &= x_+^{i\omega_+} x_-^{i\omega_-} \Theta(x_+) \Theta(x_-) + |x_+|^{i\omega_+} |x_-|^{i\omega_-} e^{\pm\pi\omega_+} \Theta(-x_+) \Theta(x_-) \\ &+ x_+^{i\omega_+} |x_-|^{i\omega_-} e^{\mp\pi\omega_-} \Theta(x_+) \Theta(-x_-) \\ &+ |x_+|^{i\omega_+} |x_-|^{i\omega_-} e^{\pm\pi\omega_+ \mp \pi\omega_-} \Theta(-x_+) \Theta(-x_-) . \end{aligned} \quad (3.20)$$

The labels ‘upper and ‘lower’ on the functions f in (3.19) indicate choosing the upper or lower signs in the exponentials in (3.20), and the coefficients c and d are undetermined functions of the momenta.

We may extract from this general expression the pure-gauge function in momentum space, $\delta \tilde{K}$, in each of the four quadrants:

$$\begin{aligned} \delta \tilde{K}_N &= c + d \\ \delta \tilde{K}_W &= e^{\pi\omega_+} c + e^{-\pi\omega_+} d \\ \delta \tilde{K}_S &= e^{\pi(\omega_+ - \omega_-)} c + e^{-\pi(\omega_+ - \omega_-)} d \\ \delta \tilde{K}_E &= e^{-\pi\omega_-} c + e^{\pi\omega_-} d \end{aligned} \quad (3.21)$$

where we have suppressed the ω_{\pm} subscripts on c and d to minimize clutter.

In order to localize support for the precursor within a single Rindler wedge, we must choose the coefficients c and d such that $\hat{K} = \tilde{K} + \delta \tilde{K}$ is zero in the other three regions. Let us attempt to localize the precursor in the east, so that only $\hat{K}_E \neq 0$. Then the coefficients must be chosen such that

$$\delta \tilde{K}_N = -\tilde{K}_N \quad \delta \tilde{K}_W = -\tilde{K}_W \quad \text{and} \quad \delta \tilde{K}_S = -\tilde{K}_S \quad (3.22)$$

where \tilde{K}_X with $X \in \{E, N, W, S\}$ is the Fourier transform of the smearing function (3.8) in the specified wedge,

$$\tilde{K}_X(\omega_+, \omega_-) \equiv \iint_X dx_+ dx_- K(0, a, z|x_+, x_-) |x_+|^{-i\omega_+ - 1} |x_-|^{-i\omega_- - 1}. \quad (3.23)$$

We have chosen the bulk field to be located at time $t = 0$, radial coordinate z , and a distance a into the eastern wedge of the bulk.

At a glance, the system (3.22) appears overdetermined, as we have three equations and only two unknown functions of the momenta, c and d . However, we shall find that the system does indeed have a consistent solution, provided that the bulk point lies within the bulk extension (the causal or entanglement wedge) of the boundary Rindler wedge in which we attempt to localize the smearing function, in this case the east. We shall return to this requirement below.

In the course of solving this system, we rely on the following relations between the Fourier transforms of the smearing function, which we prove in appendix 3.A:

$$\begin{aligned} \tilde{K}_N &= \cosh(\pi\omega_+) \tilde{K}_W \\ \tilde{K}_S &= \cosh(\pi\omega_-) \tilde{K}_W \\ \tilde{K}_E &= \cosh(\pi(\omega_+ - \omega_-)) \tilde{K}_W \end{aligned} \quad (3.24)$$

Note that the singularities in the smearing function (3.8), which occur when the argument of the logarithm is zero, do not extend into the western quadrant. This is a consequence of the fact that we chose the bulk point to be in the eastern Rindler wedge. The benefit of these relations is that they allow us to rewrite everything in terms of the Fourier transform \tilde{K}_W , which is well-defined.

With the relations (3.24) in hand, one can show that the system (3.22) is solved by

$$\begin{aligned} c &= -\frac{1}{2} e^{-\pi\omega_+} \tilde{K}_W \\ d &= -\frac{1}{2} e^{\pi\omega_+} \tilde{K}_W \end{aligned} \quad (3.25)$$

and therefore that the only non-zero portion of the momentum space smearing function, $\hat{\tilde{K}}_E$, is

$$\begin{aligned} \hat{\tilde{K}}_E &\equiv \tilde{K}_E + \delta\tilde{K}_E = \cosh(\pi(\omega_+ - \omega_-)) \tilde{K}_W + (e^{-\pi\omega_-} c + e^{\pi\omega_-} d) \\ &= -2 \sinh(\pi\omega_+) \sinh(\pi\omega_-) \tilde{K}_W. \end{aligned} \quad (3.26)$$

It then remains to obtain an explicit expression for \tilde{K}_W , which we can do by computing the Fourier transform of (3.8) in the western Rindler wedge. The

integration is performed in appendix 3.B. Substituting the result into (3.26), we have

$$\hat{K}_E = -2\pi^2 \left(\frac{z}{a}\right)^2 a^{-i(\omega_+ + \omega_-)} {}_2F_1\left(1 + i\omega_+, 1 + i\omega_-, 2, \frac{-z^2}{a^2}\right) \quad (3.27)$$

which is consistent with results found in the literature [32]. We therefore find that the smeared bulk operator (3.7) at $t = 0$, $x = a > 0$, and radial distance z , with support localized entirely within the eastern Rindler wedge, is given by

$$\begin{aligned} \Phi(0, a, z) = & -2\pi^2 \left(\frac{z}{a}\right)^2 \int d\omega_+ d\omega_- a^{-i(\omega_+ + \omega_-)} \\ & \times {}_2F_1\left(1 + i\omega_+, 1 + i\omega_-, 2, \frac{-z^2}{a^2}\right) \tilde{\mathcal{O}}_{\omega_+, \omega_-}^E \end{aligned} \quad (3.28)$$

where $\tilde{\mathcal{O}}_{\omega_+, \omega_-}^E$ is the momentum-space boundary operator, with support in the eastern wedge. We will write this explicitly in Rindler modes (cf. the Poincaré expression (3.6)) in the next section, but forgo unnecessary details here.

The action of the precursor (3.28) is UV-sensitive, and only well-defined when acting on an appropriate subclass of states. As we show explicitly in appendix 3.C, its vacuum two-point function reproduces the correct bulk correlator in the near-horizon limit.

As mentioned previously, a condition on the success of our procedure is that the bulk point be located in the entanglement wedge of the boundary region in which we attempt to localize the precursor. A natural question to ask is whether the gauge freedom in the smearing function can still be used to reconstruct a bulk point located outside the entanglement wedge. As we placed our bulk point in the eastern wedge, this would amount to trying to set the smearing function to zero in the eastern quadrant instead of the western quadrant as we did above. The set of conditions on the pure-gauge function $\delta\tilde{K}$ is then

$$\delta\tilde{K}_N = -\tilde{K}_N \quad \delta\tilde{K}_E = -\tilde{K}_E \quad \text{and} \quad \delta\tilde{K}_S = -\tilde{K}_S. \quad (3.29)$$

One can simply check that the overdetermined system of equations (3.21), (3.24) and (3.29) is now inconsistent: there no longer exists a solution for c and d . Hence we conclude that our model is consistent with the current understanding of bulk reconstruction, namely that it succeeds when the bulk point is inside – and fails when the point is outside – the causal/entanglement wedge. We shall comment more on this in the outlook, and elaborate on the distinction between the two types of bulk wedges, but first we turn to an alternative approach of localizing the bulk field, appealing instead to the entanglement structure in the CFT.

3.4 Localizing the Precursor via Entanglement

In this section we will present an alternative method for localizing the precursor. As before, our starting point is the smeared operator in Poincaré coordinates (3.7), which has non-zero support on the entire boundary and can be time-evolved to a bilocal at $t = 0$. Instead of using the gauge freedom to manipulate the support of the smearing function K however, we will now use entanglement in the field theory to map all bilocal operators into the eastern Rindler wedge. We will explicitly show that this gives the same result as that obtained in the previous section, thereby establishing that the freedom in the smearing function from gauge invariance can be equivalently understood from an entanglement perspective.

In (3.5), we expanded the CFT field ϕ in terms of Poincaré modes. We may equivalently write the mode expansion in terms of Rindler creation ($\omega < 0$) and annihilation ($\omega > 0$) operators $\beta_{\omega_{\pm}}$ with left- and right-moving⁴ Rindler momenta ω_{\pm} . These satisfy

$$[\beta_{\omega_{\pm}}, \beta_{\omega'_{\pm}}] = \omega_{\pm} \delta(\omega_{\pm} + \omega'_{\pm}) \quad \text{and} \quad \beta_{\omega_{\pm}}^{\dagger} = \beta_{-\omega_{\pm}}. \quad (3.30)$$

In light-cone coordinates $x_{\pm} \equiv t \pm x$, the Rindler expansion of the field in the eastern and western wedges (cf. figure 3.3) is, respectively,

$$\phi^E(t, x) = \int_{-\infty}^{+\infty} \frac{d\omega_+}{\omega_+} \beta_{\omega_+}^E |x_+|^{-i\omega_+} + \int_{-\infty}^{+\infty} \frac{d\omega_-}{\omega_-} \beta_{\omega_-}^E |x_-|^{i\omega_-} \quad (3.31)$$

$$\phi^W(t, x) = \int_{-\infty}^{+\infty} \frac{d\omega_+}{\omega_+} \beta_{\omega_+}^W |x_+|^{i\omega_+} + \int_{-\infty}^{+\infty} \frac{d\omega_-}{\omega_-} \beta_{\omega_-}^W |x_-|^{-i\omega_-} \quad (3.32)$$

where the Rindler mode functions are chosen such that they are positive frequency with respect to Rindler time, which we take to run upwards in both the eastern and western wedge. The light cone derivatives are

$$\begin{aligned} \partial_+ \phi^E &= -i \int_{-\infty}^{+\infty} d\omega_+ \beta_{\omega_+}^E |x_+|^{-i\omega_+-1} \\ \partial_- \phi^E &= i \int_{-\infty}^{+\infty} d\omega_- \beta_{\omega_-}^E |x_-|^{i\omega_- -1} \end{aligned} \quad (3.33)$$

$$\begin{aligned} \partial_+ \phi^W &= i \int_{-\infty}^{+\infty} d\omega_+ \beta_{\omega_+}^W |x_+|^{i\omega_+-1} \\ \partial_- \phi^W &= -i \int_{-\infty}^{+\infty} d\omega_- \beta_{\omega_-}^W |x_-|^{-i\omega_- -1} \end{aligned} \quad (3.34)$$

⁴In this section, to avoid clutter, we denote right movers by β_{ω_+} and left movers by β_{ω_-} , with no tilde on the left movers. Left and right movers commute.

and are manifestly purely left/right-moving. As a consequence, their time evolution becomes trivial:

$$\begin{aligned}\partial_+\phi(t, x) &= \partial_+\phi(0, x+t) \\ \partial_-\phi(t, x) &= \partial_-\phi(0, x-t).\end{aligned}\tag{3.35}$$

This was to be expected, since ϕ satisfies the 1+1-dimensional wave equation $\square\phi = 0$. This factorization along the null directions allows us to write the precursor, for a bulk operator shifted a distance a into the east, as a bilocal at $t = 0$:

$$\begin{aligned}\Phi(t = 0, x = a > 0, z) &= \int dx_+ dx_- K(0, a, z|x_+, x_-) \\ &\quad \times \partial_+\phi(0, x_+) \partial_-\phi(0, -x_-)\end{aligned}\tag{3.36}$$

where the smearing function (3.8), in light-cone coordinates, is

$$K(0, a, z|x_+, x_-) = \log\left(\frac{|z^2 - (x_+ - a)(x_- + a)|}{2z}\right) \equiv K.\tag{3.37}$$

Using (3.33) and (3.34), we can explicitly decompose the integral (3.36) over all four wedges:

$$\begin{aligned}\Phi(0, a, z) &= - \iint_N dx_+ dx_- \iint d\omega_+ d\omega_- K|x_+|^{-i\omega_+ - 1}|x_-|^{-i\omega_- - 1} \beta_{\omega_+}^E \beta_{\omega_-}^W \\ &\quad - \iint_S dx_+ dx_- \iint d\omega_+ d\omega_- K|x_+|^{i\omega_+ - 1}|x_-|^{i\omega_- - 1} \beta_{\omega_-}^E \beta_{\omega_+}^W \\ &\quad + \iint_E dx_+ dx_- \iint d\omega_+ d\omega_- K|x_+|^{-i\omega_+ - 1}|x_-|^{i\omega_- - 1} \beta_{\omega_-}^E \beta_{\omega_+}^E \\ &\quad + \iint_W dx_+ dx_- \iint d\omega_+ d\omega_- K|x_+|^{i\omega_+ - 1}|x_-|^{-i\omega_- - 1} \beta_{\omega_-}^W \beta_{\omega_+}^W.\end{aligned}\tag{3.38}$$

We may write this more succinctly in terms of the Fourier transform (3.23), paying careful attention to the signs of the momenta:

$$\begin{aligned}\Phi(0, a, z) &= \iint d\omega_+ d\omega_- \left(-\tilde{K}_N(\omega_+, \omega_-) \beta_{\omega_+}^E \beta_{\omega_-}^W - \tilde{K}_S(-\omega_+, -\omega_-) \beta_{\omega_+}^W \beta_{\omega_-}^E \right. \\ &\quad \left. + \tilde{K}_E(\omega_+, -\omega_-) \beta_{\omega_+}^E \beta_{\omega_-}^E + \tilde{K}_W(-\omega_+, \omega_-) \beta_{\omega_+}^W \beta_{\omega_-}^W \right).\end{aligned}\tag{3.39}$$

3.4.1 Mapping the Precursor into the Eastern Rindler Wedge

From the expression (3.39), one sees that upon time-evolving the boundary operator $\mathcal{O} = \partial_+\phi\partial_-\phi$ to the $t = 0$ Cauchy slice, one or both parts of the resulting bilocal may have support in the western wedge (indicated by β^W). We now demonstrate that the entanglement present in the Minkowski vacuum can be used to map these parts into the east. The set-up is illustrated schematically in figure 3.4.

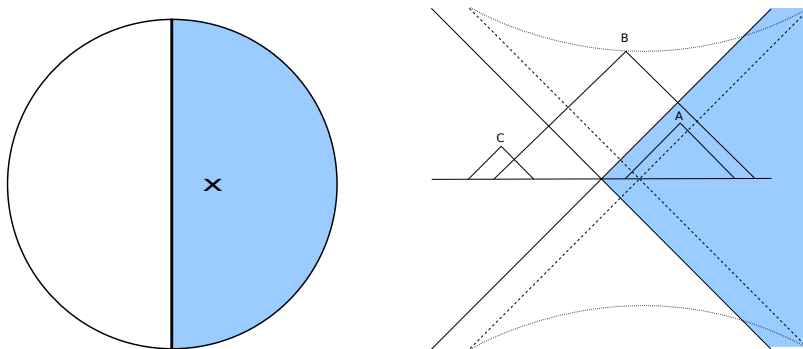


Figure 3.4: Left: $t = 0$ Cauchy slice, with a bulk point x displaced slightly into the eastern Rindler wedge (shaded). Right: time-evolution of local boundary operators to bilocals at $t = 0$. The dashed axes show the light-cone of the bulk point; the future and past singularities in the smearing function are indicated by the dotted lines. Point A falls entirely within the eastern wedge, while one leg of B , and both legs of C , must be mapped into the east using the entanglement of the Rindler vacuum. Note that with the bulk point as shown, at most one singular leg must be mapped, but this potential divergence is exactly cancelled by a decaying exponential arising from (3.40), so the resulting expression remains well-defined.

The key observation is that acting on the Minkowski vacuum with a Rindler operator, we have

$$\beta_{\omega_{\pm}}^W |0\rangle = e^{-\pi\omega_{\pm}} \beta_{-\omega_{\pm}}^E |0\rangle \quad (3.40)$$

which one can see by writing $|0\rangle \propto \bigotimes_{\omega} \sum_n e^{-\pi\omega n} |n\rangle_W \otimes |n\rangle_E$. We shall use this fact to write (3.39) entirely in terms of operators in the eastern wedge, β^E . For this mapping between western and eastern operators to succeed, we require only that both their left- and right-action on the vacuum state agree,

$$\Phi|0\rangle = \mathcal{O}_E|0\rangle \quad \text{and} \quad \langle 0|\Phi = \langle 0|\mathcal{O}_E \quad (3.41)$$

which is enough to ensure that 2-pt correlators are preserved. Our strategy is to satisfy the left equation by construction, and then check whether the right equation is also satisfied.

Performing this mapping allows us to write (3.39) as

$$\begin{aligned} \Phi(0, a, z)|0\rangle = & \iint d\omega_+ d\omega_- \left(-\tilde{K}_N(\omega_+, \omega_-) \beta_{\omega_+}^E \beta_{-\omega_-}^E e^{-\pi\omega_-} \right. \\ & -\tilde{K}_S(-\omega_+, -\omega_-) \beta_{-\omega_+}^E \beta_{\omega_-}^E e^{-\pi\omega_+} \\ & +\tilde{K}_E(\omega_+, -\omega_-) \beta_{\omega_+}^E \beta_{\omega_-}^E \\ & \left. +\tilde{K}_W(-\omega_+, \omega_-) \beta_{-\omega_+}^E \beta_{-\omega_-}^E e^{-\pi(\omega_+ + \omega_-)} \right) |0\rangle. \end{aligned} \quad (3.42)$$

Substituting the relations (3.24) gives

$$\begin{aligned} \Phi(0, a, z)|0\rangle &= \iint d\omega_+ d\omega_- \left(-\cosh(\pi\omega_+)e^{-\pi\omega_-} - \cosh(\pi\omega_-)e^{\pi\omega_+} \right. \\ &\quad \left. + \cosh(\pi(\omega_+ - \omega_-)) + e^{\pi(\omega_+ - \omega_-)} \right) \tilde{K}_W(\omega_+, \omega_-) \beta_{\omega_+}^E \beta_{-\omega_-}^E |0\rangle \end{aligned} \quad (3.43)$$

which can be simplified to

$$\Phi(0, a, z)|0\rangle = -2 \iint d\omega_+ d\omega_- \sinh(\pi\omega_+) \sinh(\pi\omega_-) \tilde{K}_W(\omega_+, \omega_-) \beta_{\omega_+}^E \beta_{-\omega_-}^E |0\rangle.$$

Plugging in in the explicit form of \tilde{K}_W , (3.68), we find

$$\begin{aligned} \Phi|0\rangle &= -2\pi^2 \left(\frac{z}{a}\right)^2 \int d\omega_+ d\omega_- a^{-i(\omega_+ + \omega_-)} \\ &\quad {}_2F_1\left(1 + i\omega_+, 1 + i\omega_-, 2, -\frac{z^2}{a^2}\right) \beta_{\omega_+}^E \beta_{-\omega_-}^E |0\rangle. \end{aligned} \quad (3.44)$$

which is precisely (3.28), with $\tilde{\mathcal{O}}_{\omega_+, \omega_-}^E = \beta_{\omega_+}^E \beta_{-\omega_-}^E$. One can check that this operator Φ satisfies the condition (3.41). This demonstrates that the entanglement structure of Minkowski space can be used to localize the precursor entirely within a single Rindler wedge, thus providing an alternative realization of the approach based on gauge freedom discussed above.

3.4.2 Mapping the Precursor in the ‘Wrong’ Rindler Wedge

To further explore this link between precursors and entanglement, let us now ask what happens if we instead attempt to map the bilocal operator into the western wedge. Since our bulk point is located in the east, we would naively expect this to fail, as this would correspond to reconstructing the bulk operator located outside the causal/entanglement wedge (cf. the end of section 3.3). Hence we refer to this as mapping the precursor into the *wrong* wedge.

The set-up is illustrated in figure 3.5. Following the same procedure as in the previous subsection, one obtains

$$\begin{aligned} \Phi(0, a, z)|0\rangle &= -2 \int d\omega_+ d\omega_- e^{\pi(\omega_- - \omega_+)} \sinh(\pi\omega_+) \sinh(\pi\omega_-) \\ &\quad \tilde{K}_W(\omega_+, \omega_-) \beta_{-\omega_+}^W \beta_{\omega_-}^W |0\rangle \\ &\propto \int d\omega_+ d\omega_- a^{-i(\omega_- + \omega_+)} e^{\pi(\omega_- - \omega_+)} \\ &\quad {}_2F_1\left(1 + i\omega_+, 1 + i\omega_-, 2, -\frac{z^2}{x^2}\right) \beta_{-\omega_+}^W \beta_{\omega_-}^W |0\rangle. \end{aligned} \quad (3.45)$$

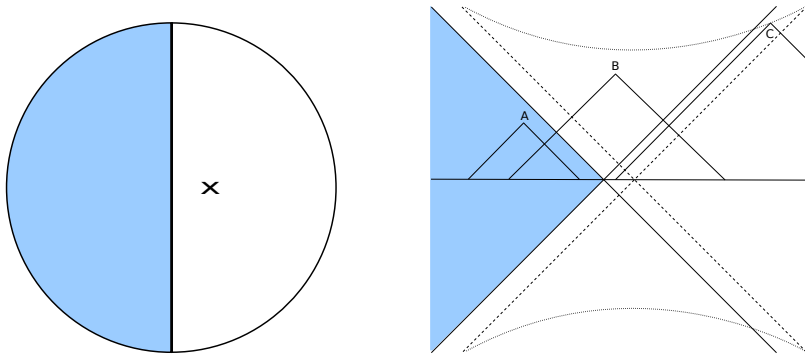


Figure 3.5: Left: $t = 0$ Cauchy slice, with a bulk point x displaced slightly into east as before, but reconstruction attempted in the western (wrong) wedge Rindler wedge (shaded). Right: time-evolution of local boundary operators to bilocals at $t = 0$. Note that while A and B can be mapped without difficulty, as discussed in the previous section, there are now points like C with two divergent legs, both of which must be mapped into the western wedge. This is one more exponential in momentum than we are capable of taming, and thus localization of the associated bulk point fails.

But upon conjugating (3.45), and taking $\omega_{\pm} \rightarrow -\omega_{\pm}$ under the integral, we find

$$\begin{aligned} \Phi^\dagger |0\rangle &\propto \int d\omega_+ d\omega_- a^{-i(\omega_- + \omega_+)} e^{-\pi(\omega_- - \omega_+)} \\ &{}_2F_1\left(1 + i\omega_+, 1 + i\omega_-, 2, -\frac{z^2}{x^2}\right) \beta_{-\omega_+}^W \beta_{\omega_-}^W |0\rangle \end{aligned} \quad (3.46)$$

in clear violation of the condition (3.41). Thus our entanglement mapping condition fails when the bulk operator lies in the complement of the selected boundary region.

The importance of this condition was recently emphasized in [80], who phrased it as the requirement of hermiticity. In particular, they proved that in order to satisfy (3.41), the field Φ must lie within the bulk entanglement wedge of the boundary region that contains the operator \mathcal{O} . Our model may therefore be taken as an explicit demonstration of this principle. Specifically, if one attempts to localize the boundary representation of a bulk operator in the complement, the resulting operator will be non-hermitian. In order to construct a well-defined precursor, the localization must be attempted within the entanglement wedge that includes the bulk field in question.

One can see that the wrong-wedge operator (3.45) is manifestly ill-behaved when acting on the Minkowski vacuum: in the limit $\omega_+ \gg 1$ and $\omega_- \ll -1$, we have two Rindler creation operators acting on $|0\rangle$, with a coefficient which grows exponentially. This means we create a state which is highly UV-sensitive (note the

singular legs that must be mapped in figure 3.5). Indeed, one can show that the two-point function $\langle 0|\Phi\Phi^\dagger|0\rangle$ diverges using the wrong-wedge operator Φ . The fact that UV-divergences occur in the same circumstance as when hermiticity is lost is suggestive, but we have not found a clear conceptual link between the two.

3.A Relating Fourier Transforms of the Smearing Function

In this appendix, we will prove the relations (3.24):

$$\begin{aligned}\tilde{K}_N(\omega_+, \omega_-) &= \cosh(\pi\omega_+) \tilde{K}_W(\omega_+, \omega_-) \\ \tilde{K}_S(\omega_+, \omega_-) &= \cosh(\pi\omega_-) \tilde{K}_W(\omega_+, \omega_-) \\ \tilde{K}_E(\omega_+, \omega_-) &= \cosh(\pi(\omega_+ - \omega_-)) \tilde{K}_W(\omega_+, \omega_-)\end{aligned}\tag{3.47}$$

where the Fourier transform of the smearing function, \tilde{K}_W , is given by (3.23), with K written in light-cone coordinates as in (3.37):

$$\begin{aligned}\tilde{K}_W(\omega_+, \omega_-) &= \int_{-\infty}^0 dx_+ \int_0^\infty dx_- \log\left(\frac{|z^2 - (x_+ - a)(x_- + a)|}{2z}\right) \\ &\quad |x_+|^{-i\omega_+ - 1} |x_-|^{-i\omega_- - 1} \\ &= \int_0^\infty dx_+ \int_0^\infty dx_- \log\left(\frac{|z^2 + (x_+ + a)(x_- + a)|}{2z}\right) \\ &\quad |x_+|^{-i\omega_+ - 1} |x_-|^{-i\omega_- - 1} \\ &= \int_{-\infty}^\infty du \int_{-\infty}^\infty dv \log\left(\frac{|z^2 + (e^u + a)(e^v + a)|}{2z}\right) e^{-i\omega_+ u} e^{-i\omega_- v}\end{aligned}\tag{3.48}$$

where in the last step we've made the change of variables $x_+ = e^u$, $x_- = e^v$. Note that the logarithm does not become singular in the western quadrant, as we shifted the bulk point into the east (cf. figure 3.4). For convenience, we may rescale the zero mode to remove the constant factor in the denominator of the argument of the logarithm. Hence, suppressing the ω_+ and ω_- subscripts, the explicit expression for δK in each of the four wedges may be written

$$\tilde{K}_W = \int_{-\infty}^\infty du \int_{-\infty}^\infty dv \log(|z^2 + (e^u + a)(e^v + a)|) e^{-i\omega_+ u} e^{-i\omega_- v}\tag{3.49}$$

$$\tilde{K}_N = \int_{-\infty}^\infty du \int_{-\infty}^\infty dv \log(|z^2 - (e^u - a)(e^v + a)|) e^{-i\omega_+ u} e^{-i\omega_- v}\tag{3.50}$$

$$\tilde{K}_E = \int_{-\infty}^\infty du \int_{-\infty}^\infty dv \log(|z^2 + (e^u - a)(e^v - a)|) e^{-i\omega_+ u} e^{-i\omega_- v}\tag{3.51}$$

$$\tilde{K}_S = \int_{-\infty}^{\infty} du \int_{-\infty}^{\infty} dv \log(|z^2 - (e^u + a)(e^v - a)|) e^{-i\omega_+ u} e^{-i\omega_- v}. \quad (3.52)$$

Let us begin by relating \tilde{K}_W and \tilde{K}_N . Define the function $f(u)$ for $u \in \mathbb{C}$ as⁵

$$f(u) \equiv \int_{-\infty}^{\infty} dv \log(z^2 + (e^u + a)(e^v + a)) e^{-i\omega_+ u} e^{-i\omega_- v}. \quad (3.53)$$

Note that integrating f over the real u -axis gives \tilde{K}_W (since $a > 0$), while integrating $f(u \pm i\pi)$ is of the same basic form as \tilde{K}_N ,

$$f(u \pm i\pi) = e^{\pm\pi\omega_+} \int_{-\infty}^{\infty} dv \log(z^2 - (e^u - a)(e^v + a)) e^{-i\omega_+ u} e^{-i\omega_- v} \quad (3.54)$$

up to a factor of $e^{\pm\pi\omega_+}$, and ambiguities due to the singularities in the logarithm. In particular, the argument of the log is negative when $z^2 < (e^u - a)(e^v + a)$, so there is a branch point at

$$u^* = \log\left(\frac{z^2}{e^v + a} + a\right) \quad (3.55)$$

and branch cuts running horizontally at $u \pm i\pi$ for $u > u^*$. Now, imagine a rectangular contour in the complex u -plane running from $-\infty$ to ∞ along the real axis, and then back the other way along $u \pm i\pi$ (that is, just inside the complex region prescribed by the branch cuts). Since we enclose no poles, the total contour integral vanishes, and we may write

$$0 = \int_{-\infty}^{\infty} du (f(u) - f(u \pm i\pi)) + \int_{\infty}^{\infty \pm i\pi} du f(u) + \int_{-\infty \pm i\pi}^{-\infty} du f(u) \quad (3.56)$$

where the last two terms are the vertical side contributions for the function evaluated at $u \rightarrow \pm\infty$ from the real axis to $\pm i\pi$. One takes the upper signs in (3.56) for the contour in the upper half-plane, which runs counter-clockwise, and the lower signs for the clockwise contour in the lower half. We then observe that the side contributions can be made to vanish by suitably deforming the contour off the real axis. Hence, dropping these terms and writing the above expression in terms of \tilde{K} , we have

$$0 = \tilde{K}_W - e^{\pm\pi\omega_+} \tilde{K}_N - e^{\pm\pi\omega_+} \int_{u^*}^{\infty} du \int_{-\infty}^{\infty} dv (\pm i\pi) e^{-i\omega_+ u} e^{-i\omega_- v} \quad (3.57)$$

where we've taken the principle value of the complex logarithm in (3.54), $\log(x) = \log|x| \pm i\pi$, where the upper/lower sign corresponds to approaching the negative

⁵For simplicity we included the v -integral in the definition of f . For the reader worried about its convergence, the following contour argument can still be made, relating the v -integrands, by defining $f(u) \equiv e^{-i\omega_- v} \log(z^2 + (e^u + a)(e^v + a)) e^{-i\omega_+ u}$ for fixed v .

real axis from the upper/lower half-plane, respectively (i.e., our choice of contour). By a linear combination of the two equations in (3.57), the third term on the r.h.s. cancels, and one obtains

$$\tilde{K}_N = \cosh(\pi\omega_+) \tilde{K}_W \quad (3.58)$$

which is the desired result. Similarly, one can show

$$\tilde{K}_S = \cosh(\pi\omega_-) \tilde{K}_W . \quad (3.59)$$

The derivation of the third relation, between \tilde{K}_W and \tilde{K}_E , follows a similar contour argument, but requires a slight change of coordinates. In particular, we first write (3.51) as

$$\tilde{K}_E = \int_{-\infty}^{\infty} dt \int_{-\infty}^{\infty} dx \log(|z^2 + (e^{t+x} - a)(e^{t-x} - a)|) e^{-i\omega t} e^{-ikx} \quad (3.60)$$

where we defined $\omega \equiv \omega_+ + \omega_-$ and $k \equiv \omega_- - \omega_+$, and similarly for \tilde{K}_W . We then define a function $g(x)$ for $x \in \mathbb{C}$,

$$g(x) \equiv \int_{-\infty}^{\infty} dt \log(z^2 + (e^{t+x} - a)(e^{t-x} - a)) e^{-i\omega t} e^{-ikx} \quad (3.61)$$

which will be related to (3.60) upon integrating along the x -axis, and observe that the integral of

$$g(x \pm i\pi) \equiv \int_{-\infty}^{\infty} dt \log(z^2 + (e^{t+x} + a)(e^{t-x} + a)) e^{-i\omega t} e^{-ikx} e^{\pm\pi k} \quad (3.62)$$

yields \tilde{K}_W .

We can now apply essentially the same argument as before. The argument of the logarithm in (3.60) is negative when $z^2 + a^2 + e^{2t} < 2ae^t \cosh x$, implying branch points at

$$x^* = \pm \cosh^{-1} \left(\frac{z^2 + a^2 + e^{2t}}{2ae^t} \right) . \quad (3.63)$$

We choose the branch cuts running out horizontally to infinity. The integration contours are then restricted to the rectangular region between the x -axis and $x \pm i\pi$, given an expression analogous to (3.56). Analytically continuing the logarithm to complex values as above, and dropping the side contributions, we have

$$0 = \tilde{K}_E - e^{\pm\pi k} \tilde{K}_W + \left(\int_{-\infty}^{-x^*} dx + \int_{x^*}^{\infty} dx \right) \int_{-\infty}^{\infty} dt (\pm i\pi) e^{-i\omega t} e^{-ikx} . \quad (3.64)$$

Taking a linear combination of these two equations, we obtain

$$\tilde{K}_E = \cosh(\pi(\omega_- - \omega_+)) \tilde{K}_W \quad (3.65)$$

as desired.

3.B Evaluating the Smearing Function

In this appendix we evaluate the Fourier integral of the smearing function in the western Rindler wedge, \tilde{K}_W (3.49),

$$\tilde{K}_W = \int_{-\infty}^{\infty} du \int_{-\infty}^{\infty} dv \log(z^2 + (e^u + a)(e^v + a)) e^{-i\omega_+ u} e^{-i\omega_- v} \quad (3.66)$$

where the argument of the log is always positive by virtue of our having shifted the bulk point into the east, as described in the main text. Integrating by parts twice, this becomes

$$\begin{aligned} \tilde{K}_W = & -\frac{1}{\omega_+ \omega_-} e^{-i\omega_+ u} e^{-i\omega_- v} \ln(z^2 + (e^u + a)(e^v + a)) \Big|_{u,v=-\infty}^{\infty} \\ & + \frac{1}{\omega_+ \omega_-} \int_{-\infty}^{\infty} du e^{-i\omega_+ u} e^{-i\omega_- v} \frac{e^u (e^v + a)}{z^2 + (e^u + a)(e^v + a)} \Big|_{v=-\infty}^{\infty} \\ & + \frac{1}{\omega_+ \omega_-} \int_{-\infty}^{\infty} dv e^{-i\omega_+ u} e^{-i\omega_- v} \frac{(e^u + a) e^v}{z^2 + (e^u + a)(e^v + a)} \Big|_{u=-\infty}^{\infty} \\ & - \frac{z^2}{\omega_+ \omega_-} \int_{-\infty}^{\infty} dudv e^{-i\omega_+ u} e^{-i\omega_- v} \frac{e^{u+v}}{(z^2 + (e^u + a)(e^v + a))^2}. \end{aligned} \quad (3.67)$$

The first three (boundary) terms can be made to vanish by a suitable contour deformation. The remaining double integral (the fourth term) can be evaluated to yield

$$\begin{aligned} \tilde{K}_W = & -\pi^2 \left(\frac{z}{a}\right)^2 a^{-i(\omega_+ + \omega_-)} \operatorname{csch}(\pi\omega_+) \operatorname{csch}(\pi\omega_-) \\ & \times {}_2F_1\left(1 + i\omega_+, 1 + i\omega_-, 2, \frac{-z^2}{a^2}\right). \end{aligned} \quad (3.68)$$

3.C Computing the Two-Point Function

As an extra check of our formalism, we include an explicit calculation of the two-point function, and show that it reduces to the correct AdS₂₊₁ correlator in the near-horizon limit. This will serve as a diagnostic of whether our expression for the bulk field constructed from boundary data entirely in the eastern wedge, (3.44)

$$\begin{aligned} \Phi(0, a, z) = & -2\pi^2 \left(\frac{z}{a}\right)^2 \int d\omega_+ d\omega_- a^{-i(\omega_+ + \omega_-)} \\ & \times {}_2F_1\left(1 + i\omega_+, 1 + i\omega_-, 2, \frac{-z^2}{a^2}\right) \beta_{\omega_+}^E \beta_{-\omega_-}^E \end{aligned} \quad (3.69)$$

is well-defined. Here $\beta_{\omega_{\pm}}^E$ are the Rindler creation ($\omega < 0$) and annihilation ($\omega > 0$) operators in the eastern wedge, as defined in the main text. Since we work entirely in the eastern wedge in what follows, we shall henceforth suppress the superscript E to minimize clutter. Inside the two-point function, we will have left/right moving Rindler operators acting on the Minkowski vacuum. As the left- and right-movers commute, the four- β correlator is

$$\begin{aligned} \langle 0 | \beta_{\omega_+} \beta_{-\omega_-} \beta_{\omega'_+} \beta_{-\omega'_-} | 0 \rangle &= \delta(\omega_+ + \omega'_+) \delta(\omega_- + \omega'_-) \\ &\times \left(\frac{\omega_+}{1 - e^{-2\pi\omega_+}} \right) \left(\frac{\omega_-}{e^{2\pi\omega_-} - 1} \right). \end{aligned} \quad (3.70)$$

The bulk two-point function we seek to examine is therefore written explicitly as

$$\begin{aligned} \langle \Phi(a_1, z_1) \Phi(a_2, z_2) \rangle &= 4\pi^4 \left(\frac{z_1 z_2}{a_1 a_2} \right)^2 \int_{-\infty}^{\infty} d\omega_+ d\omega_- d\omega'_+ d\omega'_- \delta(\omega_+ + \omega'_+) \delta(\omega_- + \omega'_-) \\ &\times a_1^{-i(\omega_+ + \omega_-)} a_2^{-i(\omega'_+ + \omega'_-)} \left(\frac{\omega_+}{1 - e^{-2\pi\omega_+}} \right) \left(\frac{-\omega_-}{1 - e^{2\pi\omega_-}} \right) \\ &\times {}_2F_1 \left(1 + i\omega_+, 1 + i\omega_-, 2, \frac{-z_1^2}{a_1^2} \right) \\ &\times {}_2F_1 \left(1 + i\omega'_+, 1 + i\omega'_-, 2, \frac{-z_2^2}{a_2^2} \right). \end{aligned}$$

By virtue of the delta functions, the integrals over primed frequencies are trivial:

$$\begin{aligned} \langle \Phi(a_1, z_1) \Phi(a_2, z_2) \rangle &= \pi^4 \left(\frac{z_1 z_2}{a_1 a_2} \right)^2 \int_{-\infty}^{\infty} d\omega_+ d\omega_- \left(\frac{a_1}{a_2} \right)^{-i(\omega_+ + \omega_-)} \\ &\times \omega_+ \omega_- (\coth(\pi\omega_+) + 1) (\coth(\pi\omega_-) - 1) \\ &\times {}_2F_1 \left(1 + i\omega_+, 1 + i\omega_-, 2, \frac{-z_1^2}{a_1^2} \right) \\ &\times {}_2F_1 \left(1 - i\omega_+, 1 - i\omega_-, 2, \frac{-z_2^2}{a_2^2} \right). \end{aligned} \quad (3.71)$$

Unfortunately, we have not succeeded in evaluating the remaining integrals exactly. However, we can investigate the behaviour in the near-horizon limit, equivalent to taking $z_1/a_1, z_2/a_2 \rightarrow \infty$. To avoid subtleties associated with the branch cut at infinity, we first performing a $z \rightarrow 1/z$ transform,

$$\begin{aligned} F(a, b, c; z) &= \frac{\Gamma(c)\Gamma(b-a)}{\Gamma(b)\Gamma(c-a)} (-z)^{-a} F(a, a-c+1, a-b+1, 1/z) \\ &+ \frac{\Gamma(c)\Gamma(a-b)}{\Gamma(a)\Gamma(c-b)} (-z)^{-b} F(b, b-c+1, -a+b+1, 1/z) \end{aligned} \quad (3.72)$$

which allows us to expand in the limit where the fourth argument of the hypergeometric function vanishes. Applying this to the product of hypergeometric functions

in (3.71), and then expanding around $z/a \rightarrow \infty$ yields, to first order,

$$\begin{aligned}
 & {}_2F_1\left(1+i\omega_+, 1+i\omega_-, 2, \frac{-z_1^2}{a_1^2}\right) {}_2F_1\left(1-i\omega_+, 1-i\omega_-, 2, \frac{-z_2^2}{a_2^2}\right) \left(\frac{a_1 a_2}{z_1 z_2}\right)^{-2} \\
 &= \left[\left(\frac{z_2}{a_2}\right)^{2i\omega_-} \frac{\Gamma(i(\omega_- - \omega_+))}{\Gamma(1+i\omega_-)\Gamma(1-i\omega_+)} + \left(\frac{z_2}{a_2}\right)^{2i\omega_+} \frac{\Gamma(-i(\omega_- - \omega_+))}{\Gamma(1-i\omega_-)\Gamma(1+i\omega_+)} \right] \\
 &\times \left[\left(\frac{z_1}{a_1}\right)^{-2i\omega_+} \frac{\Gamma(i(\omega_- - \omega_+))}{\Gamma(1+i\omega_-)\Gamma(1-i\omega_+)} + \left(\frac{z_1}{a_1}\right)^{-2i\omega_-} \frac{\Gamma(-i(\omega_- - \omega_+))}{\Gamma(1-i\omega_-)\Gamma(1+i\omega_+)} \right].
 \end{aligned}$$

Without loss of generality, we shall assume $z_2 > z_1$. Substituting this expansion into the two point function yields

$$\langle 0 | \Phi(0, a_1, z_1) \Phi(0, a_2, z_2) | 0 \rangle = \int d\omega_+ \int d\omega_- (U + L) \quad (3.73)$$

where we've defined

$$\begin{aligned}
 U &\equiv \omega_- \omega_+ e^{\pi(\omega_+ - \omega_-)} \operatorname{csch}(\pi\omega_-) \operatorname{csch}(\pi\omega_+) \left(\frac{a_1}{a_2}\right)^{-i(\omega_- + \omega_+)} \\
 &\times \left(\frac{\left(\frac{z_1^2}{a_1^2}\right)^{-i\omega_-} \Gamma(i\omega_+ - i\omega_-)}{\Gamma(1 - i\omega_-)\Gamma(i\omega_+ + 1)} + \frac{\left(\frac{z_1^2}{a_1^2}\right)^{-i\omega_+} \Gamma(i\omega_- - i\omega_+)}{\Gamma(i\omega_- + 1)\Gamma(1 - i\omega_+)} \right) \\
 &\times \left(\frac{\left(\frac{z_2^2}{a_2^2}\right)^{i\omega_-} \Gamma(i\omega_- - i\omega_+)}{\Gamma(i\omega_- + 1)\Gamma(1 - i\omega_+)} \right)
 \end{aligned} \quad (3.74)$$

$$\begin{aligned}
 L &\equiv \omega_- \omega_+ e^{\pi(\omega_+ - \omega_-)} \operatorname{csch}(\pi\omega_-) \operatorname{csch}(\pi\omega_+) \left(\frac{a_1}{a_2}\right)^{-i(\omega_- + \omega_+)} \\
 &\times \left(\frac{\left(\frac{z_1^2}{a_1^2}\right)^{-i\omega_-} \Gamma(i\omega_+ - i\omega_-)}{\Gamma(1 - i\omega_-)\Gamma(i\omega_+ + 1)} + \frac{\left(\frac{z_1^2}{a_1^2}\right)^{-i\omega_+} \Gamma(i\omega_- - i\omega_+)}{\Gamma(i\omega_- + 1)\Gamma(1 - i\omega_+)} \right) \\
 &\times \left(\frac{\left(\frac{z_2^2}{a_2^2}\right)^{i\omega_+} \Gamma(i\omega_+ - i\omega_-)}{\Gamma(1 - i\omega_-)\Gamma(i\omega_+ + 1)} \right).
 \end{aligned} \quad (3.75)$$

We will first perform the integral over ω_- , by viewing U and L as functions on the complex ω_- -plane. One can then easily show the following:

- U and L have simple poles at $\omega_- = \omega_+ \pm ni$, for $n \in \mathbb{Z}$.
- $|U(i\omega_-)| \rightarrow 0$ and $|L(-i\omega_-)| \rightarrow 0$ in the limit $\omega_- \gg 1$.

- $U + L$ has no poles on the real ω_- axis.

With these properties in hand, the integral can be performed via the residue theorem, where we close the contour in the upper/lower half-plane for U/L , respectively:

$$\begin{aligned}
 \langle \Phi \Phi \rangle &= \int d\omega_+ \int d\omega_- (U + L) \tag{3.76} \\
 &= \int d\omega_+ 2\pi i \left[-\text{Res}(L, \omega_+) + \sum_{n=1}^{\infty} (\text{Res}(U, \omega_+ + ni) - \text{Res}(L, \omega_+ - ni)) \right] \\
 &\approx \int d\omega_+ \frac{-2}{\pi} \left(\frac{z_1}{z_2} \right)^{-2i\omega_+} \left(2 \log \left(\frac{a_2}{z_2} \right) + 2\gamma + \psi(i\omega_+) + \psi(-i\omega_+) \right)
 \end{aligned}$$

where $\psi(z) = \Gamma'(z)/\Gamma(z)$ and $\gamma = -\psi(1)$. In evaluating the residues we used that $z_i/a_i \gg 1$ for $i = 1, 2$.

The integral over ω_+ is evaluated in a similar fashion. Viewing the integrand as a function in the complex ω_+ -plane, one can see that it is well behaved on the real axis, and goes to zero at $+i\infty$. Closing the integration contour in the upper half-plane, the residue theorem yields

$$\begin{aligned}
 \langle \Phi \Phi \rangle &\approx \int d\omega_+ \frac{-2}{\pi} \left(\frac{z_1}{z_2} \right)^{-2i\omega_+} \left(2 \log \left(\frac{a_2}{z_2} \right) + 2\gamma + \psi(i\omega_+) + \psi(-i\omega_+) \right) \\
 &= 2\pi i \sum_{n=1}^{\infty} \left(\frac{-2iz_1^{2n}}{\pi z_2^{2n}} \right) \propto \frac{z_1^2}{z_2^2 - z_1^2} \tag{3.77}
 \end{aligned}$$

which one can recognise as the correct two-point function for a massless scalar in AdS_{2+1} , i.e.

$$\langle \Phi(0, a_1, z_1) \Phi(0, a_2, z_2) \rangle = \frac{1}{e^S \sinh(S)} \propto \frac{z_1^2}{z_2^2 - z_1^2} \tag{3.78}$$

where the geodesic distance S in the near-horizon limit is given by $S = \log(z_2/z_1)$.

QEC from BRST

This chapter is based on the paper [4].

In chapter 3 we saw that bulk information in the CFT is ambiguous, because there are multiple non-local operators in the CFT equal to the same local bulk operator. In this chapter we will do three things. First of all, we will recast this ambiguity in the language of BRST symmetry, and conjecture that in the large N limit, the difference between two precursors is a BRST exact and ghost-free term. Second, using the BRST formalism and working in a simple model with global symmetries, we will re-derive a precursor ambiguity appearing in earlier work. Finally, we will show within this model that this BRST ambiguity has the right number of parameters to explain the freedom to localize precursors within the boundary of an entanglement wedge order by order in the large N expansion.

4.1 Introduction

The AdS/CFT correspondence is the most precise non-perturbative definition of quantum gravity. A central problem is how local bulk physics emerges from CFT data. As we saw before, this question has been studied extensively and is reasonably well-understood at large N , for small perturbations around vacuum AdS. In this limit, a bulk field Φ at a point X is defined by integrating a local CFT operator \mathcal{O} over the boundary with an appropriate smearing function K :

$$\Phi(X) = \int dt d^{d-1}x K(X|t, x) \mathcal{O}(x) + O\left(\frac{1}{N}\right). \quad (4.1)$$

This CFT operator can subsequently be time evolved to a single time slice using the CFT Hamiltonian, which gives a non-local operator P in the CFT corresponding with the field $\Phi(X)$ in the bulk. As the reader can recall from the previous chapter 3, this type of operator is called a precursor [70–72].

The study of precursors is fundamental to understanding a concrete realization of holography. There are several unresolved questions one can ask, such as how to construct precursors that correspond to bulk fields near or behind a black hole horizon. Here we focus on two particular puzzles that are related to each other, and were previously mentioned in chapter 3. At large N , bulk locality requires the precursor to commute with all local CFT operators at a fixed time, while basic properties of quantum field theory demand that only trivial operators can commute with all local operators at a given time [73]. Another is that a local bulk operator corresponds with many different precursors with different spatial support in the CFT, because the bulk field can be reconstructed in a particular spatial region of the CFT as long as it is contained in the corresponding entanglement wedge of that region.

Both of these apparent paradoxes can be resolved by requiring that different precursors are not equivalent as true CFT operators [73]. In particular, the difference between two precursors corresponding to the same bulk field seems to have no clear physical meaning, and must act trivially on some class of states. In what follows, we will refer to this perplexing feature as the ‘precursor ambiguity’.

In [73] and [69] some progress was made in giving a guiding principle for constructing the ambiguity between two precursors corresponding to the same bulk field. The former approach recasts the AdS/CFT dictionary in the language of quantum error correction (QEC). From this viewpoint, the ambiguity is an operator which acts trivially in the code subspace of QEC, which in this case is naturally thought of as the space of states corresponding to low energy excitations of the bulk. The latter work, on the other hand, proposed that gauge symmetry in the CFT can give a prescription to construct the precursor ambiguity. Moreover, they claimed that the code subspace is the full space of gauge invariant states.

Inspired by these works, we showed in chapter 3 how bulk information can be localized in the CFT by using boundary gauge invariance on one hand, and entanglement in the other. In this chapter, we will explore the former in greater detail, and explain how boundary gauge invariance can play an important role relating different precursors (corresponding to the same bulk point) to each other. We start in section 4.2 by proposing the language of BRST symmetry as a tool for making the precursor ambiguity concrete. In section 4.3, we show that this approach nicely reduces to an already identified precursor ambiguity in the presence of a global $SO(N)$ symmetry [69]. Furthermore, it has the added benefit that it generalizes to arbitrary gauge theories at any N . In section 4.4 we show in the toy model of chapter 3 how this precursor ambiguity has the right number of parameters to enable us to localize precursors in the boundary of the entanglement wedge order by order in $1/N$.

4.2 Proposal: Precursor Ambiguities from BRST

In most of the known examples of holography, the boundary theory has some gauge symmetry. The presence of these ‘unphysical’ degrees of freedom renders the naive path integral for gauge theories divergent. One approach to deal with these problems while covariantly quantizing the gauge theory is the BRST formalism [81, 82]. The rough idea is to replace the original gauge symmetry with a global symmetry, by enlarging the theory and introducing additional fields. This new rigid symmetry, the BRST symmetry, will still be present after fixing the gauge. Since the generator of the BRST symmetry Q_{BRST} is nilpotent of order two, we can construct its cohomology which will describe the gauge invariant observables of the original theory.

We propose that the natural framework to understand precursor ambiguities is the language of BRST symmetry. In particular, we claim that if P_1 and P_2 are two precursors in the large N limit corresponding with the same local bulk field $\Phi(X)$, then $P_1 - P_2 = \mathcal{O}$ where

- \mathcal{O} is BRST exact: $\mathcal{O} = \{Q_{\text{BRST}}, \tilde{\mathcal{O}}\}$
- \mathcal{O} does not contain any (anti-)ghosts.

By construction this leaves any correlation function of gauge invariant operators in arbitrary physical states invariant

$$\langle \mathcal{O}_1 \cdots \mathcal{O}_i \cdots \mathcal{O}_n \rangle = \langle \mathcal{O}_1 \cdots (\mathcal{O}_i + \{Q_{\text{BRST}}, \tilde{\mathcal{O}}\}) \cdots \mathcal{O}_n \rangle \quad (4.2)$$

since $[Q_{\text{BRST}}, \mathcal{O}_i] = 0$ for a gauge invariant operator \mathcal{O}_i , and $Q_{\text{BRST}}|\psi\rangle = 0$ for a gauge invariant state $|\psi\rangle$.

As an example, we will show in the next section 4.3 that in the case of N free scalars with a global $\text{SO}(N)$ symmetry, we can reproduce the results of [69]. That means, there exists an operator $\tilde{\mathcal{O}}$ such that

$$\{Q_{\text{BRST}}, \tilde{\mathcal{O}}\} \sim L^{ij} A^{ij} \quad (4.3)$$

where L^{ij} is the generator of the $\text{SO}(N)$ symmetry, and A^{ij} is any operator in the adjoint.

Note that while the BRST ambiguity is well-defined for any gauge theory and even at finite N , the notion of bulk locality only makes sense perturbatively in $1/N$. In order to connect the abstract BRST ambiguity to concrete equivalences between different CFT operators, we need to make use of the large N expansion. In particular, the precursor ambiguity we find, should only be valid within states where the number of excitations is small compared to N .

4.3 BRST Symmetry of N Real Scalars

In this section we will apply the BRST formalism to a theory of N real scalars. The Lagrangian for this gauge theory in the covariant gauge is given by

$$\mathcal{L} = -\frac{1}{4}(F_{\mu\nu}^a)^2 - \frac{1}{2}D^\mu\phi^i D_\mu\phi_i + \frac{\xi}{2}(B^a)^2 - B^a\partial^\mu A_\mu^a - \partial^\mu\bar{c}^a(D_\mu c)^a \quad (4.4)$$

where the auxiliary field B^a can be integrated out using $\xi B^a = \partial^\mu A_\mu^a$. We take the ϕ^i in the fundamental representation of $\text{SO}(N)$, while the ghost c^a , anti-ghost \bar{c}^a and the gauge field A_μ^a are in the adjoint. The (anti-)ghosts are scalar fermion fields. The covariant derivatives are given by

$$(D_\mu c)^a = \partial_\mu c^a + gf^{abc}A_\mu^b c^c \quad (4.5)$$

and

$$(D_\mu\phi)^i = \partial_\mu\phi^i - igA_\mu^a(T^a)_{ij}\phi^j. \quad (4.6)$$

Note that $D_\mu\phi^i$ is real since the matrices $(T^a)_{ij}$ are purely imaginary for $\text{SO}(N)$. The field strength F is given by

$$F_{\mu\nu}^a = \partial_\mu A_\nu^a - \partial_\nu A_\mu^a + gf^{abc}A_\mu^b A_\nu^c. \quad (4.7)$$

Consider the following BRST transformations:

$$\begin{aligned} \delta_B A_\mu^a &= \epsilon(D_\mu c)^a \\ \delta_B \phi^i &= ig\epsilon c^a(T^a)_{ij}\phi^j \\ \delta_B c^a &= -\frac{1}{2}g\epsilon f^{abc}c^b c^c \\ \delta_B \bar{c}^a &= \epsilon B^a \\ \delta_B B^a &= 0 \end{aligned} \quad (4.8)$$

where ϵ is a constant Grassmann parameter. The Lagrangian (4.4) is invariant under these transformations, up to a total derivative:

$$\delta_B \mathcal{L} = -\epsilon \partial^\mu (B^a (D_\mu c)^a). \quad (4.9)$$

4.3.1 The BRST Charge

In order to compute the BRST charge, we start by constructing the Noether current associated to this symmetry. Taking the boundary term into account, we get

$$J^\mu = \sum_\alpha \frac{\delta \mathcal{L}}{\delta(\partial_\mu \Phi_\alpha)} \delta_B \Phi_\alpha + B^a (D^\mu c)^a \quad (4.10)$$

where the sum runs over all possible fields in the Lagrangian, and we use left differentiation when dealing with fermionic variables. The BRST charge is then defined via

$$Q_{\text{BRST}} = \int d^{d-1}x J^0. \quad (4.11)$$

Let's start by computing the variations and defining the conjugate momenta

$$\begin{aligned} \frac{\delta \mathcal{L}}{\delta(\partial_\mu \phi^i)} &= -D^\mu \phi^i & \Pi^i &\equiv -D^0 \phi^i \\ [\phi^i(x), \Pi^j(y)] &= \delta^{ij} \delta^{(d-1)}(x-y) \end{aligned} \quad (4.12)$$

$$\begin{aligned} \frac{\delta \mathcal{L}}{\delta(\partial_\mu c^a)} &= (\partial^\mu \bar{c})^a & \pi_c^a &\equiv (\partial^0 \bar{c})^a \\ \{c^a(x), \pi_c^b(y)\} &= \delta^{ab} \delta^{(d-1)}(x-y) \end{aligned} \quad (4.13)$$

$$\begin{aligned} \frac{\delta \mathcal{L}}{\delta(\partial_\mu \bar{c}^a)} &= -(D^\mu c)^a & \pi_{\bar{c}}^a &\equiv -(D^0 c)^a \\ \{\bar{c}^a(x), \pi_{\bar{c}}^b(y)\} &= \delta^{ab} \delta^{(d-1)}(x-y) \end{aligned} \quad (4.14)$$

and finally for the gauge field

$$\begin{aligned} \frac{\delta \mathcal{L}}{\delta(\partial_\mu A_\nu^a)} &= -F^{\mu\nu,a} - \eta^{\mu\nu} B^a & \Pi^{\nu,a} &\equiv -F^{0\nu,a} - \eta^{0\nu} B^a \\ [A_\mu^a(x), \Pi^{\nu,b}(y)] &= \delta_\mu^\nu \delta^{ab} \delta^{(d-1)}(x-y). \end{aligned} \quad (4.15)$$

That gives the following Noether current

$$\begin{aligned} J^\mu &= (-F^{\mu\nu,a} - \eta^{\mu\nu} B^a) (D_\nu c)^a - ig D^\mu \phi^i c^a (T^a)_{ij} \phi^j \\ &\quad - \frac{1}{2} g (\partial^\mu \bar{c}^a) f^{abc} c^b c^c. \end{aligned} \quad (4.16)$$

The BRST charge is then given by

$$\begin{aligned} Q_{\text{BRST}} &= \int d^{d-1}x \Pi^{\nu,a} (D_\nu c)^a + ig \Pi^i c^a (T^a)_{ij} \phi^j - \frac{1}{2} g f^{abc} \pi_c^a c^b c^c \\ &= \int d^{d-1}x \Pi^{0,a} \pi_{\bar{c}}^a + \Pi^{i,a} (\partial_i c)^a - g f^{abc} \Pi^{i,c} A_i^b c^a \\ &\quad + ig \Pi^i c^a (T^a)_{ij} \phi^j - \frac{1}{2} g f^{abc} \pi_c^a c^b c^c. \end{aligned} \quad (4.17)$$

We can define the generators of the $\text{SO}(N)$ symmetry, using the Noether currents associated with the gauge transformations. The current has two contributions, one from the Yang-Mills parts F^2 and one from the matter part $(D\phi)^2$:

$$\begin{aligned} J_{\text{matter}}^a &\equiv i \Pi^i (T^a)_{ij} \phi^j & J_{\text{gauge}}^a &\equiv f^{abc} \Pi^{i,b} A_i^c \\ J^a &\equiv (J_{\text{matter}}^a + J_{\text{gauge}}^a). \end{aligned} \quad (4.18)$$

This finally leads to the the BRST charge:

$$Q_{\text{BRST}} = \int d^{d-1}x \left(g c^a J^a - \frac{1}{2} g f^{abc} \pi_c^a c^b c^c + \Pi^{0,a} \pi_c^a + \Pi^{i,a} (\partial_i c)^a \right). \quad (4.19)$$

The charge generates the BRST transformations (4.8) on the fields via

$$\delta_{\text{B}} \Phi_\alpha = \epsilon [\Phi_\alpha, Q_{\text{BRST}}]_{\pm}. \quad (4.20)$$

Using this, we can derive the BRST transformations of the conjugate momenta:

$$\begin{aligned} \delta_{\text{B}} \Pi^{0,a} &= 0 \\ \delta_{\text{B}} \Pi^{j,k} &= -g \epsilon f^{kab} c^a \Pi^{j,b} \\ \delta_{\text{B}} \Pi^k &= -i g \epsilon c^a \Pi^i (T^a)_{ik} \\ \delta_{\text{B}} \pi_c^a &= 0 \\ \delta_{\text{B}} \pi_c^b &= g \epsilon J^b - \epsilon \partial_i \Pi^{i,b} - g \epsilon f^{bde} \pi_c^d c^e \end{aligned} \quad (4.21)$$

and one can verify, using the Jacobi identity and $[T^a, T^b] = i f^{abc} T^c$, that Q_{BRST} is nilpotent when acting on the fields and their conjugate momenta, as it should.

4.3.2 Reduction to a Global $\text{SO}(N)$ Symmetry

In order to connect with previous work on precursors [69], we are interested in degrading the $\text{SO}(N)$ gauge symmetry to an ordinary global symmetry. One crude way of accomplishing this, is by setting the gauge fields $A_\mu^a = 0$. In this case, the ghosts become quantum mechanical (position independent) and the BRST charge reduces to

$$\begin{aligned} Q_{\text{BRST}} &= \int d^{d-1}x g c^a J^a - \frac{1}{2} g f^{abc} \pi_c^a c^b c^c \\ J^a &= i \Pi^i (T^a)_{ij} \phi^j \end{aligned} \quad (4.22)$$

where the global $\text{SO}(N)$ generator is given by $L^a = \int d^{d-1}x J^a(x)$.

Now consider an operator \mathcal{O}^a in the adjoint, and compute the anti-commutator of the BRST charge with $\pi_c^a \mathcal{O}^a$:

$$\begin{aligned} \{Q_{\text{BRST}}, \pi_c^d \mathcal{O}^d\} &= \int d^{d-1}x g \{c^a J^a, \pi_c^d \mathcal{O}^d\} - \frac{1}{2} g f^{abc} \{\pi_c^a c^b c^c, \pi_c^d \mathcal{O}^d\} \\ &= g \int d^{d-1}x \mathcal{O}^a J^a = g L^a \mathcal{O}^a \end{aligned} \quad (4.23)$$

where we used that the generator of global $\text{SO}(N)$ transformations rotates the operator \mathcal{O} as $[J^a, \mathcal{O}^b] = f^{abc} \mathcal{O}^c$. This expression is BRST exact by construction, and ghost-free. Adding this to a CFT operator will have no effect whatsoever within correlation functions in physical states. It is exactly the precursor ambiguity found in [69].

4.4 Localizing Precursors in a Toy Model

In the previous section, we computed the ambiguous part of the precursors as a BRST exact and ghost-free operator. This ambiguity can be viewed as the redundant, quantum error correcting part of the precursors. Once it has been identified, the physical information contained in the precursors should become clear. In this section we will study the particular ambiguity (4.23) in a holographic toy model. We will show that this ambiguity has the same structure as an HKLL series, and that it seems to contain enough freedom to localize bulk information in a particular region of the CFT by setting the smearing function to zero in that region. This hints that the procedure we did – localizing bulk information using smearing function ambiguities – to leading order in $1/N$ in the last chapter, can be carried out order by order in $1/N$.

4.4.1 The Model

The model will look familiar to the readers of chapter 3, and is a CFT containing N free scalar fields in $1 + 1$ spacetime dimensions:

$$\mathcal{L} = \sum_{i=1}^N -\frac{1}{2} \partial_\mu \phi^i \partial^\mu \phi^i. \quad (4.24)$$

There is a $\Delta = 2$ primary operator $\mathcal{O} = \partial_\mu \phi^i \partial^\mu \phi^i$ which we take to be dual to a massless scalar Φ in AdS_{2+1} .

Following (4.23), we know that the precursor ambiguity is given by $L^{ij} A^{ij}$ where A^{ij} is any operator in the adjoint of $\text{SO}(N)$ and L^{ij} is the generator of global $\text{SO}(N)$ transformations. Note that we do not gauge the $\text{SO}(N)$ transformations in this model, but only keep the global part of the $\text{SO}(N)$ transformations by setting $A_\mu^a = 0$ in the full gauge theory discussed in section 4.3. One can think of the global symmetry being present as a toy model for the full gauge theory.

Expanding the boundary fields ϕ^i in terms of left/right-moving creation and annihilation modes, one can compute the generator of global rotations

$$L^{ij} = \int \frac{dk}{2k} \left(\alpha_k^\dagger{}^{[i} \alpha_k^{j]} + \tilde{\alpha}_k^\dagger{}^{[i} \tilde{\alpha}_k^{j]} \right) \quad (4.25)$$

where the tilde denotes a right-moving polarization of the creation or annihilation modes and any zero mode contributions are left out. If there is no confusion what momentum a given mode has, we will omit the subscript k .

4.4.2 Precursor Localization Perturbatively in $1/N$

The bulk field Φ in global AdS_3 can be constructed at large N by smearing quadratic operators of the form $\mathcal{O} \sim \alpha_k \tilde{\alpha}_{k'}$ over a particular region of the CFT:

$$\Phi(X) = \int d^2x K_1(X|x) \mathcal{O}(x) + O\left(\frac{1}{\sqrt{N}}\right) \quad (4.26)$$

where the smearing function K obeys the bulk free wave equation

$$\square_{\text{AdS}_3} K_1(X|x) = 0. \quad (4.27)$$

This procedure correctly reproduces the bulk two-point function. The precursor can be obtained from (4.26) by time evolving the CFT operator to a single time slice. Extending the HKLL procedure perturbatively in $1/N$ will look schematically as follows [35, 83]:

$$\begin{aligned} \Phi(X) &= \int d^2x K_1(X|x) \mathcal{O}(x) \\ &+ \frac{1}{\sqrt{N}} \iint d^2x d^2x' K_2(X|x, x') \mathcal{O}(x) \mathcal{O}(x') + O\left(\frac{1}{N}\right) \end{aligned} \quad (4.28)$$

where the expansion parameter is $1/\sqrt{N}$ instead of $1/N$ because we are dealing with a vector-like theory [84].

In chapter 3 it was shown that, at leading order in $1/N$, the spatial support of the smearing function K_1 (and hence the information of the bulk field) can be localized in a particular Rindler wedge of the CFT due to an ambiguity in the smearing function. This freedom can be understood by noting that the term $\alpha_{k_1}^{\dagger i} \tilde{\alpha}_{k_2}^i$ can be added to \mathcal{O} within two-point functions since it annihilates the vacuum in both directions. While this two-parameter family of freedom is enough to localize the bulk field at leading order in N , one can see that it generically will be insufficient to set K_2 to zero in particular region, because this requires a four-parameter family of freedom. Since changing the smearing function corresponds with picking a different precursor, we would like to identify the aforementioned freedom in the smearing function with the precursor ambiguity. In what follows, we will explain how the precursor ambiguity $L^{ij} A^{ij}$ has enough freedom to localize bulk information order by order in $1/N$.

Start by considering the following quadratic (adjoint) operator

$$A_2^{ij} \equiv \alpha_{k_1}^{\dagger i} \tilde{\alpha}_{k_2}^j. \quad (4.29)$$

We showed that a possible ambiguity of the precursor is given by $L^{ij} A_2^{ij}$. Normal

ordering yields

$$\begin{aligned}
 \frac{1}{N^{\frac{3}{2}}} L^{ij} A_2^{ij} &= \frac{1}{N^{\frac{3}{2}}} \int \frac{dk}{2k} \left(\alpha_k^{\dagger[i} \alpha_k^{j]} + \tilde{\alpha}_k^{\dagger[i} \tilde{\alpha}_k^{j]} \right) \alpha_{k_1}^{\dagger i} \tilde{\alpha}_{k_2}^j \\
 &= \frac{(1-N)}{N^{\frac{3}{2}}} \alpha_{k_1}^{\dagger i} \tilde{\alpha}_{k_2}^i + \frac{1}{\sqrt{N}} \frac{\alpha_{k_1}^{\dagger i} L^{ij} \tilde{\alpha}_{k_2}^j}{N} \\
 &\sim \mathcal{O} + \frac{1}{\sqrt{N}} \mathcal{OO}
 \end{aligned} \tag{4.30}$$

where \mathcal{O} denotes an operator quadratic in the α 's and normalized by $1/\sqrt{N}$ such that it is $O(1)$ in N -scaling. Note that the LHS of (4.30), by construction, is zero in physical states (and hence can be added to the precursor without changing any of its correlation functions).

The piece quadratic in the α 's in (4.30) is exactly the ambiguity needed to localize the precursor in the CFT to leading order in N , as was shown in detail in chapter 3. One can now also see that one generically needs a four-parameter ambiguity if we want to be able to set K_2 in (4.28) to zero in certain regions. Even though the term \mathcal{OO}/\sqrt{N} in (4.30) has the right structure to fit in the HKLL series, it does not have enough freedom to set K_2 to zero (it has only 2 free parameters, while we need 4). It can be done, however, by constructing a new operator which annihilates $SO(N)$ -invariant states and is quartic in the α 's:

$$A_4^{ij} \equiv A_2^{ij} - \frac{1}{N} A_2^{ij} \alpha_{k_3}^{\dagger m} \alpha_{k_4}^m. \tag{4.31}$$

The ambiguity in the precursor to order $\frac{1}{\sqrt{N}}$ is then given by $L^{ij} A_4^{ij}$. Normal ordering yields

$$L^{ij} A_4^{ij} = L^{ij} A_2^{ij} + T_4 + T_6 \tag{4.32}$$

where

$$T_4 = \alpha_{k_1}^{\dagger i} \alpha_{k_3}^{\dagger i} \tilde{\alpha}_{k_2}^m \alpha_{k_4}^m - \alpha_{k_3}^{\dagger i} \tilde{\alpha}_{k_2}^i \alpha_{k_1}^{\dagger m} \alpha_{k_4}^m + (1-N) \alpha_{k_1}^{\dagger i} \tilde{\alpha}_{k_2}^i \alpha_{k_3}^{\dagger m} \alpha_{k_4}^m \tag{4.33}$$

$$\begin{aligned}
 T_6 &= \alpha_k^{\dagger i} \alpha_{k_1}^{\dagger i} \alpha_{k_3}^{\dagger m} \tilde{\alpha}_{k_2}^j \alpha_k^j \alpha_{k_4}^m - \alpha_k^{\dagger j} \alpha_{k_1}^{\dagger i} \alpha_{k_3}^{\dagger m} \tilde{\alpha}_{k_2}^j \alpha_k^i \alpha_{k_4}^m \\
 &\quad + \tilde{\alpha}_k^{\dagger i} \alpha_{k_1}^{\dagger i} \alpha_{k_3}^{\dagger m} \tilde{\alpha}_{k_2}^j \tilde{\alpha}_k^j \alpha_{k_4}^m - \tilde{\alpha}_k^{\dagger j} \alpha_{k_1}^{\dagger i} \alpha_{k_3}^{\dagger m} \tilde{\alpha}_{k_2}^j \tilde{\alpha}_k^i \alpha_{k_4}^m
 \end{aligned} \tag{4.34}$$

and repeated momenta are integrated over appropriately. By T_4 we denote the ambiguity to quartic order in $L^{ij} A_4^{ij}$ and similarly with T_6 to hexic order. As before, T_4 and T_6 scale the same with respect to N in any gauge invariant state. Also they do not contribute in three-point functions of the bulk field.

Again we find that all the terms nicely arrange themselves in the right structure of an HKLL series:

$$\frac{1}{N^{\frac{3}{2}}} L^{ij} A_4^{ij} \sim \mathcal{O} + \frac{1}{\sqrt{N}} \mathcal{O}\mathcal{O} + \frac{1}{N} \mathcal{O}\mathcal{O}\mathcal{O} \quad (4.35)$$

where \mathcal{O} schematically denotes an operator quadratic in the α 's and normalized by $1/\sqrt{N}$ such that it is $O(1)$ in N -scaling. The main difference with $L^{ij} A_2^{ij}$ is that the term quartic in the α 's now gets a new contribution from T_4 , which does have four independent parameters, and hence in principle has enough freedom to localize the smearing function K_2 .

Doing so also introduced a term like α^6 . The connected piece of this will be down in $1/N$ relative to α^4 . If T_4 fixes the ambiguity at order $1/\sqrt{N}$, T_6 will contribute towards fixing it at order $1/N$. Thus, continuing this reasoning and choosing an improved operator A^{ij} , we will be able to fix the ambiguity in the precursor to any order in $1/N$ perturbatively.

We can now summarize how this recursive procedure works to localize bulk information order by order in N . When the operator we want to smear A_2^{ij} is quadratic, the ambiguity in the precursor to the quadratic order is given by $(1-N)\alpha_{k_1}^i \tilde{\alpha}_{k_2}^j$. These modes are labeled by two different momenta. Since we are working in two spacetime dimensions, they are able to fix all the ambiguity in the precursor up to quadratic level.

But fixing the quadratic level, introduces a quartic piece: $\alpha_{k_1}^i L^{ij} \tilde{\alpha}_{k_2}^j$. This piece has insufficient freedom to localize the precursor up to $1/\sqrt{N}$ corrections. To fix the ambiguity to the quartic level, one introduces a quartic ambiguity $L^{ij} A_4^{ij}$. This gives a piece T_4 which has four independent momenta and hence can now fix any ambiguity in the precursor up to quartic order. However, doing so also introduced a hexic piece T_6 . This hexic term makes the precursor ambiguous to order six. We can repeat the procedure, smear a different A^{ij} and then fix the ambiguity in the precursor up to order six.

Surprisingly, each term at a higher order is $\frac{1}{\sqrt{N}}$ relative to the current order. Hence, this procedure can be carried out order by order in $\frac{1}{\sqrt{N}}$ and thus fixes all the ambiguity in the interacting HKLL series in this toy model. While it is not explicitly demonstrated in this thesis, we would expect similar story to hold for matter fields are in the adjoint.

One should note that, while the quadratic and quartic piece in the ambiguity (4.30) (and similarly for the quartic and hexic piece in the ambiguity (4.35)) have the correct 'naive' N -scaling ($\alpha \sim N^{\frac{1}{4}}$) to be arranged in an HKLL series, their real N -scaling is the same. This means that neither term in (4.30) or (4.35) is small compared to the other. For clarity, we will elaborate on this a bit more in the next section 4.4.3.

4.4.3 N -Scaling

Within physical states, both terms on the RHS of (4.30) will be equal and opposite. In particular, they must have the same N -scaling (in contrary to what was claimed in [69]), even though naive N -counting would suggest otherwise. In order to explicitly see that both terms have the same N -scaling in $SO(N)$ -invariant states, we pick the following three states and label the operators as follows:

States	Operators
$ \psi'_1\rangle = \frac{1}{\sqrt{N}} \alpha_{k_3}^{\dagger m} \alpha_{k_4}^{\dagger m} 0\rangle$	$\mathcal{O}_1 = \alpha_{k_1}^{\dagger i} L^{ij} \tilde{\alpha}_{k_2}^j / N^{\frac{3}{2}}$
$ \psi''_1\rangle = \frac{1}{\sqrt{N}} \tilde{\alpha}_{k_3}^{\dagger m} \tilde{\alpha}_{k_4}^{\dagger m} 0\rangle$	$\mathcal{O}_2 = \alpha_{k_1}^{\dagger i} \tilde{\alpha}_{k_2}^i / \sqrt{N}$
$ \psi_2\rangle = \frac{1}{\sqrt{N}} \tilde{\alpha}_{k_5}^{\dagger m} \alpha_{k_6}^{\dagger m} 0\rangle$	

In order to assign a N -scaling to \mathcal{O}_2 , one could check its two-point function. However, since this operator has vanishing two-point functions, we investigate the three-point function and find that it goes like $1/\sqrt{N}$. This justifies us to call assign an $O(1)$ N -scaling to \mathcal{O}_2 . We will estimate the size of \mathcal{O}_1 and \mathcal{O}_2 in the subspace spanned by the three states above. Let us denote the matrix elements of an arbitrary operator \mathcal{O} in the above subspace as

$$\mathcal{O} = \begin{pmatrix} \langle \psi'_1 | \mathcal{O} | \psi'_1 \rangle & \langle \psi'_1 | \mathcal{O} | \psi''_1 \rangle & \langle \psi'_1 | \mathcal{O} | \psi_2 \rangle \\ \langle \psi''_1 | \mathcal{O} | \psi'_1 \rangle & \langle \psi''_1 | \mathcal{O} | \psi''_1 \rangle & \langle \psi''_1 | \mathcal{O} | \psi_2 \rangle \\ \langle \psi_2 | \mathcal{O} | \psi'_1 \rangle & \langle \psi_2 | \mathcal{O} | \psi''_1 \rangle & \langle \psi_2 | \mathcal{O} | \psi_2 \rangle \end{pmatrix}.$$

Then we get the following matrix elements for \mathcal{O}_1 and \mathcal{O}_2

$$\mathcal{O}_1 = \frac{1}{\sqrt{N}} \begin{pmatrix} 0 & 0 & 1 \\ 0 & 0 & 0 \\ 0 & 1 & 0 \end{pmatrix} \quad \mathcal{O}_2 = \frac{1}{\sqrt{N}} \begin{pmatrix} 0 & 0 & 1 \\ 0 & 0 & 0 \\ 0 & 1 & 0 \end{pmatrix}. \quad (4.36)$$

We can see that both the pieces in $L^{ij} A_2^{ij}$ scale in the same way with respect to N , as expected. Naively, one could expect the part quartic in the α 's to be down to part quadratic in the α 's by a factor $1/\sqrt{N}$. For these particular operators that doesn't happen, because the disconnected piece in \mathcal{O}_1 enhances its N -scaling.

Applying similar arguments to (4.35), we conclude T_6 must have the same N -scaling as T_4 . Again, the reason why this does not agree with naive N -scaling, is due to the contribution from the disconnected piece in T_6 .

Sub-AdS Scale Locality in $\text{AdS}_3/\text{CFT}_2$

This chapter is based on the paper [3].

In this chapter, we investigate sub-AdS scale locality in our familiar weakly coupled toy model of the $\text{AdS}_3/\text{CFT}_2$ correspondence. We will find that this simple model has the correct density of states at low and high energies to be dual to Einstein gravity coupled to matter in AdS_3 . The bulk correlation functions also have the correct behavior at leading order in the large N expansion, but deviations appear at order $1/N$. We will interpret this as evidence for non-locality of the theory, which is consistent with the presence of an infinite tower of massless higher spin fields. Our analysis leads to the conjecture that any large N CFT_2 that is both modular invariant, and exhibits the correct low-energy density of states, is dual to a gravitational theory with sub-AdS scale locality.

5.1 Introduction

The AdS/CFT correspondence has enabled tremendous progress in our understanding of quantum gravity. However, many important questions remain unanswered. Which CFTs are dual to bulk theories of Einstein gravity, with or without matter fields? What is the simplest CFT that reproduces the basic features of Einstein gravity? How does sub-AdS scale locality emerge in AdS/CFT? The goal of the present chapter is to address these questions in the context of an explicit toy model.

We will focus on $\text{AdS}_3/\text{CFT}_2$, where it is simplest to obtain precise answers to these rather grand questions. Indeed, the $\text{AdS}_3/\text{CFT}_2$ duality is a particularly constrained example of holography. Einstein gravity is topological in three dimensions, so there are no propagating gravitons. Additionally, two-dimensional

CFTs are highly constrained by the presence of the additional Virasoro symmetry. Nevertheless, many important features of quantum gravity, for example aspects of black hole physics, are still captured in three-dimensional gravity. The more constrained 3-dimensional framework thus provides a tractable environment amenable to precise results, while yielding insights that generalize to higher dimensions.

We will investigate the question of sub-AdS scale locality, by exploring the detailed properties of an explicit toy model for holography. The model, originally introduced in [69] and refined in chapter 3, consists of N massless free bosons restricted to the singlet sector of the global $O(N)$ symmetry. This model can be thought of as the two-dimensional version of the GKPY duality [84, 85]. The theory has a scalar operator \mathcal{O} dual to a massless scalar field in the bulk, defined as

$$\mathcal{O} = \partial\phi^I \bar{\partial}\phi^I. \quad (5.1)$$

The model was used to explicitly show how one can localize bulk operators within a given spatial region in chapter 3, where the connection between freedom in the smearing function and quantum error correction was investigated. In chapter 4 we explained the precursor ambiguity using gauge invariance and BRST. In this chapter, we investigate more refined properties of the model, including its spectrum and $1/N$ effects in correlation functions. We will show that the density of states is given by

$$\rho(\Delta) \sim \begin{cases} \exp\left(\gamma\Delta^{\frac{2}{3}}\right) & 1 \ll \Delta \lesssim N \\ \exp\left(2\pi\sqrt{\frac{N}{3}}\Delta\right) & \Delta \gg N. \end{cases} \quad (5.2)$$

The high energy spectrum is given by the Cardy formula. This is actually surprising, since the theory is not modular invariant. The projection to $O(N)$ singlets breaks modular invariance, and hence Cardy's formula does not *a priori* apply. However, we will argue – based on an explicit proof for $SO(3)$ – that this projection is only a subleading effect at energies much larger than N . Note that because modular invariance is broken, the regime of validity of the Cardy formula does not extend to $\Delta \sim N$ even though the growth of the low energy spectrum (5.2) satisfies the sparseness criterion. In the intermediate range, the spectrum will interpolate smoothly between the two regimes in (5.2).

The low-energy spectrum is compatible with a local quantum field theory in AdS₃. However, the spectrum contains an infinite tower of higher spin fields which ultimately cause the breakdown of sub-AdS scale locality. We will demonstrate this breakdown from properties of the Lorentzian four-point function of the operator \mathcal{O} . In particular, there is no divergence at order $O(1/N)$ when the boundary points form a bulk Landau diagram [43, 86–89]. Furthermore, the bulk theory is a

Vasiliev higher spin theory [90], and the effective Lagrangian contains interactions with an unbounded number of derivatives. In fact, it turns out that this model is equivalent to a sector of the coset models described in [91, 92], with a $\mathcal{W}_\infty^{(e)}$ symmetry at $\lambda = 1$.

Our model demonstrates that the ‘locality criterium’ on the spectrum (mentioned below in section 5.2), is actually not a sufficient condition for sub-AdS scale locality. However, the model was constructed by taking a modular invariant theory and projecting out many states. The result is manifestly not modular invariant, and restoring it with the addition of twisted sectors would completely destroy the sparseness of the low lying states. This was shown in a similar context in [93]. Our theory can therefore not satisfy both the locality criterion and modular invariance simultaneously. We believe that these arguments extend beyond our specific toy model, which will lead us to formulate a conjecture about sub-AdS scale locality.

5.2 Some Criteria for Bulk Locality

In the strongest interpretation of the AdS/CFT correspondence, every two dimensional CFT is dual to a theory of quantum gravity in AdS_3 . In some sense, the CFT defines the theory of quantum gravity in the bulk. The CFT data, namely the full set of correlation functions, can be interpreted as scattering amplitudes in the dual theory. The central charge is given by the AdS radius in Planck units [94],

$$c = \frac{3L_{\text{AdS}}}{2G_N} . \tag{5.3}$$

However, a generic CFT will not correspond to a theory of weakly coupled gravity. Rather, there exists a set of conditions the field theory must satisfy in order for it to have a well-behaved geometric dual. Identifying this list of necessary and/or sufficient conditions has been the focus of much recent effort [43, 95–101]. Here we briefly summarize the important constraints that will be relevant to the present work. We start with the weakest assumption, and incrementally carve out a smaller and smaller subset of the space of all two-dimensional CFTs.

1. **The large N criterion.** First, the relation (5.3) makes it clear that a weakly coupled gravitational theory requires large central charge. In particular, the large N limit in the CFT corresponds with the semi-classical limit of the gravitational theory. Since the central charge is a measure for the degrees of freedom in the CFT, this criterion heuristically says that the CFT needs sufficient degrees of freedom in order to be able to make up the holographic (radial direction). Furthermore, if we want to be able to dial the gravitational

coupling constant, we need a family of two dimensional CFT's labelled by a parameter N such that $c \sim N$. However, as we will explicitly show later in this chapter, large central charge is insufficient to have bulk locality, which brings us to the next criterion.

2. **The convergence criterion.** To obtain a sensible semi-classical limit, further constraints must be imposed. Chief among them is the requirement that the spectrum of the theory remains well-defined in the large N limit [99–101]. Specifically, we require that the density of states $\rho_N(\Delta)$ remains finite in the $N \rightarrow \infty$ limit at fixed energy Δ :

$$\lim_{N \rightarrow \infty} \rho_N(\Delta) \equiv \rho_\infty(\Delta) < \infty \quad \text{for any finite, fixed } \Delta. \quad (5.4)$$

This criterion can be seen as demanding that perturbation theory remains valid in the bulk, since the latter requires a finite number of bulk fields at every given energy. It is important to note that this is only a criterion on the perturbative spectrum of the gravitational theory, and therefore it says nothing about black holes; as $N \rightarrow \infty$, the energy Δ of the lightest black hole diverges.

This criterion explains why N free bosons, free fermions, or any theory that is a direct product, cannot be a good holographic theory. To see this, note that free bosons have N operators at dimension $\Delta = 1$ hence it will fail to satisfy this criterion. If we want this theory to be a ‘good’ holographic dual, most of the states have to be projected out. This can be done by orbifolding, or by considering a gauge theory. It should come as no surprise that most of the holographic dualities we know, involve gauge theories.

3. **The sparseness criterion.** The phase structure of Einstein gravity in AdS₃ is such that there are two saddle points that dominate the finite temperature partition function at low and high temperature: thermal AdS and the BTZ black hole. These saddles exchange dominance in the Hawking-Page phase transition at the self-dual temperature $\beta = 2\pi$ such that the partition function reads

$$\log \mathcal{Z}(\beta) = \frac{c}{12} \max \left(\beta, \frac{4\pi^2}{\beta} \right) + O(c^0) \quad (5.5)$$

where we take $c \sim N$. In [97], it was shown that in order for a CFT to reproduce this phase structure in the large N limit, the density of light operators must be bounded by

$$\rho(\Delta) \lesssim \exp(2\pi\Delta) \quad \text{for} \quad \Delta \leq \frac{c}{12}. \quad (5.6)$$

We refer to this as the sparseness criterion. It was also shown in [97] that a CFT which satisfies this sparseness condition (and is modular invariant)

will have an extended Cardy regime (which is usually only valid for $\Delta \gg c$) in the limit of large central charge:

$$\rho(\Delta) = \exp\left(2\pi\sqrt{\frac{c}{3}\left(\Delta - \frac{c}{12}\right)}\right) \quad \text{for} \quad \Delta \geq \frac{c}{12}. \quad (5.7)$$

This extended Cardy formula reproduces the Bekenstein-Hawking formula for the entropy of the BTZ black hole as soon as it dominates the canonical ensemble.

Note, however, that this sparseness constraint is rather weak. It corresponds to a Hagedorn growth typical of string theories in which the string and AdS scales are equal. Thus it allows for theories that are drastically different from Einstein gravity (such as symmetric product orbifolds), and in particular theories that are non-local on sub-AdS scales. The fact that such string theories can reproduce the phase structure of Einstein gravity is a peculiarity of AdS₃ (see [102] for a discussion of higher dimensions). It is therefore necessary to impose a stronger constraint on the CFT in order to ensure that we recover a bulk dual that is local on sub-AdS scales, which motivates the fourth and final criterion on our list.

4. **The locality criterion.** If the perturbative sector of the bulk theory is to behave as a local quantum field theory in AdS, then the CFT must satisfy the following condition on the density of states:

$$\rho(\Delta) \sim \exp\left(\gamma\Delta^{\frac{D-1}{D}}\right) \quad \text{for} \quad 1 \ll \Delta \ll N \quad (5.8)$$

where γ is some order-one coefficient, and D is a (positive) integer with a natural interpretation: it is the total number of bulk dimensions whose sizes are comparable to the AdS radius. The free energy resulting from such a density of states will be compatible with bulk thermodynamics of a local quantum field theory in D dimensions, namely $F \propto V_D T^{D+1}$, with a proportionality constant that depends on γ . This criterion is therefore necessary to reproduce the correct bulk thermodynamics at low temperatures.

One may wonder, after carving out this subspace of field theories, whether these four criteria are in fact sufficient to ensure locality on sub-AdS scales. In this chapter we will show that they are not, by investigating sub-AdS scale locality in our weakly coupled toy model. Despite its simplicity, our model reproduces a surprising number of the desired features of a theory dual to Einstein gravity coupled to matter in AdS₃. This includes the correct density of states at both low and high energies, as well as the correct bulk correlation functions at leading order in the large N expansion. Non-local effects seem to emerge at order $1/N$. However, a deeper pathology of our toy model is the lack of modular invariance;

indeed, any attempt to restore modular invariance would drastically change the properties of the low lying spectrum, and hence displace us beyond the subspace of holographic CFT's we so carefully circumscribed above. For this reason, we are led to the following conjecture:

Sub-AdS Locality Conjecture:

In the large N limit, every CFT₂ that satisfies the locality criterion, and has modular invariance, is dual to a bulk gravitational theory with sub-AdS scale locality.

The evidence for this conjecture is essentially experimental, based largely on our intuition with orbifold CFTs. The basic reasoning is as follows: starting from a large N theory with a global symmetry and many low lying states, one can try to project out states until the bound (5.8) is satisfied. In order to preserve modular invariance, twisted sectors must be added in proportion to the severity of the projection. In [99, 101], it was shown that for any orbifold by a permutation group $G \subseteq S_N$, the locality criterion cannot be satisfied. This leaves the possibility that a projection by a bigger group such as $O(N)$ could achieve this criterion. However, although this works for the untwisted sector, modular invariance forces the inclusion of so many twisted sectors that the spectrum grows even faster than Hagedorn [93, 103]. None of the existent orbifold constructions seem to work, even for non-discrete groups.

Of course, the absence of known counterexamples does not constitute a proof of our conjecture, though it would be interesting to try to construct one. In this line of thought, the CFT data that could most likely be used to prove (or disprove) our conjecture are the OPE coefficients, as they contain the dynamical information of the CFT that, for example, could be translated as a diagnostic for bulk locality using singularities of the four-point functions. Upon imposing (5.8) and demanding modular invariance, one could try to constrain the OPE coefficients using bootstrap techniques along the lines of [96, 98, 104]. It would also be interesting to understand how our conjecture relates to other criteria, such as the gap in the operator dimensions discussed in section 1.3.6 of the introduction. We will not attempt to tackle these questions in this thesis, but instead focus on the properties and consequences of this particular model.

The remainder of this chapter is organized as follows: in section 5.3, we discuss properties of the spectrum of our toy model at both low and high energies. In section 5.4, we comment on bulk locality in our toy model, using properties of correlation functions at leading and subleading order in the $1/N$ expansion. We computed (analytically up to level 4, and numerically for higher levels) explicit expressions for the first few single-trace primaries at finite N , which are collected in appendix 5.A.

5.3 The Holographic Toy Model Revisited

5.3.1 The Model

The model we consider was defined in chapter 3 as a refinement of an earlier version proposed in [69]. We will summarize it quickly for convenience. The CFT consists of N free massless scalars in two dimensions. The Lagrangian is

$$\mathcal{L} = \partial_\mu \phi^I \partial^\mu \phi^I \quad (5.9)$$

where the scalars ϕ^I transform in the fundamental representation of a global $O(N)$ symmetry. The Hilbert space of such a theory is given by

$$\mathcal{H}_N = \mathcal{H}^{\otimes N} \quad (5.10)$$

where \mathcal{H} is the Hilbert space of a single free boson. We wish to consider the subspace of states that are invariant under the $O(N)$ symmetry, namely the singlet sector. Therefore the relevant Hilbert space is

$$\mathcal{H}_{\text{singlet}} = \mathcal{H}^{\otimes N} / O(N) . \quad (5.11)$$

It is important to specify the procedure by which we impose such a constraint. In general field theories, the way to do so with local dynamics is by gauging the symmetry. This will enforce Gauss' Law and project to the singlet sector. However, preserving conformal invariance in the process is more subtle.

In two dimensions, there is a very natural way to enforce a singlet constraint while preserving conformal invariance: orbifolding. The orbifolding procedure (which is usually done for a discrete group) enforces the singlet constraint, but also adds new operators to the theory from the twisted sectors. Indeed, a CFT_2 orbifold should really be thought of as a discrete gauge theory in two dimensions, where the twisted sectors are the degrees of freedom arising from the holonomies of the gauge field. Note that the inclusion of the twisted sector states comes from demanding that the theory is modular invariant on the torus. Projecting to the singlet sector without adding twisted sectors manifestly breaks modular invariance.

Throughout this chapter we will only consider the untwisted sector, which is tantamount to imposing the singlet constraint by hand. As a consequence, our theory will not be modular invariant. This has some important ramifications, some of which we address when we discuss the high energy spectrum below. That said, we wish to emphasize that the singlet sector nonetheless retains many desirable properties. For example, the sector is closed: only singlet operators appear in the OPE of any two singlet operators. This implies in particular that the four-point function of any singlet operators obeys the crossing relations.

5.3.2 Spectrum of Primaries

In this section, we describe the spectrum of singlet operators in our CFT. We will be particularly interested in the single-trace Virasoro primaries, since every such operator is dual to a new bulk field, while multi-trace primaries correspond to multi-particle states.

In both the holomorphic and anti-holomorphic sectors, the spectrum of the theory is characterized by the appearance of one new single trace Virasoro primary at every even level $h, \bar{h} \geq 4$. The general expression for these operators may be written as [105]

$$W^s(z) = \frac{2^{s-3}s!}{(2s-3)!!} \sum_{l=1}^{s-1} \frac{(-1)^l}{s-1} \binom{s-1}{l} \binom{s-1}{s-l} \partial^l \phi^I \partial^{s-l} \phi^I + O\left(\frac{1}{N}\right). \quad (5.12)$$

Note that these operators are not exactly single trace, but their multi-trace components are suppressed by powers of $1/N$. We give explicit expressions to all orders in $1/N$ for the holomorphic primaries up to level 8 in appendix 5.A, and indeed find that the multi-trace components are always suppressed by higher powers of N . These fields correspond to conserved higher spin currents that couple to massless higher-spin fields in the bulk, and have been shown to generate a non-linear $\mathcal{W}_\infty^{(e)}[\lambda = 1]$ algebra [105]. In the (anti-)holomorphic sector there is only one $\mathcal{W}_\infty^{(e)}$ primary, the identity, which generates all the Virasoro primaries.

In the mixed sector, the theory contains one single-trace scalar operator $\mathcal{O} = \partial\phi^I \bar{\partial}\phi^I$ with dimension $(h, \bar{h}) = (1, 1)$. This operator is also a $\mathcal{W}_\infty^{(e)}$ primary, and naturally induces an infinite tower of multi-trace \mathcal{W}_∞ primary operators (corresponding to multi-particle states in the bulk) given schematically by

$$\mathcal{O}_{n_i, \bar{n}_i}^k =: \sum_{n_i, \bar{n}_i} a_{n_1 \dots n_k \bar{n}_1 \dots \bar{n}_k} \partial^{n_1} \bar{\partial}^{\bar{n}_1} \mathcal{O} \partial^{n_2} \bar{\partial}^{\bar{n}_2} \mathcal{O} \dots \partial^{n_k} \bar{\partial}^{\bar{n}_k} \mathcal{O} : + O\left(\frac{1}{N}\right) \quad (5.13)$$

for an appropriate choice of coefficients a_{n_i, \bar{n}_i} . A generic choice of these coefficient will not lead to a primary, since the global descendants of the lower dimensional operators must be subtracted out. Along with their global and \mathcal{W}_∞ descendants, the operators (5.13) generate the entire spectrum of the theory in the limit $N \rightarrow \infty$. At finite N , there are new primary operators that appear at $\Delta = N$. These will play an important role when we discuss the high energy part of the spectrum.

It is worth mentioning that we do not include zero modes. The standard vertex operators $e^{ik^I \phi^I}$ are not invariant under the $O(N)$ symmetry and are thus projected out. However, this still allows for operators of the form $e^{\lambda \phi^I \phi^I}$. We will not consider such operators, and instead implicitly further project to states that are invariant under $ISO(N)$ symmetries $\phi^I \rightarrow R^{IJ} \phi^J + C^I$.

5.3.3 Density of States

Low Energies: $1 \ll \Delta \ll N$

We first compute the asymptotic density of perturbative states, i.e., states whose energy is parametrically smaller than N . States whose energy scales with N are typically associated to non-perturbative objects such as a black holes, and will be the focus of the next sub-section.

We will consider free bosons on the cylinder, where the excitations are given by oscillators a_{-j}^I . The index j denotes the energy of the oscillator, hence a single-oscillator state would have $h = j$. In order to compute the density of perturbative states $\rho(\Delta)$, we consider $n < N$ oscillators a^I , each in the fundamental representation of $O(N)$. The singlet constraint forces us to contract all indices to form an invariant state. If n is even, this can be done in $(n-1)!!$ different ways, while if n is odd, the singlet constraint implies $\rho(\Delta) = 0$. The density of states for an n -oscillator state can therefore be estimated as

$$\rho_n(\Delta) \sim (n-1)!! \cdot \frac{1}{n!} \int_0^\Delta d\Delta_1 \dots \int_0^\Delta d\Delta_n \delta\left(\Delta - \sum_i \Delta_i\right) \quad (5.14)$$

$$= (n-1)!! \frac{\Delta^{n-1}}{n!(n-1)!} = \frac{\Delta^{n-1}}{n!(n-2)!!} \quad (5.15)$$

where the factor of $1/n!$ in (5.14) approximates the number of ways of distributing the energy Δ over n oscillators. The total density of states is then

$$\rho(\Delta) \sim \sum_{n=1}^{\Delta} 2^n \rho_n(\Delta) \quad (5.16)$$

$$\rho_n(\Delta) \approx e^{n \log \Delta - \frac{3}{2} n \log n} \quad \text{for } n \gg 1$$

where the factor of 2^n accounts for the inclusion of both left- and right-movers. We may evaluate this sum by performing a saddle-point approximation on n . The dominant saddle is at $n_0 = (2\Delta)^{\frac{2}{3}} e^{-1}$, which yields

$$\rho(\Delta) \sim e^{\gamma \Delta^{\frac{2}{3}}}, \quad 1 \ll \Delta \ll N. \quad (5.17)$$

Note that, in addition to the saddle point, we made two other approximations in the course of obtaining this result: the factor of 2^n from the choice of a or \bar{a} , and the double factorial $(n-1)!!$ from pair contractions. These two factors are only exact when all the oscillators have different momenta, otherwise one should include an appropriate symmetrization factor. Our approximations thus yield an overcounting of the total number of states, but those are subdominant in the

regime under consideration. This is the reason for the undetermined coefficient γ in (5.17), which cannot be determined from this analysis.

It is however possible to express the perturbative partition function analytically. The contribution of the $\mathcal{W}_\infty^{(e)}$ identity character gives [92]

$$\mathcal{Z}_{\text{higher spins}} = \prod_{s \in 2\mathbb{N}^*} \prod_{n \geq s} \frac{1}{|1 - q^n|^2} \equiv |M^e(q)|^2, \quad (5.18)$$

where M^e is the modified MacMahon function. The contribution of our real scalar field with conformal dimension one, including all its multi-trace operators and global descendants, was shown in [106] to be

$$\mathcal{Z}_{\text{scalar}} = \prod_{l, l'=0}^{\infty} \frac{1}{1 - q^{1+l} \bar{q}^{1+l'}}. \quad (5.19)$$

The total perturbative partition function is therefore given by [91]

$$\mathcal{Z}(q, \bar{q}) = (q\bar{q})^{-\frac{c}{24}} |M^e(q)|^2 \prod_{l, l'=0}^{\infty} \frac{1}{1 - q^{1+l} \bar{q}^{1+l'}} \quad (5.20)$$

from which the appropriate coefficient could in principle be extracted. In practice, this requires knowledge of the asymptotics of the modified MacMahon function. However, the asymptotics of the coefficient of q^n in the standard MacMahon function, where the product is over all (i.e. odd and even) spins, is known to be $\rho(n) \sim e^{3\zeta(3)(n/2)^{2/3}}$, and one expects a similar formula for the growth of the modified MacMahon function, but with different numerical factors. Thus, in conjunction with the upper bound on the density of states derived above, this demonstrates that our theory satisfies the locality criterion. We now turn to the density of high energy states.

Asymptotically High Energies: $1 \ll N \ll \Delta$

Here we will show that the density of states at asymptotically high energies $\Delta \gg N$ has a Cardy growth. We will do this by showing that the density of states in this regime has the same leading asymptotics as the product theory and the correction is only polynomial in the energy. We will show that

$$e^{2\pi\sqrt{\frac{N}{3}}\Delta} \sim \rho_{\text{product}}(\Delta) \geq \rho_{\text{singlet}}(\Delta) \geq \frac{\rho_{\text{product}}(\Delta)}{\Delta^p}, \quad \Delta \gg N \quad (5.21)$$

for some power p .

Before embarking on the proof, some general comments are in order. The result (5.21) may seem surprising since it implies that the Cardy formula also holds

asymptotically in the singlet theory, even though the theory is not modular invariant. This is a consequence of the nature of the projection, which preserves certain properties of the full theory even though modular invariance is lost. To see this, consider an orbifold by a discrete group G . The singlet sector (equivalently, the untwisted sector) partition function is given by

$$Z_N(q, \bar{q}) = \frac{1}{|G|} \sum_{g \in G} \text{Tr}_{\mathcal{H}^{\otimes N}} \left[g q^{L_0 - c/24} \bar{q}^{\bar{L}_0 - \bar{c}/24} \right]. \quad (5.22)$$

A lower bound to the density of states can be obtained by only considering the term in this sum where the group element g is the identity

$$Z_N(q, \bar{q}) = \frac{1}{|G|} \text{Tr}_{\mathcal{H}^{\otimes N}} \left[q^{L_0 - c/24} \bar{q}^{\bar{L}_0 - \bar{c}/24} \right] = \frac{1}{|G|} Z(q, \bar{q})^N \quad (5.23)$$

where Z is the partition function of one free boson. For any discrete group, $|G|$ is a finite number, and will constitute only a small correction for sufficiently large temperatures. Performing an inverse Laplace transform to obtain the density of states, we find that the growth is Cardy up to some subleading correction from $|G|$. Since an upper bound to the density of states is given by considering the product theory, which has Cardy growth, this shows that for any discrete orbifold, even the non-modular invariant singlet theory still has a Cardy growth. Unfortunately, such an argument fails for projections by continuous groups. However, the analogue of the correction coming from $|G|$ can still be calculated in our $O(N)$ example. It is no longer constant in the energy, but it is still subleading compared to the Cardy growth.

The proof of (5.21) proceeds as follows. A generic state will be of the form

$$a_{-1}^{n_1} a_{-2}^{n_2} \cdots a_{-k}^{n_k} |0\rangle \quad (5.24)$$

with energy $\Delta = \sum_{i=1}^k i \cdot n_i$. Since we can take the energy to be arbitrarily large, many of the oscillators will have the same momenta and must therefore be appropriately symmetrized. Hence in order to estimate the number of singlets at a given energy Δ , we must find the multiplicity of the trivial representation in

$$\text{Sym}(n_1) \otimes \cdots \otimes \text{Sym}(n_k) \quad (5.25)$$

where $\text{Sym}(n_1)$ denotes the symmetric tensor product of n_1 fundamentals.

Since this is a rather cumbersome counting problem, we will do the explicit computation for $SO(3)$. The argument for general N will be very similar and only the power p of the suppression in (5.21) will change.

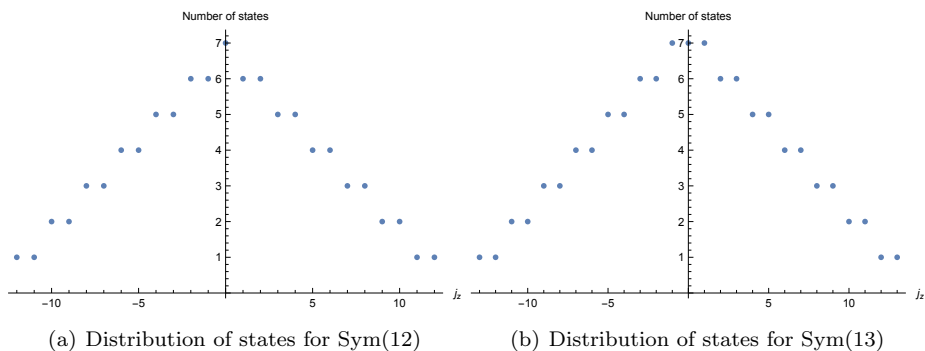


Figure 5.1: Distribution of the number of states per j_z for Sym(12) and Sym(13)

Proof for SO(3)

Consider the symmetric product of n fundamentals of SO(3). The generating function for the number of states at a given j_z in the symmetric tensor product Sym(n) is given by

$$z(x, n) = \sum_{j_z=-n}^n (\# \text{ states}) x^{j_z} = \left(\sum_{i=-m/2}^{m/2} x^{2i} \right) \left(\sum_{i=-n}^n x^i \right) \quad (5.26)$$

$$m = \left\lfloor \frac{n}{2} \right\rfloor \quad \text{and} \quad n = \left\lceil \frac{n}{2} \right\rceil.$$

The states form a triangular distribution which is symmetric around $j_z = 0$. The total number of states is $\frac{(n+1)(n+2)}{2}$, and the variance is given by $\frac{n(n+3)}{6}$. See figures 5.1(a) and 5.1(b) for examples of this distribution at even and odd n .

Now, when tensoring together Sym(n_1) \otimes \cdots \otimes Sym(n_k), we know that the angular momentum in the z -direction is additive:

$$j_z^{\text{Total}} = \sum_{i=1}^k j_z^i. \quad (5.27)$$

This enables us to extract the number of singlets with the following formula:

$$\# \text{ singlets} = (\# \text{ states with } j_z^{\text{Total}} = 0) - (\# \text{ states with } j_z^{\text{Total}} = 1). \quad (5.28)$$

This expression can be understood by observing that any irrep of SO(3) with spin strictly greater than zero has one state with $j_z = 0$ for each state with $j_z = 1$. Hence any difference between the two must come from a spin zero singlet. For example, one can see from figures 5.1(a) and 5.1(b) that Sym(12) has 1 singlet, while Sym(13) has none.

The distribution of j_z^{Total} can be obtained using the central limit theorem. We view the j_z^i as independent discrete random variables with mean 0 and variance σ_i^2 . j_z^{Total} has mean zero and variance $\sigma_{\text{Total}}^2 = \sum_{i=1}^k \sigma_i^2$. Note that $\sigma_{\text{Total}}^2 \rightarrow \infty$ as $k \rightarrow \infty$. Since there exists a constant A such that $|j_z^i| \leq A$ for all i , the central limit theorem implies that j_z^{Total} is approximately Gaussian. More precisely, for $a < b$:

$$\lim_{n \rightarrow \infty} P\left(a < \frac{j_z^{\text{Total}}}{\sigma_{\text{Total}}} < b\right) = \frac{1}{\sqrt{2\pi}} \int_a^b dx e^{-\frac{x^2}{2}}. \quad (5.29)$$

This implies that in the regime of very large energies, where we sum over a large number of j_z^i , we can approximate the distribution of j_z^{Total} by

$$P(j_z^{\text{Total}}) \approx \frac{1}{\sqrt{2\pi}\sigma} e^{-\frac{(j_z^{\text{Total}})^2}{2\sigma^2}} \quad (5.30)$$

with variance

$$\begin{aligned} \sigma^2 &= \sum_i \sigma_i^2 = \sum_i \frac{n_i(n_i + 3)}{6} \\ &\leq \sum_i n_i^2 \leq \left(\sum_i i \cdot n_i\right)^2 \\ &\leq \Delta^2. \end{aligned} \quad (5.31)$$

Note that this distribution is normalized, so that $P(j_z^{\text{Total}} = 0) - P(j_z^{\text{Total}} = 1)$ gives the ratio of singlets to the total number of states in the product theory. In the large E limit, we may take σ arbitrarily large to obtain

$$\begin{aligned} P(j_z^{\text{Total}} = 0) - P(j_z^{\text{Total}} = 1) &\approx \frac{1}{\sqrt{2\pi}\sigma} \left(\frac{1}{2\sigma^2}\right) \\ &= \frac{1}{\sqrt{8\pi}\sigma^3} \geq \frac{1}{\sqrt{8\pi}\Delta^3} \end{aligned} \quad (5.32)$$

and hence we conclude

$$\rho_{\text{product}}(\Delta) \geq \rho_{\text{singlet}}(\Delta) \geq \frac{\rho_{\text{product}}(\Delta)}{\Delta^3}. \quad (5.33)$$

5.4 Bulk Locality in the Toy Model

5.4.1 Locality and Reconstruction

In this section, we review how bulk locality emerges in the model, and probe the breakdown thereof. We shall work in Lorentzian signature in the CFT. The field theory contains an operator $\mathcal{O} = \partial_+ \phi^I \partial_- \phi^I$ with conformal dimension $\Delta = 2$,

which is dual to a massless scalar Φ in AdS₃. In chapter 3, this holographic toy model was used to investigate bulk locality and reconstruction of Φ in the large N limit. At leading order in $1/N$, the bulk field is free, and can be reconstructed on the boundary by integrating the CFT operator against a suitable smearing function

$$\Phi(X) = \int dxdt K(X|x, t)\mathcal{O}(x, t) + O\left(\frac{1}{N}\right). \quad (5.34)$$

This prescription correctly reproduces the bulk two-point function from the CFT.

We now demonstrate explicitly how bulk locality emerges at large N in this model. Expanding the bulk field Φ into mode functions in Poincaré AdS₃, we have

$$\Phi(t, x, z) = \int d\omega dk (\alpha_{\omega k} g_{\omega k}(t, z, x) + \text{h.c.}). \quad (5.35)$$

A local bulk field should satisfy the equal-time commutation relations

$$\begin{aligned} [\Phi(x, z), \Phi(x', z')] &= [\Pi(x, z), \Pi(x', z')] = 0 \\ [\Phi(x, z), \Pi(x', z')] &\sim \delta(x - x')\delta(z - z') \end{aligned} \quad (5.36)$$

which in turn require

$$[\alpha_{\omega k}, \alpha_{\omega' k'}] = [\alpha_{\omega k}^\dagger, \alpha_{\omega' k'}^\dagger] = 0 \quad (5.37)$$

$$[\alpha_{\omega k}, \alpha_{\omega' k'}^\dagger] \sim \delta(\omega - \omega')\delta(k - k'). \quad (5.38)$$

Via the extrapolate dictionary, we can relate the bulk creation and annihilation operators above to the those in the CFT by demanding that $\lim_{z \rightarrow 0} z^{-\Delta} \Phi(t, x, z) \leftrightarrow \partial_+ \phi^I \partial_- \phi^I$. This implies

$$\alpha_{\omega k} \sim \frac{a_{\omega+k}^I \tilde{a}_{\omega-k}^I}{\sqrt{N}} = \frac{a_{\omega+}^I \tilde{a}_{\omega-}^I}{\sqrt{N}} \quad (5.39)$$

where the a 's are the left- and right-moving Fourier modes of the boundary fields ϕ^I . Equation (5.39) is essentially the statement that a bulk particle corresponds to a pair of left- and right-moving excitations in the CFT. Note that $\omega_\pm < 0$ corresponds to a creation operator, and that $a_{\omega_\pm}^\dagger = a_{-\omega_\pm}$. Translating the bulk commutation relations (5.37) and (5.38) into the CFT using $[a_\omega^I, a_{\omega'}^J] = \omega \delta(\omega + \omega') \delta^{IJ}$ yields

$$\begin{aligned} \frac{1}{N} [a_{\omega_+}^I \tilde{a}_{\omega_-}^I, a_{\omega'_+}^J \tilde{a}_{\omega'_-}^J] &= \omega_+ \omega_- \delta(\omega_+ + \omega'_+) \delta(\omega_- + \omega'_-) \\ &+ \frac{1}{N} \left(\omega_- a_{\omega_+}^I a_{\omega'_+}^I \delta(\omega_- + \omega'_-) + \omega_+ \tilde{a}_{\omega_-}^I \tilde{a}_{\omega'_-}^I \delta(\omega_+ + \omega'_+) \right) \end{aligned} \quad (5.40)$$

which becomes local when N is large (i.e., when the last two terms can be dropped).

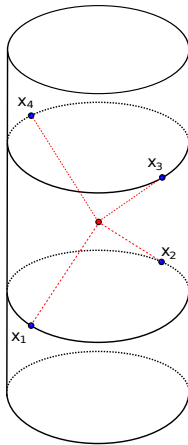


Figure 5.2: Four CFT insertions that are not lightlike separated in the CFT, but whose bulk lightcones intersect in a point.

5.4.2 3- and 4-point Correlation Functions

At next-to-leading order in $1/N$, we expect the bulk dual of our CFT to be non-local, despite having the density of states of a local quantum field theory in $2+1$ -dimensions. As detailed in section 5.3.2, the bulk contains massless higher spin fields, which strongly suggests locality violation since the effective Lagrangian will be unbounded in the number of derivatives. To quantify the non-locality, we calculate the 3- and 4-point functions of our primary field \mathcal{O} . As explained in the introduction 1.3.6, the 4-point functions provide a strong test of bulk locality [43, 86–89]. Any theory with a nontrivial S-matrix *in the flat space limit* must have certain lightcone singularities in the 4-point function. These singularities arise when the bulk interaction point is lightlike connected to all 4 boundary points, none of which are lightlike separated in the boundary theory; see figure 5.2. Such singularities do not occur in a CFT at finite N , but they can appear in the large N limit.

The 3-point function of the operator \mathcal{O} is zero,

$$\langle \mathcal{O}\mathcal{O}\mathcal{O} \rangle = 0 . \quad (5.41)$$

This is easily seen since each \mathcal{O} contains one left-mover and one right-mover, so the 3-point function contains 3 left-movers. Since the boundary theory is free, the vacuum expectation value of an odd number of left-movers is zero.

The 4-point function contains a factorized piece, which dominates at large N , and a subleading connected piece. Defining the operator \mathcal{O} with a normalization that

makes the 2-point function order one in N-scaling,

$$\mathcal{O} = \frac{1}{\sqrt{N}} \partial_+ \phi^I \partial_- \phi^I \quad (5.42)$$

the 4-point function is

$$\begin{aligned} \langle \mathcal{O}(x_1) \mathcal{O}(x_2) \mathcal{O}(x_3) \mathcal{O}(x_4) \rangle &= \frac{1}{N^2} \langle \partial_+ \phi^I(x_1) \partial_- \phi^I(x_1) \partial_+ \phi^J(x_2) \partial_- \phi^J(x_2) \\ &\times \partial_+ \phi^K(x_3) \partial_- \phi^K(x_3) \partial_+ \phi^L(x_4) \partial_- \phi^L(x_4) \rangle. \end{aligned} \quad (5.43)$$

We can then use the fact that

$$\begin{aligned} \langle \partial_+ \phi^I(x_1) \partial_+ \phi^J(x_2) \rangle &= \frac{\delta^{IJ}}{(x_1^+ - x_2^+)^2} \\ \langle \partial_+ \phi^I(x_1) \partial_- \phi^J(x_2) \rangle &= 0 \end{aligned} \quad (5.44)$$

to obtain

$$\begin{aligned} \langle \mathcal{O}(x_1) \mathcal{O}(x_2) \mathcal{O}(x_3) \mathcal{O}(x_4) \rangle &= \text{disconnected} \\ &+ \frac{1}{N} \frac{1}{(x_1^+ - x_2^+)^2 (x_1^- - x_3^-)^2 (x_2^- - x_4^-)^2 (x_3^+ - x_4^+)^2} + \text{permutations} \end{aligned} \quad (5.45)$$

where, with our normalization conventions, the disconnected piece is of order N^0 .

Examining this expression for the full 4-point function, it is clear that singularities arise only when some pair of points are lightlike separated on the boundary, such that they have the same value of x^+ or x^- . There are no additional singularities, which would appear if the bulk theory were truly described by Einstein gravity coupled to matter. This leaves us with two non-exclusive possibilities: the bulk theory is either non-local or has a trivial S-matrix in the flat-space limit¹. There is some evidence for the latter on general grounds so we cannot conclude directly from the singularity structure that the bulk theory is non-local. However, we have found above that the bulk theory contains an infinite tower of massless higher-spin fields, indicating that it is non-local in the sense that the Lagrangian contains an arbitrarily large number of derivatives. It would be interesting to better quantify the degree of non-locality in the bulk (see for example [112]), and to determine whether the commutators can be corrected order-by-order in $1/N$. We will not address these questions any further in this thesis.

¹Determining the space of permissible field redefinitions that reveals the S-matrix to be trivial despite the presence of interaction terms is an open area of research. We will not attempt to address the issue here, but refer the reader to the higher-spin literature, e.g. [107–112].

5.A Holomorphic Primaries

Here we give explicit expressions for the holomorphic Virasoro primaries at *finite* N , up to $h = 8$. We will work on the cylinder and discuss primary states. The comparison with the operators on the plane can be performed via the state-operator correspondence; e.g., the spin 4 operator is given in [105]. To see that our states are single-trace in the large N limit, some care is needed in the estimation of the magnitude of a given term. Terms with more oscillators naturally weigh more since they have several sums. Each oscillator carries an effective weight of $N^{1/4}$, which follows from considering any normalized state,

$$\mathcal{N}a_1 \dots a_k |0\rangle \sim N^{-k/4} a_1 \dots a_k |0\rangle. \quad (5.46)$$

The states below are given up to an overall normalization.

There is one new primary at $h = 4$:

$$\mathcal{W}_4 = a_{-1}^I a_{-3}^I - \frac{3}{4} a_{-2}^I a_{-2}^I - \frac{3}{2(N+2)} a_{-1}^I a_{-1}^I a_{-1}^J a_{-1}^J. \quad (5.47)$$

At $h = 6$, there is also one new primary given by

$$\begin{aligned} \mathcal{W}_6 = & a_{-1}^I a_{-5}^I - \frac{5}{2} a_{-2}^I a_{-4}^I + \frac{5}{3} a_{-3}^I a_{-3}^I + \frac{5(8N+7)}{4(N-1)(N+2)} a_{-1}^I a_{-1}^I a_{-2}^J a_{-2}^J \\ & + \frac{5(N-16)}{4(N-1)(N+2)} a_{-1}^I a_{-1}^J a_{-2}^I a_{-2}^J - \frac{15}{N+2} a_{-1}^I a_{-1}^J a_{-1}^I a_{-3}^I \\ & + \frac{15}{(N+2)(N+4)} a_{-1}^I a_{-1}^I a_{-1}^J a_{-1}^J a_{-1}^K a_{-1}^K. \end{aligned} \quad (5.48)$$

There are 2 new primaries at $h = 8$. An orthogonal basis can be chosen such that one of these becomes single-trace at large N , while the other remains multi-trace. The former may be written:

$$\begin{aligned} \mathcal{W}_8 = & -\frac{N+2}{28} a_{-1}^I a_{-7}^I + \frac{N+2}{8} a_{-2}^I a_{-6}^I - \frac{N+2}{4} a_{-3}^I a_{-5}^I \\ & + \frac{5(N+2)}{32} a_{-4}^I a_{-4}^I + a_{-1}^I a_{-1}^J a_{-1}^J a_{-5}^I - \frac{45}{32} a_{-2}^I a_{-2}^I a_{-2}^I a_{-2}^J \\ & - \frac{4N+3}{2(N-1)} a_{-1}^I a_{-1}^I a_{-2}^J a_{-4}^J + \frac{5(3N+8)}{12(N-1)} a_{-1}^I a_{-1}^I a_{-3}^J a_{-3}^J - \frac{N-8}{2(N-1)} a_{-1}^I a_{-1}^J a_{-2}^J a_{-4}^I \\ & - \frac{28-N}{4(N-1)} a_{-1}^I a_{-2}^J a_{-2}^I a_{-3}^J - \frac{5(5N+6)}{12(N-1)} a_{-1}^I a_{-1}^J a_{-3}^I a_{-3}^J + \frac{14N+13}{4(N-1)} a_{-1}^I a_{-2}^J a_{-2}^I a_{-3}^I \\ & - \frac{5}{4(N-1)} a_{-1}^I a_{-1}^I a_{-1}^J a_{-1}^J a_{-2}^K a_{-2}^K + \frac{5}{4(N-1)} a_{-1}^I a_{-1}^J a_{-1}^K a_{-1}^K a_{-2}^I a_{-2}^J. \end{aligned} \quad (5.49)$$

Similarly, there are 3 new primaries at $h = 10$, only one of which will be single-trace at large N . And there are 6 new primaries at $h = 12$, only one of which is single-trace at large N . For their explicit form, we refer the reader to the appendices in the paper [3].

Conclusions & Outlook

In this final chapter we will wrap up and summarize the results we have obtained throughout this thesis, providing some concluding remarks and discussing a few unresolved questions.

6.1 Burning Black Holes

Black holes are one of the favorite tools of a theorist to study the properties of (quantum) gravity, e.g. by studying black hole thermodynamics and microstate counting. Their main use in this thesis, however, is to learn about another puzzling aspect due to the fact that black holes emit Hawking radiation: the firewall paradox. This states that there seems to be a conflict between three basic postulates that we took for granted in a regime where we thought we could trust our theory, i.e. doing low energy effective field theory on a weakly curved background:

- unitarity: black hole formation and evaporation is a unitary process.
- locality: operators that are spacelike separated commute.
- the equivalence principle: a freely falling observer does not experience anything special at the horizon.

Resolving this conflict should teach us about quantum gravity, and in particular whether and why quantum gravity corrections would suddenly be important in this low energy regime.

We took a pragmatic step towards resolving the firewall paradox in chapter 2, where we have shown that for static black holes in $3 + 1$ and higher dimensions, there does not exist a causal patch that contains all the ingredients necessary to construct the firewall paradox at the level of s -wave Hawking quanta (which is the predominant form of Hawking radiation due to the angular momentum barrier). In that case black hole complementarity can come to the rescue, since no single observer would be able to see the violation of any physical law.

A possible exception to this principle arises when considering the Schwarzschild black hole in $3+1$ dimensions, and we presented a detailed analysis of the infalling geometry for this case. Our results indicate that the infalling observer is always missing some finite amount of information about the s -wave. Though it remains to show precisely how much angular resolution the observer can afford to lose before reconstruction of the partner mode becomes impossible in principle, our analysis suggests that it is at best difficult in practice. We focused on the situation for s -waves, as this version of the firewall paradox is the simplest and most robust in our view. Although it would be interesting to consider the consequences for high- l modes, this requires a more thorough understanding of the degree to which black hole mining disrupts the entanglement of the quantum state. A more detailed analysis of localization of partner modes may shed more light on this direction.

We conclude that for static black holes in $3+1$ and higher dimensions, black hole complementarity is sufficient to evade at least the simplest version of the firewall paradox. While this is not enough to settle the debate, it necessitates a more careful formulation of the paradox. In particular, two classes of proposed resolutions are worth mentioning. First of all, instead of giving up on the equivalence principle like AMPS did, it has been suggested that a violation of locality can also provide an outcome for firewalls, effectively violating the assumption that P and R are independent in figure 2.1. The challenge is to explain why tiny non-localities could conspire to have rather large effects; or why they are important to solve the firewall problem, but can be neglected when doing all other physics problems. A proposal that makes use of a rather dramatic violation of locality is known under the name ER=EPR [113], and suggests that entanglement is caused by tiny wormholes, that in this case connect the interior of the black hole with the exterior. Although a cute proposal, one may wonder whether entanglement (a quantum mechanical property) can really be explained using wormholes. It would be interesting to see whether further evidence can be found or not.

Secondly there is a class of holographic arguments, making a case that typical CFT states dual to a black hole, will contain firewalls [57, 58]. They seem quite robust and not sensitive to the causal patch arguments made in chapter 2. An advantage of the holographic description is that black hole evaporation is manifestly unitary in the CFT, although it is far from clear how this happens from the bulk point of view. Various holographically inspired resolutions have been proposed, some of the most interesting ones suggesting a state-dependent way of doing AdS/CFT in order to avoid firewalls by reconstructing bulk fields near (or even behind) the horizon [114–118]. There is no doubt that, in order to settle these issues and ultimately understand quantum gravity, a detailed study of the bulk-boundary mapping and (sub-AdS scale) locality in AdS/CFT is required. These questions brought us to the chapters 3, 4 and 5 in this thesis.

6.2 Precarious Precursors

The AdS/CFT correspondence turned out to be an exciting laboratory, radically and rapidly changing the décor of modern high energy theory research. It maps the strongly coupled phase of a gauge theory to a particularly well understood low energy limit of string theory (supergravity), and vice versa. Since AdS/CFT is a duality between the full string theory and gauge theory, it should provide hints for dealing with string theories and gauge theories well beyond perturbative regimes. Therefore, holography allows us to explore gauge and string theories in ways which were inaccessible before. This exploration takes place from two point of views. First of all from a fundamental viewpoint, where AdS/CFT provides a non-perturbative definition of quantum gravity in AdS in terms of an holographically dual CFT living on the boundary. Secondly from a more phenomenological viewpoint, where new developments like AdS/QCD (which predicted the universal viscosity to entropy ratio for a large class of strongly interacting field theories [119]) or AdS/CMT (which provides a stringy description of strongly coupled condensed matter systems such as superconductors or superfluids) gave rise to entire new fields of theoretical physics.

In order to make ‘practical’ use of the correspondence, a dictionary for translating gauge theory problems into string theory ones (and vice versa) is necessary. A central problem is how to reconstruct gravitational bulk physics from boundary data. We saw that the boundary duals of local operators deep in the bulk have highly non-local representations in the CFT, known as precursors. Following the HKLL construction, these can be localized to the boundary region of an AdS-Rindler wedge that contains the bulk field. This immediately raises the question of redundant boundary duals: a bulk field that falls within multiple boundary wedges must have multiple, different boundary representations. We are therefore left with the problem of how inequivalent precursors can all give rise to the same bulk operator.

In chapter 3, we addressed this question using an improved version of the holographic toy model in [69]. There it was argued that the non-uniqueness of precursors is a simple consequence of boundary gauge invariance, an idea on which we elaborated later in chapter 4. We provided an explicit demonstration of this proposal, explained how boundary gauge invariance leads to an ambiguity in the smearing function, and used the ambiguity to localize precursors within a single Rindler wedge. This supports the claim that gauge invariance may be deeply connected to the emergence of the dual spacetime [4, 69]. In section 3.3, this was accomplished without any mention of boundary entanglement. Rather, it relied only on the freedom to add unphysical modes to the precursor.

In contrast, entanglement is essential for a quantum error correction scheme to succeed [73]. Indeed, it has been postulated that the entanglement between boundary regions plays a crucial role in the emergence of the bulk spacetime, and there are reasons to believe that the entanglement – as opposed to the causal – wedge is the more natural bulk dual for holographic reconstruction [80, 120–126]. In the interest of further exploring the link between entanglement and localization, we showed explicitly in section 3.4 that the entanglement between boundary Rindler wedges can likewise be used to localize the bulk information to within a single region, provided that the bulk point is contained in the particular Rindler wedge, in complete agreement with the previous approach based on ambiguities in the smearing function.

Our model may also be useful for diagnosing proposals for the description of operators behind the black hole horizon, such as [117, 127], since the bulk spacetime we considered does have a Rindler horizon. In addition, it may clarify subtleties in the CFT operators dual to bulk fields outside the black hole horizon, which have the same properties as our Rindler precursors.

It is interesting to ask whether our model continues to agree with expectations about the full AdS/CFT correspondence when we consider more complicated boundary regions, such as disconnected intervals. The analogous set-up for a disconnected boundary region is shown in figure 6.1. The shaded region is the entanglement wedge for the given, disconnected boundary region. When this region becomes sufficiently large, the bulk minimal surface transitions to the new global minimum, whereupon the entanglement wedge suddenly includes the bulk point [5, 128]. The question we wish to ask is whether our model generalizes to agree with the corresponding reconstruction prescription. Specifically, can the precursor corresponding to a bulk point within the shaded bulk region be localized within the (disconnected) boundary of this region?

Generalizing our results to multiple, disconnected boundary regions requires either an explicit formula for the pure-gauge smearing function δK , or a general prescription for when a particular bilocal can be mapped into a given wedge. We cannot present a general solution, but instead comment on what one might expect given the obtained results, in the interest of comparing them with reconstruction proposals involving the entanglement wedge [80] and quantum error correction [73]. Naïvely generalizing our results for the case of a single boundary region, we would suspect that the precursor cannot be mapped to a healthy operator within the boundary wedge, if some bilocals that are evolved back from the lightcone singularity, have both points outside the CFT region under interest. This simple criterion would imply that our simple model fails to reproduce the expected result, namely that bulk operators in the entanglement wedge can be mapped to

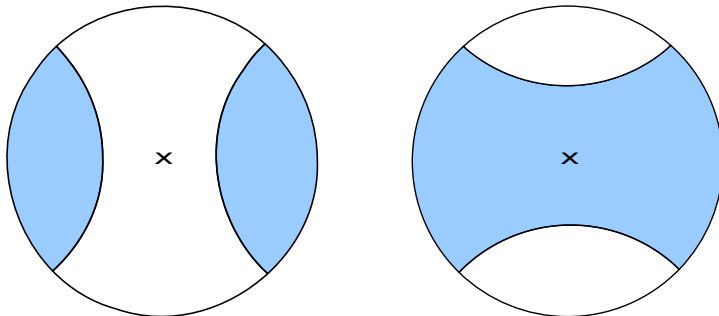


Figure 6.1: Time slice of global AdS, with the entanglement wedge for a disconnected region (shaded). If the region is sufficiently small (left), the bulk point labelled x will not be included, and hence the shaded boundary region contains no information about it. However, as the boundary region is increased, the bulk minimal surfaces that define the entanglement wedge eventually transition to a new global minimum (right), whereupon the shaded boundary region abruptly gains information about the given bulk point. Intuitively, one needs ‘enough’ of the boundary to reconstruct the bulk.

precursors in the corresponding boundary region. It should perhaps not be too surprising that our weakly-coupled model does not have enough features to reproduce the entanglement wedge reconstruction, because expectations about the entanglement wedge are based on the Ryu-Takayanagi (RT) formula for the entanglement entropy. It is known that a simple free field model on the boundary will not reproduce the correct RT formula for the entanglement entropy of multiple intervals [129]. Thus, while our model appears to generalize naturally to disconnected *causal* wedges, there is no obvious generalization that would correctly reproduce the *entanglement* wedge prescription. Understanding precisely how the entanglement structure, or the gauge freedom, conspires to produce localized precursors describing the interior of the entanglement wedge of general boundary regions, would be very illuminating.

In chapter 4 we focused on the paradoxical property that different precursors can correspond to the same bulk field. In particular, the difference between two such precursors, while it is a nontrivial operator in the CFT, does not seem to have any physical meaning in the bulk. We conjectured that, in the large N limit, such an operator is BRST exact and ghost-free, and showed that by construction it can be freely added to operators inside physical correlation functions. That is exactly the property we would want a precursor ambiguity to have. This constitutes preliminary evidence that precursors are related to the underlying gauge symmetry of the field theory. To support our claim, we re-derived the precursor ambiguity in the same, simple holographic toy model that was used in chapter 3 to modify the spatial support of the smearing function.

Several interesting follow-up directions remain to be explored. One could for example study precursors in the toy model in nontrivial states (such as thermal states), but more importantly, one would like to generalize the construction to a proper gauge theory with local gauge invariance. Perhaps the simplest example of a field theoretic precursor ambiguity is to consider the dual of the bulk operator one obtains by integrating a bulk field over a symmetric minimal surface. Such operators were studied in [130,131], and to lowest order in the $1/N$ expansion in the field theory they are given by appropriately smearing the boundary value of the bulk scalar over the causal diamond (defined using the boundary of the bulk minimal surface). There are two equivalent choices of causal diamonds for a given symmetric minimal surface. Together, they contain a full Cauchy slice for the field theory. Hence, there are two inequivalent boundary representations of the same bulk operator, and the difference between these two is an example of a precursor ambiguity. We would therefore like to conjecture that there exists an operator Y such that this difference is given by $\{Y, Q_{\text{BRST}}\}$. It would be very interesting to try and construct such an operator Y .

Finally, in chapter 5, we discussed the broader issue of bulk locality in $\text{AdS}_3/\text{CFT}_2$. Dissecting the toy model used in chapter 3 showed the presence of an infinite tower of higher spins in the bulk. While this typically gives rise to a non-local theory (in the sense that the bulk Lagrangian will contain an infinite number of derivatives), surprisingly, a detailed analysis showed that it has the right low- and high energy density of states to be dual to a local gravitational theory in the bulk. However, because the model is pathological – it is not modular invariant due to projecting out all states which are not $\text{SO}(N)$ singlets – we were led to conjecture that at large N all CFT_2 's that have a density of states which is bounded by that of a local QFT in D -dimensions (cf. the locality criterion discussed in section 5.2) and are modular invariant, will be dual to a gravitational bulk theory with sub-AdS scale locality.

Evidence for this is largely circumstantial, and based on the absence of a counterexample and our intuition with orbifold CFT's that restoring modular invariance requires a drastic modification of the spectrum, violating the locality criterion. A lot of future work remains to be done to completely understand which CFTs have local bulk duals. To prove the conjecture one would have to impose modular invariance and the constraint on the density of states, and try to translate this to conditions on the OPE coefficients, perhaps using bootstrap-like techniques. Since the OPE's define the CFT (together with its spectrum) and contain all the dynamical information, we would expect them to play a key role. It would also be interesting to understand how our conjecture relates to other criteria, such as the Lorentzian four-point function and the gap in the operator dimensions as explained in the introduction.

The mystery of why and how the CFT organizes its degrees of freedom in such a way to give rise to a bulk theory with (sub-AdS scale) locality, remains a – for me personally, probably *the* – great miracle of AdS/CFT. Although progress has been made, more research is necessary to fully apprehend what this tells us about quantum gravity. Theoretical physicists are determined to do what is needed, and a better understanding of the laws of nature will ultimately and inevitably follow. Whether that would require jumping in burning black holes, dealing with precarious precursors, or studying further aspects of gauge/gravity duality.

Bibliography

- [1] B. Freivogel, R. A. Jefferson, L. Kabir, and I.-S. Yang, “Geometry of the Infalling Causal Patch,” *Phys. Rev.* **D91** no. 4, (2015) 044036, arXiv:1406.6043 [hep-th].
- [2] B. Freivogel, R. A. Jefferson, and L. Kabir, “Precursors, Gauge Invariance, and Quantum Error Correction in AdS/CFT,” *JHEP* **04** (2016) 119, arXiv:1602.04811 [hep-th].
- [3] A. Belin, B. Freivogel, R. A. Jefferson, and L. Kabir, “Sub-AdS Scale Locality in AdS₃/CFT₂,” *JHEP* **04** (2017) 147, arXiv:1611.08601 [hep-th].
- [4] J. de Boer, B. Freivogel, L. Kabir, and S. F. Lokhande, “Precursors and BRST Symmetry,” arXiv:1612.05265 [hep-th].
- [5] B. Freivogel, R. A. Jefferson, L. Kabir, B. Mosk, and I.-S. Yang, “Casting Shadows on Holographic Reconstruction,” *Phys. Rev.* **D91** no. 8, (2015) 086013, arXiv:1412.5175 [hep-th].
- [6] F. V. Dimitrakopoulos, L. Kabir, B. Mosk, M. Parikh, and J. P. van der Schaar, “Vacua and correlators in hyperbolic de Sitter space,” *JHEP* **06** (2015) 095, arXiv:1502.00113 [hep-th].
- [7] A. Einstein, “The Foundation of the General Theory of Relativity,” *Annalen Phys.* **49** (1916) 769–822. [Annalen Phys.14,517(2005)].
- [8] K. Schwarzschild, “On the gravitational field of a mass point according to Einstein’s theory,” *Sitzungsber. Preuss. Akad. Wiss. Berlin (Math. Phys.)* **1916** (1916) 189–196, arXiv:physics/9905030 [physics].
- [9] S. W. Hawking, “Black holes in general relativity,” *Commun. Math. Phys.* **25** (1972) 152–166.
- [10] J. D. Bekenstein, “Black holes and entropy,” *Phys.Rev.* **D7** (1973) 2333–2346.
- [11] S. Hawking, “Particle Creation by Black Holes,” *Commun.Math.Phys.* **43** (1975) 199–220.

- [12] A. Strominger and C. Vafa, “Microscopic origin of the Bekenstein-Hawking entropy,” *Phys.Lett.* **B379** (1996) 99–104, arXiv:hep-th/9601029 [hep-th].
- [13] G. Gibbons and S. Hawking, “Cosmological Event Horizons, Thermodynamics, and Particle Creation,” *Phys.Rev.* **D15** (1977) 2738–2751.
- [14] M. Banados, C. Teitelboim, and J. Zanelli, “The Black hole in three-dimensional space-time,” *Phys. Rev. Lett.* **69** (1992) 1849–1851, arXiv:hep-th/9204099 [hep-th].
- [15] S. W. Hawking and D. N. Page, “Thermodynamics of Black Holes in anti-De Sitter Space,” *Commun. Math. Phys.* **87** (1983) 577.
- [16] L. Kabir, “Quiver Models: Quantum Metrics & Monte Carlo,” *MSc Dissertation, Unpublished* (2013) .
- [17] G. ’t Hooft, “Dimensional reduction in quantum gravity,” arXiv:gr-qc/9310026 [gr-qc].
- [18] L. Susskind, “The World as a hologram,” *J.Math.Phys.* **36** (1995) 6377–6396, arXiv:hep-th/9409089 [hep-th].
- [19] J. M. Maldacena, “The Large N limit of superconformal field theories and supergravity,” *Adv.Theor.Math.Phys.* **2** (1998) 231–252, arXiv:hep-th/9711200 [hep-th].
- [20] G. ’t Hooft, “A Planar Diagram Theory for Strong Interactions,” *Nucl.Phys.* **B72** (1974) 461.
- [21] S. Coleman, *Aspects of Symmetry*. Cambridge Univ. Press, Cambridge, 1985.
- [22] D. Z. Freedman and A. Van Proeyen, *Supergravity*. Cambridge Univ. Press, Cambridge, 2012.
- [23] O. Aharony, S. S. Gubser, J. M. Maldacena, H. Ooguri, and Y. Oz, “Large N field theories, string theory and gravity,” *Phys. Rept.* **323** (2000) 183–386, arXiv:hep-th/9905111 [hep-th].
- [24] E. Witten, “Anti-de Sitter space and holography,” *Adv.Theor.Math.Phys.* **2** (1998) 253–291, arXiv:hep-th/9802150 [hep-th].
- [25] S. Gubser, I. R. Klebanov, and A. M. Polyakov, “Gauge theory correlators from noncritical string theory,” *Phys.Lett.* **B428** (1998) 105–114, arXiv:hep-th/9802109 [hep-th].

- [26] L. Susskind and E. Witten, “The Holographic bound in anti-de Sitter space,” arXiv:hep-th/9805114 [hep-th].
- [27] T. Banks, M. R. Douglas, G. T. Horowitz, and E. J. Martinec, “AdS dynamics from conformal field theory,” arXiv:hep-th/9808016 [hep-th].
- [28] I. R. Klebanov and E. Witten, “AdS / CFT correspondence and symmetry breaking,” *Nucl.Phys.* **B556** (1999) 89–114, arXiv:hep-th/9905104 [hep-th].
- [29] L. Mezincescu and P. Townsend, “Stability at a Local Maximum in Higher Dimensional Anti-de Sitter Space and Applications to Supergravity,” *Annals Phys.* **160** (1985) 406.
- [30] D. Harlow and D. Stanford, “Operator Dictionaries and Wave Functions in AdS/CFT and dS/CFT,” arXiv:1104.2621 [hep-th].
- [31] A. Hamilton, D. N. Kabat, G. Lifschytz, and D. A. Lowe, “Local bulk operators in AdS/CFT: A Boundary view of horizons and locality,” *Phys. Rev.* **D73** (2006) 086003, arXiv:hep-th/0506118 [hep-th].
- [32] A. Hamilton, D. N. Kabat, G. Lifschytz, and D. A. Lowe, “Holographic representation of local bulk operators,” *Phys. Rev.* **D74** (2006) 066009, arXiv:hep-th/0606141 [hep-th].
- [33] A. Hamilton, D. N. Kabat, G. Lifschytz, and D. A. Lowe, “Local bulk operators in AdS/CFT: A Holographic description of the black hole interior,” *Phys. Rev.* **D75** (2007) 106001, arXiv:hep-th/0612053 [hep-th]. [Erratum: *Phys. Rev.*D75,129902(2007)].
- [34] A. Hamilton, D. N. Kabat, G. Lifschytz, and D. A. Lowe, “Local bulk operators in AdS/CFT and the fate of the BTZ singularity,” *AMS/IP Stud. Adv. Math.* **44** (2008) 85–100, arXiv:0710.4334 [hep-th].
- [35] D. Kabat, G. Lifschytz, and D. A. Lowe, “Constructing local bulk observables in interacting AdS/CFT,” *Phys. Rev.* **D83** (2011) 106009, arXiv:1102.2910 [hep-th].
- [36] D. Kabat, G. Lifschytz, S. Roy, and D. Sarkar, “Holographic representation of bulk fields with spin in AdS/CFT,” *Phys. Rev.* **D86** (2012) 026004, arXiv:1204.0126 [hep-th].
- [37] D. Kabat and G. Lifschytz, “CFT representation of interacting bulk gauge fields in AdS,” *Phys. Rev.* **D87** no. 8, (2013) 086004, arXiv:1212.3788 [hep-th].

- [38] D. Kabat and G. Lifschytz, “Decoding the hologram: Scalar fields interacting with gravity,” *Phys. Rev.* **D89** no. 6, (2014) 066010, arXiv:1311.3020 [hep-th].
- [39] D. Kabat and G. Lifschytz, “Finite N and the failure of bulk locality: Black holes in AdS/CFT,” *JHEP* **09** (2014) 077, arXiv:1405.6394 [hep-th].
- [40] D. Kabat and G. Lifschytz, “Bulk equations of motion from CFT correlators,” *JHEP* **09** (2015) 059, arXiv:1505.03755 [hep-th].
- [41] D. Kabat and G. Lifschytz, “Locality, bulk equations of motion and the conformal bootstrap,” *JHEP* **10** (2016) 091, arXiv:1603.06800 [hep-th].
- [42] S. Leichenauer and V. Rosenhaus, “AdS black holes, the bulk-boundary dictionary, and smearing functions,” *Phys. Rev.* **D88** no. 2, (2013) 026003, arXiv:1304.6821 [hep-th].
- [43] I. Heemskerk, J. Penedones, J. Polchinski, and J. Sully, “Holography from Conformal Field Theory,” *JHEP* **10** (2009) 079, arXiv:0907.0151 [hep-th].
- [44] A. Almheiri, D. Marolf, J. Polchinski, and J. Sully, “Black Holes: Complementarity or Firewalls?,” *JHEP* **02** (2013) 062, arXiv:1207.3123 [hep-th].
- [45] D. N. Page, “Information in black hole radiation,” *Phys. Rev. Lett.* **71** (1993) 3743–3746, arXiv:hep-th/9306083 [hep-th].
- [46] D. N. Page, “Time Dependence of Hawking Radiation Entropy,” *JCAP* **1309** (2013) 028, arXiv:1301.4995 [hep-th].
- [47] S. W. Hawking, “Breakdown of Predictability in Gravitational Collapse,” *Phys. Rev.* **D14** (1976) 2460–2473.
- [48] S. D. Mathur, “The Information paradox: A Pedagogical introduction,” *Class. Quant. Grav.* **26** (2009) 224001, arXiv:0909.1038 [hep-th].
- [49] S. L. Braunstein, S. Pirandola, and K. Życzkowski, “Better Late than Never: Information Retrieval from Black Holes,” *Phys. Rev. Lett.* **110** no. 10, (2013) 101301, arXiv:0907.1190 [quant-ph].
- [50] L. Susskind, L. Thorlacius, and J. Uglum, “The Stretched horizon and black hole complementarity,” *Phys. Rev.* **D48** (1993) 3743–3761, arXiv:hep-th/9306069 [hep-th].
- [51] L. Susskind, “String theory and the principles of black hole complementarity,” *Phys. Rev. Lett.* **71** (1993) 2367–2368, arXiv:hep-th/9307168 [hep-th].

- [52] L. Susskind and L. Thorlacius, “Gedanken experiments involving black holes,” *Phys. Rev.* **D49** (1994) 966–974, arXiv:hep-th/9308100 [hep-th].
- [53] K. Schoutens, H. L. Verlinde, and E. P. Verlinde, “Black hole evaporation and quantum gravity,”
- [54] Y. Kiem, H. L. Verlinde, and E. P. Verlinde, “Black hole horizons and complementarity,” *Phys. Rev.* **D52** (1995) 7053–7065, arXiv:hep-th/9502074 [hep-th].
- [55] I. Ilgin and I.-S. Yang, “Causal Patch Complementarity: The Inside Story for Old Black Holes,” *Phys. Rev.* **D89** no. 4, (2014) 044007, arXiv:1311.1219 [hep-th].
- [56] B. Freivogel, “Energy and Information Near Black Hole Horizons,” *JCAP* **1407** (2014) 041, arXiv:1401.5340 [hep-th].
- [57] D. Marolf and J. Polchinski, “Gauge/Gravity Duality and the Black Hole Interior,” *Phys. Rev. Lett.* **111** (2013) 171301, arXiv:1307.4706 [hep-th].
- [58] A. Almheiri, D. Marolf, J. Polchinski, D. Stanford, and J. Sully, “An Apologia for Firewalls,” *JHEP* **09** (2013) 018, arXiv:1304.6483 [hep-th].
- [59] D. Harlow and P. Hayden, “Quantum Computation vs. Firewalls,” *JHEP* **06** (2013) 085, arXiv:1301.4504 [hep-th].
- [60] L. Hui and I.-S. Yang, “Complementarity plus backreaction is enough,” *Phys. Rev.* **D89** no. 8, (2014) 084011, arXiv:1308.6268 [hep-th].
- [61] R. Bousso, B. Freivogel, S. Leichenauer, V. Rosenhaus, and C. Zukowski, “Null Geodesics, Local CFT Operators and AdS/CFT for Subregions,” *Phys. Rev.* **D88** (2013) 064057, arXiv:1209.4641 [hep-th].
- [62] S.-J. Rey and V. Rosenhaus, “Scanning Tunneling Macroscopy, Black Holes, and AdS/CFT Bulk Locality,” *JHEP* **07** (2014) 050, arXiv:1403.3943 [hep-th].
- [63] A. R. Brown, “Tensile Strength and the Mining of Black Holes,” *Phys. Rev. Lett.* **111** no. 21, (2013) 211301, arXiv:1207.3342 [gr-qc].
- [64] R. Bousso, B. Freivogel, and S. Leichenauer, “Saturating the holographic entropy bound,” *Phys. Rev.* **D82** (2010) 084024, arXiv:1003.3012 [hep-th].
- [65] K. Martel and E. Poisson, “Regular coordinate systems for Schwarzschild and other spherical space-times,” *Am. J. Phys.* **69** (2001) 476–480, arXiv:gr-qc/0001069 [gr-qc].

- [66] L. Susskind, “Black Hole Complementarity and the Harlow-Hayden Conjecture,” arXiv:1301.4505 [hep-th].
- [67] R. Cleve, D. Gottesman, and H.-K. Lo, “How to share a quantum secret,” *Phys. Rev. Lett.* **83** (1999) 648–651, arXiv:quant-ph/9901025 [quant-ph].
- [68] M. Hillery, V. Bužek, and A. Berthiaume, “Quantum secret sharing,” *Phys. Rev.* **A59** (1999) 1829, arXiv:quant-ph/9806063 [quant-ph].
- [69] E. Mintun, J. Polchinski, and V. Rosenhaus, “Bulk-Boundary Duality, Gauge Invariance, and Quantum Error Corrections,” *Phys. Rev. Lett.* **115** no. 15, (2015) 151601, arXiv:1501.06577 [hep-th].
- [70] J. Polchinski, L. Susskind, and N. Toumbas, “Negative energy, superluminality and holography,” *Phys. Rev.* **D60** (1999) 084006, arXiv:hep-th/9903228 [hep-th].
- [71] S. B. Giddings and M. Lippert, “Precursors, black holes, and a locality bound,” *Phys. Rev.* **D65** (2002) 024006, arXiv:hep-th/0103231 [hep-th].
- [72] B. Freivogel, S. B. Giddings, and M. Lippert, “Toward a theory of precursors,” *Phys. Rev.* **D66** (2002) 106002, arXiv:hep-th/0207083 [hep-th].
- [73] A. Almheiri, X. Dong, and D. Harlow, “Bulk Locality and Quantum Error Correction in AdS/CFT,” *JHEP* **04** (2015) 163, arXiv:1411.7041 [hep-th].
- [74] R. Haag, *Local quantum physics: Fields, particles, algebras*. 1992.
- [75] B. Chilian and K. Fredenhagen, “The Time slice axiom in perturbative quantum field theory on globally hyperbolic spacetimes,” *Commun. Math. Phys.* **287** (2009) 513–522, arXiv:0802.1642 [math-ph].
- [76] F. Pastawski, B. Yoshida, D. Harlow, and J. Preskill, “Holographic quantum error-correcting codes: Toy models for the bulk/boundary correspondence,” *JHEP* **06** (2015) 149, arXiv:1503.06237 [hep-th].
- [77] Z. Yang, P. Hayden, and X.-L. Qi, “Bidirectional holographic codes and sub-AdS locality,” *JHEP* **01** (2016) 175, arXiv:1510.03784 [hep-th].
- [78] P. Hayden, S. Nezami, X.-L. Qi, N. Thomas, M. Walter, and Z. Yang, “Holographic duality from random tensor networks,” *JHEP* **11** (2016) 009, arXiv:1601.01694 [hep-th].
- [79] T. Andrade and D. Marolf, “AdS/CFT beyond the unitarity bound,” *JHEP* **01** (2012) 049, arXiv:1105.6337 [hep-th].

- [80] X. Dong, D. Harlow, and A. C. Wall, “Reconstruction of Bulk Operators within the Entanglement Wedge in Gauge-Gravity Duality,” *Phys. Rev. Lett.* **117** no. 2, (2016) 021601, arXiv:1601.05416 [hep-th].
- [81] C. Becchi, A. Rouet, and R. Stora, “Renormalization of Gauge Theories,” *Annals Phys.* **98** (1976) 287–321.
- [82] I. V. Tyutin, “Gauge Invariance in Field Theory and Statistical Physics in Operator Formalism,” arXiv:0812.0580 [hep-th].
- [83] I. Heemskerk, D. Marolf, J. Polchinski, and J. Sully, “Bulk and Transhorizon Measurements in AdS/CFT,” *JHEP* **10** (2012) 165, arXiv:1201.3664 [hep-th].
- [84] I. Klebanov and A. Polyakov, “AdS dual of the critical O(N) vector model,” *Phys.Lett.* **B550** (2002) 213–219, arXiv:hep-th/0210114 [hep-th].
- [85] S. Giombi and X. Yin, “The Higher Spin/Vector Model Duality,” *J. Phys.* **A46** (2013) 214003, arXiv:1208.4036 [hep-th].
- [86] S. B. Giddings, “Flat space scattering and bulk locality in the AdS / CFT correspondence,” *Phys. Rev.* **D61** (2000) 106008, arXiv:hep-th/9907129 [hep-th].
- [87] M. Gary, S. B. Giddings, and J. Penedones, “Local bulk S-matrix elements and CFT singularities,” *Phys. Rev.* **D80** (2009) 085005, arXiv:0903.4437 [hep-th].
- [88] M. Gary and S. B. Giddings, “The Flat space S-matrix from the AdS/CFT correspondence?,” *Phys. Rev.* **D80** (2009) 046008, arXiv:0904.3544 [hep-th].
- [89] J. Maldacena, D. Simmons-Duffin, and A. Zhiboedov, “Looking for a bulk point,” arXiv:1509.03612 [hep-th].
- [90] M. A. Vasiliev, “Higher spin gauge theories in four-dimensions, three-dimensions, and two-dimensions,” *Int. J. Mod. Phys.* **D5** (1996) 763–797, arXiv:hep-th/9611024 [hep-th].
- [91] M. R. Gaberdiel and C. Vollenweider, “Minimal Model Holography for SO(2N),” *JHEP* **08** (2011) 104, arXiv:1106.2634 [hep-th].
- [92] C. Candu, M. R. Gaberdiel, M. Kelm, and C. Vollenweider, “Even spin minimal model holography,” *JHEP* **01** (2013) 185, arXiv:1211.3113 [hep-th].

- [93] S. Banerjee, A. Castro, S. Hellerman, E. Hijano, A. Lepage-Jutier, A. Maloney, and S. Shenker, “Smoothed Transitions in Higher Spin AdS Gravity,” *Class. Quant. Grav.* **30** (2013) 104001, arXiv:1209.5396 [hep-th].
- [94] J. D. Brown and M. Henneaux, “Central Charges in the Canonical Realization of Asymptotic Symmetries: An Example from Three-Dimensional Gravity,” *Commun. Math. Phys.* **104** (1986) 207–226.
- [95] S. El-Showk and K. Papadodimas, “Emergent Spacetime and Holographic CFTs,” *JHEP* **10** (2012) 106, arXiv:1101.4163 [hep-th].
- [96] A. L. Fitzpatrick and J. Kaplan, “AdS Field Theory from Conformal Field Theory,” *JHEP* **02** (2013) 054, arXiv:1208.0337 [hep-th].
- [97] T. Hartman, C. A. Keller, and B. Stoica, “Universal Spectrum of 2d Conformal Field Theory in the Large c Limit,” *JHEP* **09** (2014) 118, arXiv:1405.5137 [hep-th].
- [98] A. L. Fitzpatrick, J. Kaplan, and M. T. Walters, “Universality of Long-Distance AdS Physics from the CFT Bootstrap,” *JHEP* **08** (2014) 145, arXiv:1403.6829 [hep-th].
- [99] A. Belin, C. A. Keller, and A. Maloney, “String Universality for Permutation Orbifolds,” *Phys. Rev.* **D91** no. 10, (2015) 106005, arXiv:1412.7159 [hep-th].
- [100] F. M. Haehl and M. Rangamani, “Permutation orbifolds and holography,” *JHEP* **03** (2015) 163, arXiv:1412.2759 [hep-th].
- [101] A. Belin, C. A. Keller, and A. Maloney, “Permutation Orbifolds in the large N Limit,” arXiv:1509.01256 [hep-th].
- [102] A. Belin, J. de Boer, J. Kruthoff, B. Michel, E. Shaghoulian, and M. Shyani, “Universality of Sparse $d > 2$ Conformal Field Theory at Large N ,” arXiv:1610.06186 [hep-th].
- [103] M. R. Gaberdiel, R. Gopakumar, and M. Rangamani, “The Spectrum of Light States in Large N Minimal Models,” *JHEP* **01** (2014) 116, arXiv:1310.1744 [hep-th].
- [104] P. Kraus and A. Maloney, “A Cardy Formula for Three-Point Coefficients: How the Black Hole Got its Spots,” arXiv:1608.03284 [hep-th].
- [105] M. R. Gaberdiel, K. Jin, and W. Li, “Perturbations of $W(\infty)$ CFTs,” *JHEP* **10** (2013) 162, arXiv:1307.4087 [hep-th].
- [106] S. Giombi, A. Maloney, and X. Yin, “One-loop Partition Functions of 3D Gravity,” *JHEP* **08** (2008) 007, arXiv:0804.1773 [hep-th].

- [107] M. A. Vasiliev, “Star-Product Functions in Higher-Spin Theory and Locality,” *JHEP* **06** (2015) 031, arXiv:1502.02271 [hep-th].
- [108] E. D. Skvortsov and M. Taronna, “On Locality, Holography and Unfolding,” *JHEP* **11** (2015) 044, arXiv:1508.04764 [hep-th].
- [109] M. Taronna, “Pseudo-local Theories: A Functional Class Proposal,” in *Proceedings, International Workshop on Higher Spin Gauge Theories: Singapore, Singapore, November 4-6, 2015*. 2017.
- [110] M. A. Vasiliev, “Current Interactions, Locality and Holography from the 0-Form Sector of Nonlinear Higher-Spin Equations,” arXiv:1605.02662 [hep-th].
- [111] M. Taronna, “A Note on Field Redefinitions and Higher-Spin Equations,” *EPJ Web Conf.* **125** (2016) 05025, arXiv:1607.04718 [hep-th].
- [112] X. Bekaert, J. Erdmenger, D. Ponomarev, and C. Sleight, “Bulk quartic vertices from boundary four-point correlators,” in *Proceedings, International Workshop on Higher Spin Gauge Theories: Singapore, Singapore, November 4-6, 2015*. 2017.
- [113] J. Maldacena and L. Susskind, “Cool horizons for entangled black holes,” *Fortsch.Phys.* **61** (2013) 781–811, arXiv:1306.0533 [hep-th].
- [114] K. Papadodimas and S. Raju, “An Infalling Observer in AdS/CFT,” *JHEP* **10** (2013) 212, arXiv:1211.6767 [hep-th].
- [115] K. Papadodimas and S. Raju, “Black Hole Interior in the Holographic Correspondence and the Information Paradox,” *Phys.Rev.Lett.* **112** no. 5, (2014) 051301, arXiv:1310.6334 [hep-th].
- [116] K. Papadodimas and S. Raju, “State-Dependent Bulk-Boundary Maps and Black Hole Complementarity,” *Phys. Rev.* **D89** no. 8, (2014) 086010, arXiv:1310.6335 [hep-th].
- [117] K. Papadodimas and S. Raju, “Local Operators in the Eternal Black Hole,” *Phys. Rev. Lett.* **115** no. 21, (2015) 211601, arXiv:1502.06692 [hep-th].
- [118] K. Papadodimas and S. Raju, “Remarks on the necessity and implications of state-dependence in the black hole interior,” *Phys. Rev.* **D93** no. 8, (2016) 084049, arXiv:1503.08825 [hep-th].
- [119] P. Kovtun, D. Son, and A. Starinets, “Viscosity in strongly interacting quantum field theories from black hole physics,” *Phys.Rev.Lett.* **94** (2005) 111601, arXiv:hep-th/0405231 [hep-th].

- [120] B. Czech, J. L. Karczmarek, F. Nogueira, and M. Van Raamsdonk, “The Gravity Dual of a Density Matrix,” *Class. Quant. Grav.* **29** (2012) 155009, arXiv:1204.1330 [hep-th].
- [121] A. Lewkowycz and J. Maldacena, “Generalized gravitational entropy,” *JHEP* **1308** (2013) 090, arXiv:1304.4926 [hep-th].
- [122] D. L. Jafferis, A. Lewkowycz, J. Maldacena, and S. J. Suh, “Relative entropy equals bulk relative entropy,” *JHEP* **06** (2016) 004, arXiv:1512.06431 [hep-th].
- [123] T. Faulkner, A. Lewkowycz, and J. Maldacena, “Quantum corrections to holographic entanglement entropy,” *JHEP* **1311** (2013) 074, arXiv:1307.2892.
- [124] M. Headrick, V. E. Hubeny, A. Lawrence, and M. Rangamani, “Causality & holographic entanglement entropy,” *JHEP* **12** (2014) 162, arXiv:1408.6300 [hep-th].
- [125] N. Bao and I. H. Kim, “Precursor problem and holographic mutual information,” arXiv:1601.07616 [hep-th].
- [126] A. C. Wall, “Maximin Surfaces, and the Strong Subadditivity of the Covariant Holographic Entanglement Entropy,” *Class. Quant. Grav.* **31** no. 22, (2014) 225007, arXiv:1211.3494 [hep-th].
- [127] M. Guica and D. L. Jafferis, “On the construction of charged operators inside an eternal black hole,” arXiv:1511.05627 [hep-th].
- [128] V. E. Hubeny, H. Maxfield, M. Rangamani, and E. Tonni, “Holographic entanglement plateaux,” *JHEP* **08** (2013) 092, arXiv:1306.4004 [hep-th].
- [129] S. Leichenauer and M. Moosa, “Entanglement Tsunami in (1+1)-Dimensions,” *Phys. Rev.* **D92** (2015) 126004, arXiv:1505.04225 [hep-th].
- [130] B. Czech, L. Lamprou, S. McCandlish, B. Mosk, and J. Sully, “A Stereoscopic Look into the Bulk,” *JHEP* **07** (2016) 129, arXiv:1604.03110 [hep-th].
- [131] J. de Boer, F. M. Haehl, M. P. Heller, and R. C. Myers, “Entanglement, holography and causal diamonds,” *JHEP* **08** (2016) 162, arXiv:1606.03307 [hep-th].

Contributions to Publications

Here I give a brief overview of my personal contributions to the publications on which this thesis is based on. For each of my publications, I participated and contributed in all conceptual discussions from which the intellectual content originated. Writing the papers was always done in close collaboration with the co-authors. Note that in theoretical high energy physics, the authors are always listed alphabetically, so the order does not reflect individual contributions.

- [1] B. Freivogel, R. Jefferson, L. Kabir and I-S. Yang

Geometry of the Infalling Causal Patch

Phys. Rev. **D91 no. 4**, 044036 (2015), arXiv:1406.6043 [hep-th].

I did the analysis for black holes in AdS and dS, suggested the use of PG coordinates to study the infalling observer for the $D = 4$ Schwarzschild black hole, and performed the analytics in section 3.

- [2] B. Freivogel, R. Jefferson and L. Kabir

Precursors, Gauge Invariance, and Quantum Error Correction in AdS/CFT

JHEP **1604**, 119 (2016), arXiv:1602.04811 [hep-th].

I performed the calculations in section 3 (except the analytical continuation of the Rindler modes), section 4 and the appendices.

- [3] A. Belin, B. Freivogel, R. Jefferson and L. Kabir

Sub-AdS Scale Locality in AdS₃/CFT₂

JHEP **1704**, 147 (2017), arXiv:1611.08601 [hep-th].

I carried out the analysis of the low- and high energy density of states in section 2, and did the bulk locality computations in section 3.1. I analytically computed the Virasoro primaries at finite N up to level 4.

- [4] J. de Boer, B. Freivogel, L. Kabir and S. F. Lokhande

Precursors and BRST Symmetry

arXiv:1612.05265 [hep-th].

I performed the computations in sections 2 & 3, and the computations in section 4.3. I contributed to formulating the conjecture.

Samenvatting

BULK-LOKALITEIT GEBROKEN: GLOEIENDE ZWARTE GATEN & PRECAIRE PRECURSOREN

Deze thesis tracht een overzicht te geven van een deel van het onderzoek dat ik verricht heb tijdens mijn doctoraatsstudies in Amsterdam. Mijn onderzoek spitst zich toe op hoe fundamentele onderwerpen zoals algemene relativiteitstheorie, thermodynamica en kwantummechanica aan elkaar gerelateerd blijken. Er bestaan verschillende connecties, die tot uiting komen in zwarte gaten, holografie, en de AdS/CFT correspondentie in het bijzonder. In deze samenvatting zal ik dan ook proberen een korte valoriserende introductie te geven tot deze onderwerpen, en tegelijkertijd mijn wetenschappelijke bijdrage bondig toe te lichten.

Introductie

In het begin van vorige eeuw werden de fundamentele principes van de kwantummechanica gelegd, een theorie die kleine deeltjes zoals moleculen en atomen beschrijft. Het combineren van de kwantummechanica met de principes van een andere ontdekking uit het begin van vorige eeuw – de speciale relativiteitstheorie – leidde tot een van de grootste triomfen uit de 20^e eeuwse natuurkunde: het standaardmodel van de deeltjesfysica. Deze theorie geeft ons één enkele beschrijving van alle waargenomen fundamentele deeltjes, samen met drie van de vier natuurkrachten: de sterke-, zwakke-, en elektromagnetische kracht. Het standaardmodel werd onderworpen aan verschillende experimenten, en blijkt keer op keer stand te houden, tot op de kleinste afmetingen die waargenomen kunnen worden met behulp van de huidige deeltjesversnellers.

De vierde – en misschien wel bekendste – kracht wordt niet beschreven door het standaardmodel: de zwaartekracht. Deze kracht, die beschreven wordt door Einsteins algemene relativiteitstheorie, is verantwoordelijk voor het beschrijven van grote, massieve deeltjes zoals planeten die rond de zon draaien. Hoewel zwaarte-

kracht niet in het standaardmodel opgenomen is, heeft dit verrassend genoeg nooit tot discrepanties geleid in experimenten met deeltjesversnellers. Dit komt omdat zwaartekracht de zwakste van de vier fundamentele krachten is, zoals iedereen die ooit een paperclip met een magneet optilde, zelf heeft kunnen ondervinden.

Ondanks dat zwaartekracht de zwakste is van de vier, is het de enige kracht die werkt op grote afstanden (van macroscopische tot zelfs kosmologische schaal), en dus alomtegenwoordig is in de typische situaties van ons dagelijkse leven. Daarom is het bestuderen van de zwaartekracht toch uiterst interessant. Een manier om de zwaartekracht te bestuderen, is door te kijken wat er gebeurt als ze zeer sterk is, wat bereikt kan worden door objecten heel zwaar te maken. Wat blijkt dan? Het is niet mogelijk om de dichtheid van een object onbeperkt te laten toenemen. Wanneer een object voldoende massief wordt, stort het in elkaar onder druk van zijn eigen gewicht en vormt het één van de meest fascinerende objecten uit de natuurkunde: zwarte gaten. Merk op dat zwarte gaten niet louter een theoretisch begrip zijn, maar ook door astronomen waargenomen worden in ons universum. Het zijn namelijk de eindproducten van zware, uitdovende sterren wanneer deze op het einde van hun leven in elkaar storten.

Het ontbreken van zwaartekracht in het standaardmodel is niet de enige reden waarom het werk van natuurkundigen nog niet vervolledigd is. Het standaardmodel bevat namelijk verschillende onbepaalde parameters (zoals de massa's van elementaire deeltjes) die niet door de theorie verklaard worden. Bovendien is onze huidige beschrijving van de zwaartekracht – de algemene relativiteitstheorie – onvolledig: in situaties waarin de zwaartekracht heel sterk is (zoals in het centrum van zwarte gaten) of toegepast moet worden op heel kleine (kwantummechanische) afstanden zoals bij het begin van ons universum, loopt de beschrijving helemaal mis. In het wilde weg toepassen van algemene relativiteitstheorie op kleine afstanden is inconsistent. Dit alles blijft theoretisch natuurkundigen motiveren om te zoeken naar een 'betere' theorie: een kwantummechanische theorie van de zwaartekracht, die liefst ook nog de interactie met drie andere fundamentele krachten beschrijft. Zo een goede 'geünificeerde' theorie moet dus zowel het standaardmodel als de algemene relativiteitstheorie bevatten.

Een van de meest veelbelovende kandidaten voor zo'n alomvattende theorie is de snaartheorie. De fundamentele bouwstenen van deze theorie zijn geen deeltjes, maar wel trillende, uitgestrekte objecten: snaren en membranen. De verschillende trillingswijzen van een snaar kunnen worden geïnterpreteerd als fundamentele deeltjes. In het bijzonder kan worden aangetoond dat onder deze deeltjes zich het zogenaamde 'graviton' bevindt, dat de zwaartekracht veroorzaakt. Bovendien kunnen de membranen gebruikt worden om modellen in snaartheorie te bouwen die dezelfde eigenschappen als het standaardmodel vertonen. Dit stemt natuurkundigen

hoopvol dat snaartheorie zowel het standaardmodel, als een kwantumtheorie van de zwaartekracht kan beschrijven.

Het bestuderen van snaartheorie heeft reeds tot ettelijke successen in natuur- en wiskunde geleid. Daarenboven, en bijzonder relevant voor deze thesis, heeft snaartheorie geleid tot een van de meest merkwaardige en krachtige ideeën in de theoretische natuurkunde: de AdS/CFT correspondentie. Hierover wordt verder uitgeweid in de sectie ‘precaire precursoren’.

Gloeiende Zwarte Gat

Een zwart gat kan voorgesteld worden als een bol, waarbij het oppervlak van de bol overeenkomt met de horizon van het zwarte gat. Eenmaal hier voorbij, is de zwaartekracht zo sterk dat er geen weg meer terug is. Zelfs licht kan niet meer ontsnappen aan de zwaartekracht wanneer het binnen de horizon van het zwarte gat komt, vandaar de naam: *zwart* gat. Eenmaal binnen de horizon eindigt alles onvermijdelijk in het centrum van de bol, waar de ‘singulariteit’ van het zwarte gat zich bevindt: een punt waar de massadichtheid oneindig wordt. In de buurt van de singulariteit is de zwaartekracht zo sterk dat de algemene relativiteitstheorie geen correcte beschrijving meer geeft, en een theorie van kwantumgravitatie noodzakelijk is om te verklaren wat er gebeurt.

In de jaren 70 werd verrassend genoeg duidelijk dat zwarte gaten toch niet zo zwart zijn: Hawking toonde aan dat zwarte gaten een temperatuur hebben, en thermische straling uitzenden. Dit impliceert dat een zwart gat langzaam energie verliest en kleiner wordt: het verdampt. Het gaf aanleiding tot de ‘informatie paradox’: gooi een object in een zwart gat en wacht tot het zwarte gat volledig verdampt is. Het eindresultaat is een hoopje thermische straling die geen enkele informatie meer over dat object bevat. Dit mag banaal lijken, maar signaleert een fundamenteel probleem met tijdsevolutie van de onderliggende theorie.

In 2012 ontstond een nieuwe, gerelateerde paradox. Er werd voor verdampende zwarte gaten pijnlijk aangetoond dat drie fundamentele natuurkundige principes onderling inconsistent zijn. Eerst en vooral is er het equivalentie principe waarop de algemene relativiteitstheorie gebaseerd is. Dit zegt dat een waarnemer in vrije val altijd hetzelfde observeert, ongeacht of hij hier op aarde valt, of hij nu door de horizon van een zwart gat valt. Ten tweede zijn er de wetten van de kwantummechanica, en ten derde het principe van de lokaliteit, wat zegt dat processen die voldoende ver van elkaar verwijderd zijn, elkaar niet kunnen beïnvloeden. Het feit dat deze drie principes inconsistent zouden zijn wanneer toegepast op een verdampend zwart gat, kwam als een shock.

Sommige natuurkundigen besloten dan maar het equivalentie principe op te geven, en concludeerden dat een waarnemer in vrije val nooit de binnenkant van een zwart gat zal zien, maar verbrand wordt op de horizon door een muur van hoge energie deeltjes. Deze paradox werd dan ook toepasselijk de ‘firewall’ paradox gedoopt.

Dit brengt ons naar de inhoud van één van mijn onderzoeken. In hoofdstuk 2 van deze thesis heb ik geprobeerd de firewall paradox te ontcrachten, door te laten zien dat een waarnemer die in een zwart gat valt, onmogelijk alle drie principes kan meten om de paradox te kunnen construeren. Dit heb ik meetkundig aangetoond voor een grote klasse zwarte gaten in verschillende ruimtes en dimensies. Het geeft een pragmatische uitweg voor de paradox: als een waarnemer niet in de mogelijkheid verkeert om alle drie principes te verifiëren, kan deze dus niet tot de conclusie komen dat ze onderling inconsistent zijn. Dit maakt dat er geen reden is om van het equivalentie principe af te stappen, en de waarnemer kan dus zonder problemen door de horizon van een zwart gat vallen.

Echter, dit is geen sluitend bewijs om de firewall paradox voorgoed op te bergen. Hoewel het onderzoek suggereert dat voor een grote klasse zwarte gaten het niet mogelijk is om de paradox waar te nemen, zijn er andere, in het bijzonder holografische (verder hierover meer) argumenten voor firewalls die robuust blijken te zijn tegen de meetkundige argumenten die ik gemaakt heb. Verder onderzoek is nodig, en ik ben ervan overtuigd dat een sluitende resolutie van deze paradox tot diepere inzichten in kwantumgravitatie zal leiden.

Precaire Precursoren

Zwarte gaten zijn thermodynamische objecten; ze worden niet alleen gekarakteriseerd door temperatuur, maar ook door entropie: een grootheid die de hoeveelheid informatie meet. Het bijzondere is dat zwarte gaten een entropie hebben die gegeven wordt door hun oppervlakte, en niet door hun volume (zoals men zou verwachten bij een gas of andere familiere vorm van materie). In zekere zin betekent dit dat alle informatie van het zwarte gat, zich op de horizon (de rand) ervan bevindt. Dit fascinerende gegeven kan worden beschouwd als gevolg van het *holografisch principe*, wat stelt dat elke gravitationele theorie in een bepaald volume beschreven kan worden door een andere theorie, die leeft op het oppervlak dat dat volume omsluit. Dit merkwaardig principe wordt door theoretisch natuurkundigen beschouwd als één van de eigenschappen die een kwantummechanische theorie van de zwaartekracht zal hebben.

Al snel werd vermoed dat ook snaartheorie holografisch is, en het onderzoek culmineerde in 1997 met een van de grootste successen uit de snaartheorie: een concrete

realisatie van het holografisch principe, genaamd de Anti-de Sitter/Conforme velden (Field) Theorie correspondentie. AdS is een negatief gekromde ruimte uit de algemene relativiteitstheorie, en CFT een bijzonder symmetrische, kwantummechanische deeltjestheorie. AdS/CFT is een dualiteit (m.a.w. equivalentie) tussen twee totaal verschillende theorieën: enerzijds is er snaartheorie die leeft in AdS, en anderzijds is er de CFT die leeft op de rand van de AdS ruimte. Hiermee wordt nu ook duidelijk waarom dit een voorbeeld van het holografisch principe genoemd wordt: de gravitationele snaartheorie in AdS (ook wel de bulk genoemd), is exact gelijk aan een niet-gravitationele theorie die op de rand leeft!

AdS/CFT is zonder twijfel een van de grootste doorbraken in de theoretische natuurkunde van de afgelopen 20 jaar. De kracht van AdS/CFT zit hem in het feit dat het mogelijk is om een (vaak moeilijk) snaartheorie probleem in AdS te vertalen naar een ander, equivalent probleem in de CFT, dat meestal gemakkelijker op te lossen valt; en omgekeerd natuurlijk ook. Wat ik zelf het meest interessant vind, is dat AdS/CFT ons zo een unieke blik op snaartheorie in AdS biedt, dat toelaat kwantummechanische aspecten van zwaartekracht te bestuderen, door deze te vertalen naar een equivalent probleem in de CFT. Deze vertaling is verre van triviaal, en vraagt als het ware een woordenboek om het ene probleem in het andere om te schrijven. Hoewel zo'n vertaling cruciaal is voor de verdere ontwikkeling van AdS/CFT, zijn nog vele aspecten onbegrepen. Het is dan ook hier dat ik in mijn onderzoek een bijdrage geleverd heb, zoals uiteengezet in hoofdstukken 3, 4 en 5.

Een van mijn favoriete objecten om te bestuderen in AdS/CFT zijn de zogenaamde precursoren: een ingewikkeld en vaak niet-lokaal object in de CFT dat, wanneer het vertaald wordt naar de AdS bulk, eenvoudigweg overeenkomt met één lokaal punt. Net omdat de CFT op de rand van AdS leeft, is het interessant om te onderzoeken hoe verschillende punten in de bulk, die gescheiden leven in deze 'extra' dimensie weg van rand, in de CFT gereconstrueerd worden. Dit vertaalt zich in dat precursoren vaak heel verrassende en zelfs paradoxale eigenschappen hebben, zoals de titel al doet vermoeden. In het bijzonder, indien deze punten in de bulk voldoende ver van elkaar verwijderd zijn, zouden deze niet met elkaar mogen interageren, iets wat lokaliteit in de bulk genoemd wordt. Het bestaan van lokaliteit in de bulk is een, voor mij misschien wel het, mirakel van AdS/CFT, en zonder twijfel een van de minst begrepen maar meest fascinerende aspecten van de correspondentie.

Aangezien alle informatie van een punt in de gravitationele bulk bevat zit in de precursor, heb ik onderzocht hoe en waar in de CFT deze informatie gecodeerd wordt. Ik heb aangetoond dat precursoren niet uniek zijn (d.w.z. meerdere precursoren kunnen met hetzelfde punt in AdS corresponderen), en laat zien dat het gebrek aan uniciteit gebruikt kan worden om informatie in een bepaalde regio van

de CFT te lokaliseren. Vervolgens poneer ik ook een vermoeden dat precursoren die met eenzelfde bulk punt corresponderen, relateert aan de onderliggende symmetrieën in de CFT. Dit is verrassend, aangezien voorheen gedacht werd dat deze symmetrieën (ijksymmetrie in het bijzonder) geen fysische rol spelen in AdS/CFT. Tenslotte stel ik de vraag welke eigenschappen een CFT moet hebben, om ‘goede’, lokale gravitationele theorieën te beschrijven, zoals Einsteins zwaartekrachtstheorie waarin we lijken te leven. Dit is geen eenvoudige vraag, en om vooruitgang te maken heb ik een simpel model van de AdS/CFT correspondentie bestudeerd. Dit liet me toe om de kenmerken bloot te leggen van dergelijke holografische CFTs.

De AdS/CFT correspondentie heeft het bestuderen van kwantumgravitatie fundamenteel veranderd, en maakte van holografie een van de meest waardevolle en interessante ideeën uit de theoretische natuurkunde in de afgelopen 20 jaar. Het onderzoeksveld breidt zich snel uit en focust zich niet enkel op kwantumgravitatie, maar omvat nu ook deelgebieden die holografie (en snaartheorie in het bijzonder) gebruiken om meer te leren over kernfysica en de theorie van gecondenseerde materie zoals supergeleiders en -fluida.